Aus der Klinik für Dermatologie, Venerologie und Allergologie
und HTCC – Hauttumorcentrum Charité der Medizinischen Fakultät
Charité – Universitätsmedizin Berlin

DISSERTATION

Entscheidende Rolle Reaktiver Sauerstoffspezies für die bekämpfung von Kutanen SCC-Zellen
Crucial Role of Reactive Oxygen Species for targeting of Cutaneous SCC Cells

zur Erlangung des akademischen Grades
Doctor medicinae (Dr. med.)

vorgelegt der Medizinischen Fakultät
Charité – Universitätsmedizin Berlin

von

Jiaqi Zhu
aus Changchun, Jilin, China

Datum der Promotion: ....25.06.2023....

Table of content

List of table and figures

List of Abbreviations

Abbreviation	Meaning
AK	Actinic keratosis
AKT	PKB Protein kinase B
AML	Acute myeloid leukemia
ASK1	Apoptosis signal-regulated kinase 1
BCA	Bicinchoninic acid
BSA	Bovine serum albumin
CDK	Cell cycle-dependent kinase
c-FILP	Cellular FLICE-inhibitory proteins
cIAPS	Cellular inhibitor of apoptosis proteins
cSCC	Cutaneous squamous cell carcinoma
COX-2	Cyclooxygenase-2
CTCL	Cutaneous T-cell lymphoma
DMSO	Dimethylsulfoxid
DR5/TRAIL-R2	Death receptor 5
DCF	Dichlorofluorescin
EC	Epicatechin
ECG	Epicatechin gallate
EDTA	Ethylenediaminetetraacetic acid
ELISA	Enzyme-Linked ImmunoSorbent Assay
EGC	Epigallocatechin
EGCG	Epigallocatechin gallate/ Epigallocatechin-3-gallate
FACS	Fluorescence-activated cell sorting analyses
FCS	Fetal calf serum
FDA	Food and Drug Administration
FLT3-ITD	FMS-like tyrosine kinase-3 internal tandem duplication
H2DCF-DA	2',7'-dichlorodihydrofluorescein diacetate
ICDA	Inhibitors of DNAse
LDH	Lactate dehydrogenase
MnSOD	Manganese-dependent superoxide dismutase
MMP	Mitochondrial membrane potential
MOMP	Mitochondrial outer membrane permeability
NAC	N-acetylcysteine
NSAID	Nonsteroidal anti-inflammatory drugs
NOX2/4	Nicotinamide-adenine dinucleotide phosphate oxidase 2/4
PBS	Phosphate buffered saline
PE	Polyphenon E
PKC	Protein kinase C
QVD-Oph	Quinoline-Val-Asp-Difluorophenoxymethylketone
ROS	Reactive oxygen species
RPMI	Roswell Park Memorial Institute
SDS	Sodiumdodecylsulfat
SOD2/3	Superoxide dismutase 2/3
STAT3	Signal transducer and activator of transcription 3

TMRM+	Tetramethylrhodamin-methylester
TRAIL	Tumor necrosis factor-related apoptosis inducing-ligand
XIAP	X- linked inhibitory apoptosis protein

1. Abstract

Cutaneous squamous cell carcinoma (cSCC) accounts for 20% of all skin cancers. Actinic keratoses (AK) is the precursors of cSCC, and there is still no effective way to stop its progression into cSCC. Effective medicines are needed to combat the current high incidence of of cSCC and AK. Non-steroidal anti-inflammatory drugs as celecoxib, indirubin derivatives or sinecatechins (Veregen, Polyphenon E, PE) represent promising candidates. Here, the efficacy and mode of action of celecoxib, three indirubin derivatives and PE were investigated in four cSCC cell lines. The indirubin derivatives caused loss of cell proliferation and viability as well as induced apoptosis. Celecoxib obtained a strong anti-proliferative effect in four representative cSCC cell lines. Apoptosis were further enhanced and loss of cell viability were increased, when the indirubin derivatives or celecoxib were combined with TRAIL (Tumor necrosis factor-related apoptosis inducing-ligand). In both combined treatments, pro-apoptotic caspase cascades were activated. Also, the TRAIL receptor DR5, the pro-apoptotic Puma and the p21 were up-regulated, whereas anti-apoptotic factors (survivin and XIAP) were down-regulated. PE also caused strong reduction in cell proliferation and cell viability but not apoptosis. For celecoxib and indirubin derivatives, a strong and early increase in reactive oxygen species (ROS) was characteristic, while for PE, ROS decreased early and increased later. For indirubin derivatives, the relation between high ROS and apoptosis could be shown by anti-oxidative pre-treatment, while for celecoxib, the production of ROS was strong so that it could not be prevented by anti-oxidants. For PE, the relation between low ROS and inhibition of cell proliferation and cell viability could be shown by anti-oxidative pre-treatment. Thus, high ROS may induce apoptosis, while low ROS may inhibit cell proliferation and cell viability in cSCC cells. These data illuminate the different mechanisms of ROS in the treatment of cSCC as well as provide the basis to understand how pro- and anti-tumorigenic ROS signalling pathways may be effectively used in cancer therapy.

1. Zusammenfassung

Das kutane Plattenepithelkarzinom (cSCC) macht 20 % aller Hautkrebserkrankungen aus. Aktinische Keratosen (AK) sind die Vorstufen von cSCC, und es gibt immer noch keine wirksame Methode, um ihr Fortschreiten zu cSCC zu verhindern. Es werden wirksame Arzneimittel benötigt, um die derzeit hohe Inzidenz von cSCC und AK zu bekämpfen. Nicht-steroidale Entzündungshemmer wie Celecoxib, Indirubin-Derivate oder Sinecatechine (Veregen, Polyphenon E, PE) sind vielversprechende Kandidaten. Hier wurden die Wirksamkeit und die Wirkungsweise von Celecoxib, drei Indirubin-Derivaten und PE in vier cSCC-Zelllinien untersucht. Die Indirubin-Derivate führten zu einem Verlust der Zellproliferation und der Lebensfähigkeit und induzierten Apoptose. Celecoxib erzielte bei vier repräsentativen cSCC-Zelllinien eine starke anti-proliferative Wirkung. Die Apoptose und der Verlust der Lebensfähigkeit der Zellen wurden noch verstärkt, wenn die Indirubin-Derivate oder Celecoxib mit TRAIL (Tumor-Nekrose-Faktor-bezogener Apoptose-Induktions-Ligand) kombiniert wurden. Bei beiden kombinierten Behandlungen wurden pro-apoptotische Caspase-Kaskaden aktiviert. Außerdem wurden der TRAIL-Rezeptor DR5, das pro-apoptotische Bcl-2-Protein Puma und der Zellzyklusinhibitor p21 hochreguliert, während anti-apoptotische Faktoren (Survivin und XIAP) herunterreguliert wurden. PE führte auch zu einem starken Rückgang der Zellproliferation und der Lebensfähigkeit der Zellen, aber nicht zur Induktion der Apoptose. Für Celecoxib und Indirubin-Derivate war ein starker und früher Anstieg reaktiver Sauerstoffspezies (ROS) charakteristisch, während bei PE die ROS früh ab- und später zunahmen. Bei Indirubin-Derivaten konnte der Zusammenhang zwischen hohen ROS und Apoptose durch eine antioxidative Vorbehandlung aufgezeigt werden, während bei Celecoxib die Produktion von ROS so stark war, dass sie durch Antioxidantien nicht verhindert werden konnte. Bei PE konnte der Zusammenhang zwischen niedrigen ROS und der Hemmung der Zellproliferation und Zelllebensfähigkeit durch eine antioxidative Vorbehandlung nachgewiesen werden. Somit kann ein hoher ROS-Gehalt Apoptose auslösen, während ein

niedriger ROS-Gehalt die Zellproliferation und Zelllebensfähigkeit von cSCC-Zellen hemmen kann. Diese Daten beleuchten die verschiedenen Mechanismen von ROS bei der Behandlung von cSCC und liefern die Grundlage für das Verständnis, wie pro- und antitumoröse ROS-Signalwege in der Krebstherapie wirksam eingesetzt werden können.

2. Introduction

2. 1 Actinic keratosis and cutaneous SCC

Actinic keratosis (AK), produced in tumorigenic epidermal keratinocytes, is mainly located in sun-exposed areas of the skin. AK is characterised by an exceptionally high incidence ranging from 11% to 60% in caucasian individuals above 40 years (1). Clinical and subclinical lesions often coexist over large areas and have also been described as field cancerization (2). AK lesions have the potential to transform into aggressive cutaneous squamous cell carcinoma (cSCC), therefore, AK has been defined as cSCC in situ and treatment of AK is important (3). Cutaneous SCC is a malignant proliferation of the skin epithelium that accounts for 20% to 50% of all skin cancers (4) and accounts for 20% of skin cancer deaths worldwide (5). Often, cSCC exhibits a relatively benign clinical behaviour, and most cSCC can be successfully eradicated by surgical resection, sometimes in combination with adjuvant radiotherapy or chemotherapy. Moreover, some of patients with advanced and metastatic cSCC may benefit from systemic therapy (6). However, a proportion of cSCC has features associated with a high likelihood of recurrence and metastasis, as well as drug resistance associated with a high mortality rate. These are still issues that need to be addressed in the treatment of cSCC (7). Therefore, there is an urgent need for novel and alternative treatment options.

2. 2 Induction of apoptosis in cancer therapy

Induction of apoptosis to eliminate neoplastic cells is a major target of treatment for cancer, and resistance to therapy is often interpreted as a deficiency of apoptosis (8). Therefore, eliminating resistance to apoptosis induction during treatment is a critical step for treating cSCC and reducing drug resistance (9). Apoptosis can be induced through extrinsic and intrinsic pathways. Death ligands can initiate extrinsic induction of apoptosis. The death ligand TRAIL has become widely known for its anti-cancer potential, while it remains generally unaffected in normal cells

(10, 11). Death receptor activation is followed by the formation of cell membrane-bound death-inducing signalling complexes that lead to the activation of promoter caspases including caspase-8 and caspase-10 (12). Activate effector caspases, such as caspases-3, -6 and -7, which can be cleaved and activated by initiator caspases, can cleave several death substrates to fragment DNA and induce apoptosis (13).

On the other hand, intrinsic pro-apoptotic pathways can be activated the reaction to cellular stress situations, including high levels of ROS and anti-cancer treatments such as chemotherapy. It is dependent on MOMP, loss of MMP and release of mitochondrial factors such as cytochrome c, which may trigger activation of caspase-9 (14). This procedure is under a critical control of the pro-apoptotic and anti-apoptotic Bcl-2 protein family. Bcl-2 performs its anti-apoptotic function by binding and inhibiting of Bax, belonging to pro-apoptotic family (14, 15). Normally, induction of apoptosis and inhibition of cell proliferation are regulated in parallel.

Cell proliferation is critically regulated by CDK 1/2/4/6, which mediate retinoblastoma (Rb) protein phosphorylation, thus resulting in E2F transcription factor-induced gene expression and activation of the cell cycle (16). On the other hand, the INK4 family (p15, p16, p18, and p19) as well as of the Cip/Kip family (p21, p27 and p57) can prevent cell cycle progression (17). While CDK inhibitors critically control cell proliferation in normal cells, they may be downregulated or abolished in cancer (18).

2. 3 Different treatments of cSCC

Treatment options for cSCC include surgery, chemotherapy, radiotherapy, photodynamic therapy and molecular targeted therapy. Of these, surgery is by far the most common and important one. Many cSCCs can be treated surgically, and the ten-year survival rate for cSCC after surgery is over 90%, but it decreases dramatically once metastasis occurs (19). The frequency of lymph node metastases is about 4%, while the mortality rate is close to 2% (20). Especially, When cSCC and AK occur at specific sites, the lesions are too large and numerous,

the patient is too old or the tumor has metastasised distantly, other medical treatments such as radiotherapy, PDT and/or chemotherapy may be better options (21). Given that, precise and targeted therapies are required.

2. 4 Celecoxib

The NSAID and COX-2 inhibitor celecoxib has received particular interest for its anti-tumor activity (22). Efficiency in colorectal adenomas has been shown in clinical trials to yield its FDA approval for patients with familial adenomatous polyposis (23-25). A growing number of experiments have demonstrated that the anti-cancer activity of celecoxib may be more related to COX-2-independent effects than to COX-2-dependent mechanisms (26-28).

2. 5 Indirubin derivatives

Indirubin has been recognized as the effective component of Danggui LonghuiWan to treat chronic and inflammatory diseases. In the 1980s, clinical results obtained during the treatment of patients with chronic granulocytic leukemia with indirubin, stimulating the study of this compound (29, 30). Owing to the native form with the limited anti-tumor activity, several laboratories are currently investigating new derivatives to enhance its efficacy (31-33).

2. 6 Sinecatechins (Polyphenon E)

The green tea extract Sinecatechins (Polyphenon E, PE; Veregen®, Aresus Pharma GmbH, Strausberg, Germany) represents another promising candidate for tumor therapy (34). For the most abundant catechin, EGCG, inhibition of cell proliferation and induction of apoptosis of mammary carcinoma, lung cancer and gastric cancer cells has been reported (35-37).

2. 7 The role of ROS

ROS, including H_2O_2, superoxide anion radicals, hydroxyl radical, singlet oxygen, and alpha-oxygen are often considered to be by-products of oxygen depletion and cellular metabolism (38, 39). ROS play key roles in many cellular processes, including cell differentiation, proliferation and cell death, through regulating key signalling pathways (40). The balance of ROS is essential for cell survival, signalling and protection. Detoxification of ROS achieved through non-enzymatic or enzymatic anti-oxidants are involved in the scavenging of different types of ROS. Increased levels of ROS may favour tumorigenesis, leading to DNA, protein and lipid damage and may promote genetic instability (41-45). ROS may also act as signalling molecules in cancer development, contributing to abnormal cell growth, metastasis, resistance to apoptosis, angiogenesis, and in some types of cancer impaired differentiation (46, 47). The main function of anti-oxidant defence in tumor cells is to prevent excessive ROS accumulation and to maintain tumor-friendly ROS levels, allowing disease progression and resistance to apoptosis (48).

However, when ROS rises to toxic levels, it depletes the capacity of the tumor cells' antioxidant system, disrupts ROS homeostasis of the tumor cells and subsequently inducing cell cycle arrest, apoptosis and senescence (49, 50). Thus, ROS anti-tumor signalling could be a target for cancer therapy. A number of chemotherapeutic agents widely used to treat cancer have been described as increasing the production of ROS, causing irreparable damage and cell death. These include anthracyclines, cisplatin, bleomycin and arsenic trioxide (51). In previous studies of our group, they described that increased ROS can result in induction of apoptosis, as shown for indirubin derivatives in cutaneous T-cell lymphoma and melanoma cells (52, 53). Mitochondrial leakage or other sources can generate ROS (54), but relationship with the depicted apoptotic pathways is not well understood so far.

Here, the pro-apoptotic effects of celecoxib, indirubin derivatives and PE were investigated in cSCCs cells, and the efficiency of combination therapy was shown. Downstream signalling

pathways has been revealed and the role of ROS in three treatments has been explored. The results may help to improve the treatment of cSCC/AK.

3. Materials and Methods

3. 1 Cell culture and treatment

Four representative cSCC cell lines (SCL-I, SCL-II, SCC-12 and SCC-13) were included in this study. Most assays were performed in 24-well plates after seeding 5 $\times 10^4$ cells per well. Celecoxib (BioMol, Hamburg, Germany; 1000-8672) was used at 25–100 µM. Indirubin derivatives (DKP-071, DKP-073 and DKP-184) (55) were used at 2.5–20 µM. PE was applied in concentrations of 10–200 µg/ml. Cells were also treated with agonistic anti-CD95 antibody (CH-11, IgM mouse; Beckman Coulter, Krefeld, Germany; 100 ng/mL), and Killer TRAIL™ (Adipogen, San Diego USA, AG-40T-0001; 50 ng/mL). To inhibit caspases, pan-caspase inhibitor QVD-Oph (Abcam, Cambridge, UK; 10 µM) was applied 1 h earlier before agonist application.

3. 2 Cell proliferation

Cell proliferation was evaluated by WST-1 assays (Roche Diagnostics, Penzberg, Germany), the assay was quantified in an ELISA reader at 440 nm. As the enzyme activity is only present in metabolically active cells, the readout reflects both the numbers and viability of cells.

3. 3 Apoptosis induction, cytotoxicity and cell viability

Cell cycle analysis was used to determined apoptosis. Cells were stained for 1 h with propidium iodide. Due to the washing out of small DNA fragments, nuclei with less DNA than G1 (sub-G1) correspond to cells with DNA fragmentation (apoptotic cells). Cytotoxicity was determined in cell culture supernatants by quantification of released LDH activity. Cell viability was determined by staining cells with calcein-AM (PromoCell, Heidelberg, Germany), which is converted in viable cells through intracellular esterases to the green-fluorescent dye calcein.

3. 4 Mitochondrial membrane potential

Loss of MMP was determined by staining cells with the fluorescent dye tetramethylrhodamine-6-maleimide ($TMRM^+$; Sigma-Aldrich, Darmstadt, Germany). Cells were stained for 20 min at 37°C in 1 µM $TMRM^+$ and measured by flow cytometry.

3. 5 Analysis of ROS

To determine the levels of intracellular ROS, cells were stained with the cell-permeable and non-fluorescent chemical 2', 7'-dichlorodihydrofluorescein diacetate (H2DCF-DA; D-399, Thermo Fisher Scientific, Hennigsdorf, Germany, 10 µM). Before starting treatment with other effectors, cells were pre-incubated for 1 h with H_2DCF-DA (10 µM). Cells were treated with 1 mM H_2O_2 for 1 h as positive controls. Different antioxidant treatments were utilized with the purpose of suppressing treatment-induced ROS levels. Antioxidants were generally applied at 1 h before starting treatment.

3. 6 Western Blotting

Total protein extracts were obtained by cell lysis buffer containing 150 mM NaCl, EDTA (1 mM), 1% NP-40; 50 mM Tris (pH 8.0), as well as phosphatase and protease inhibitors. Following SDS polyacrylamide gel electrophoresis, proteins were blotted on nitrocellulose membranes.

Table 1. Antibodies of western blotting

Antibodies		Manufacturer
Primary Antibodies	Rabbit-anti-Cleaved caspase-3 Rabbit-anti-Caspase-6,7 and9 Mouse- anti- Caspase-8 Rabbit-anti-XIAP, Mcl-1, Bad, Bcl-2 and Bcl-w	Cell Signaling Danvers, MA, USA

	Mouse- anti- c-Filp, survivin, p21, puma and β-actin Rabbit-anti-DR5	Santa Cruz, Texas, USA Abcam , Cambridge, UK
Secondary Antibodies	peroxidase- goat anti-rabbit peroxidase- goat anti-mouse	Dako, Hamburg, Germany

3. 7 Statistical analysis

We performed the experiments in at least three separate experiments to ensure that the results were repeatable. We used Student's t-test to determine statistical significance. A statistically signifcant p value<0.05 was adopted. Western blot signals were quantified by densitometry using Fusion-Capt Advance software (Vilber Lourmat, Collégien, France), values were normalized by the respective β-actin values and median values were formed from each two independent experiments (independent cell extracts).

4. Results

4. 1 Decrease of cSCC Cell Proliferation

Quantitative WST-1 assays were utilized to evaluate cell proliferation. As for celecoxib, the anti-proliferative potential was evaluated in SCL-II as well as SCC-12. We found a dose-dependent, anti-proliferative effect of celecoxib (Figure 1A). The antiproliferative effect was not dependent on direct cytotoxicity and was identified by LDH release assays at 2 h (data not shown).

The efficacy of three derivatives (DKP-071, -073, -184) of indirubin and PE were investigated in four cSCC cell lines. As for indirubin derivatives, at 24 h, cell proliferation rates were generally decreased in cSCC cells by three derivatives, reaching 30%, 29% and 48% in SCL-I, 72%, 77% and 83% in SCL-II, 50%, 48% and 79% in SCC-12 as well as 41%, 22% and 57% in SCC-13 (Figure 1B). These antiproliferative effects were further enhanced by the binding of indirubin derivatives to TRAIL (data not shown).

As for PE, effects on cell proliferation were investigated in cSCC cell lines in response to increasing dose of PE (10–200 µg/ml). At 24 h, PE resulted in a strong and dose-dependent decrease of cell numbers in four cell lines (Figure 1C). Then, after 24 h, the effects further enhanced at 48h. Thus, PE (100/200 µg/ml) decreased cell proliferation to 43%/ 22% (SCL-I), 29%/ 19% (SCL-II), 39%/ 29% (SCC-12) as well as 37%/ 24% (SCC-13) at 48 h (data not shown).

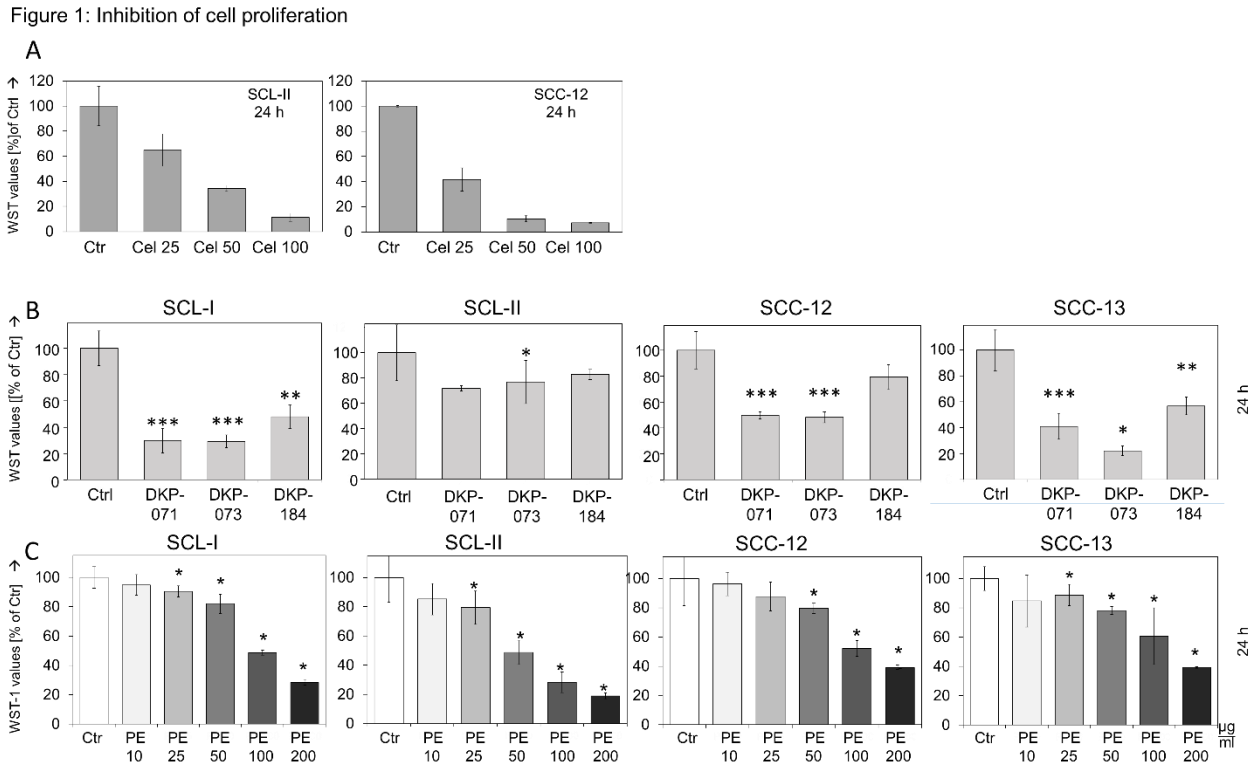

Figure 1. Decrease of cSCC Cell Proliferation. Cell proliferation was evaluated by WST-1 assay in cSCC cells at 24 h with (A) celecoxib (25, 50, 100 μM), (B) indirubin derivatives (DKP-071, -073 and -184, 10 μM) and (C) PE (10 -200 μg/ml).

4. 2 Induction of Apoptosis and Loss of Cell Viability

In compared to the inhibitory effect of celecoxib on cell proliferation, the induction of apoptosis by celecoxib was not significant. Treatment with 25 and 50 μM celecoxib resulted in less than 5% apoptosis at 24 h and 48 h (Figure 2A). Meanwhile, at 25 and 50 μM the effect on cell viability was minimal. Only for 100 μM celecoxib, a stronger effect was found (Figure 3A).

Although cell proliferation was also obviously influenced by medium concentrations of celecoxib, the direct influence on apoptosis and cell viability was of limited significance. To enhance the pro-apoptotic function of celecoxib, it was in combination with TRAIL as well as with CH-11. As a result, the induction of apoptosis was increased in four cell lines. (Figure 2A). The enhancement of apoptosis is often accompanied by a reciprocal loss of cell viability. Combining celecoxib with death ligands caused a significant decrease in cell viability within

48 h (Figure 3A), which proved that celecoxib and death ligands were effective combination partners.

As for indirubin derivatives, when three derivatives were applied alone, apoptosis induction was shown at 24 h. The combination of indirubin derivatives (10 μM) and TRAIL (50 ng/mL) further enhanced apoptosis rates (40%-80%; Figure 2B). A more evident combination effect was observed at the 24 h cell viability level, as the combination of DKP-071 or DKP-073 with TRAIL almost completely abolished cell viability (<10%). (Figure 3B).

As for PE, the reduction in cell proliferation after PE treatment coincided with a strong reduction in cell survival at 24 h and 48 h. Thus, PE (200 μg/mL) reduced the number of surviving cells to 3%-16% in four cell lines at 48 h (untreated controls: 53% - 90%; Figure 3C). In contrast, the induction of apoptosis remained at a low level, reaching at maximum 13% +/- 7% in SCL-II and 14% +/- 4% in SCC-13 after 48 h (Figure 2C). However, the pro-apoptotic capacity of PE was not further enhanced when combined with TRAIL (data not shown).

Figure 2 Induction of Apoptosis

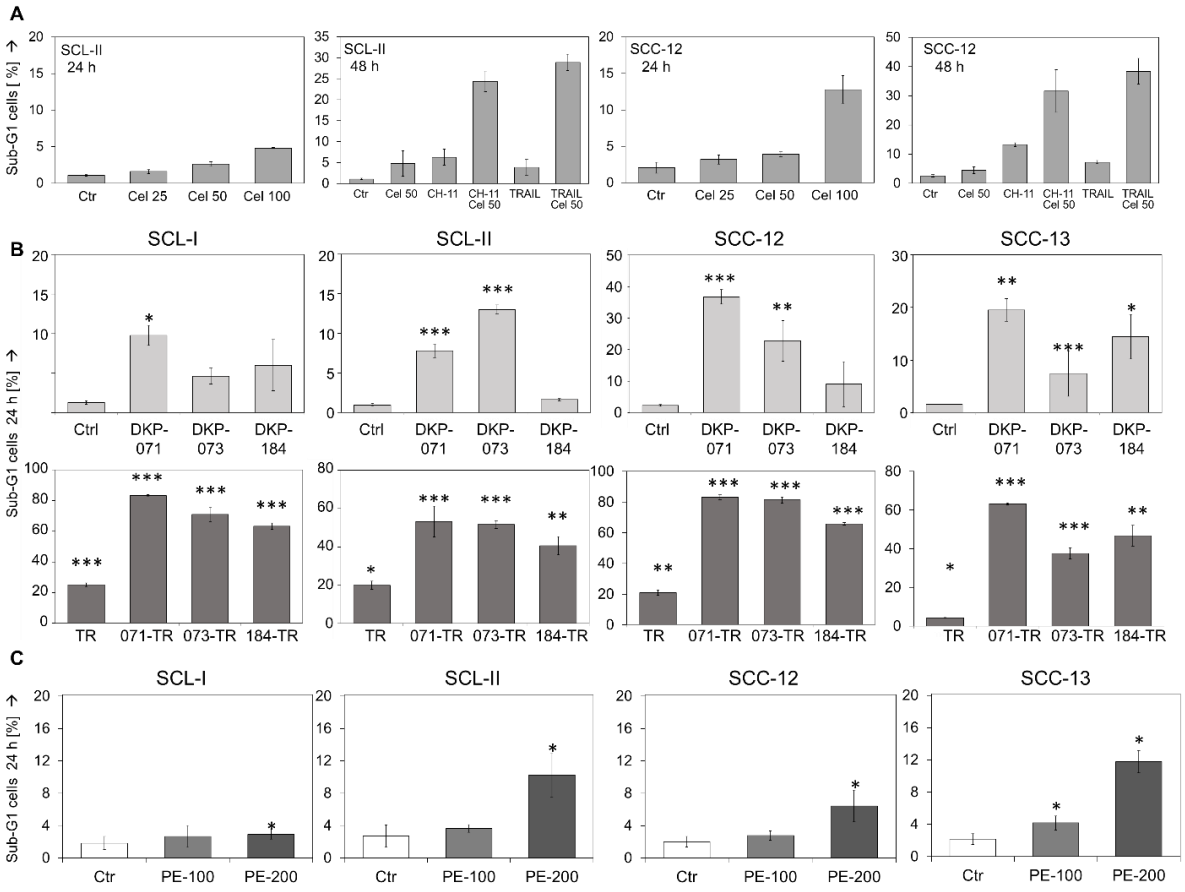

Figure 2. Apoptosis induction. Apoptotic cells were recognized as sub-G1 cells in cell cycle analysis and were characterized by DNA fragmentation. (A) Apoptotic cells were determined at 24 h in response to celecoxib (25, 50 and 100 µM), and celecoxib (50 µM), CH-11 (100 ng/ml), TRAIL (50 ng/ml) or combinations at 48 h. (B) Cells were treated with DKP-071, -073 and -184 (10 µM), TRAIL (TR; 50 ng/mL) or the combinations at 24 h. (C) Cells were treated with PE (100, 200 µg/ml) for 24 h and 48 h.

Figure 3: Loss of cell Viability

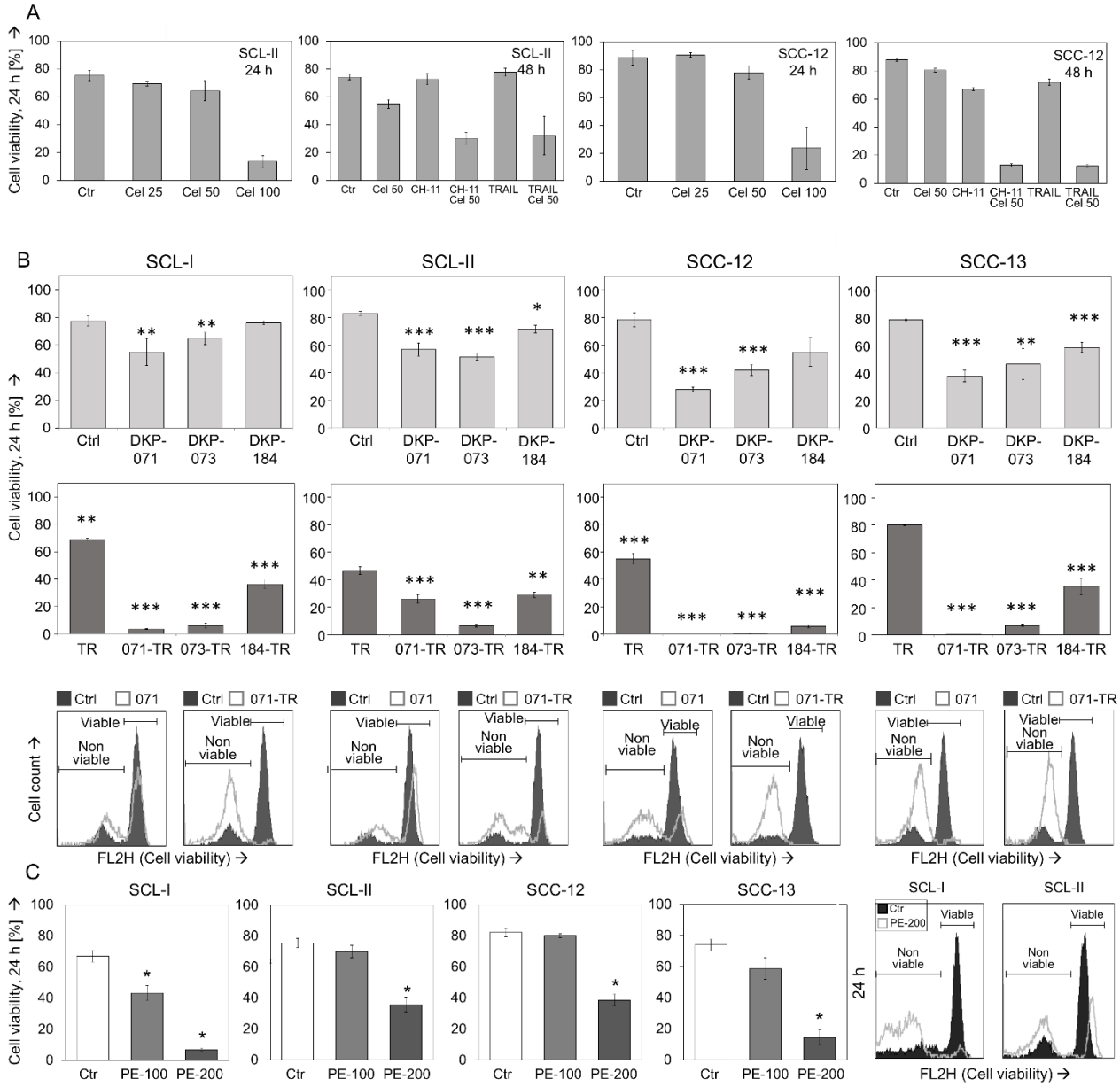

Figure 3. Loss of cell viability. (A) Viable cells were determined at 24 h in response to celecoxib (25, 50 and 100 µM), and celecoxib (50 µM), CH-11 (100 ng/ml), TRAIL (50 ng/ml) or combinations at 48 h. (B) Cells were treated with DKP-071, -073 and -184 (10 µM), TRAIL (TR; 50 ng/mL) or the combinations at 24 h. (C) Cells were treated with PE (100, 200 µg/ml) for 24 h and 48 h.

4. 3 Changes of mitochondrial membrane potential

Maintenance of MMP represents a critical issue of viable cells, and early loss of MMP may be a feature of activation of intrinsic, pro-apoptotic pathways. For the mechanism of action of different treatments in cSCC cells, he changes in MMP were evaluated.

There are no obvious effects on MMP levels neither in the early phase (3 h) nor late phase (24 h), when celecoxib applied alone. However, when the combination treatment was used, a significant loss of MMP (up to 90%) was observed at 24 h, indicating a strong apoptosis was induced (Figure 4A). Thus, the loss of MMP occurred either simultaneously or as a consequence of induced apoptosis.

As for indirubin derivatives, when cells were treated with indirubin derivatives alone, there is an early loss of MMP (4 h) in SCL-I, SCC-12 and SCC-13 (Figure 4B). But, at 24 h, SCL-II had a delayed response with obvious loss of MMP (Figure 4C), no effects at 4 h. Apoptosis and loss of cell viability were not apparent at 4 h, suggesting that the loss of MMP represents an initial effect and is not secondary to cell death.

As for PE, although induced apoptosis was only moderate after PE (200 μg/ml) treatment (Figure 2C), obvious loss of MMP appeared at 24 hours (Figure 4D) but not an earlier time (4 hours of treatment, data not shown). The 24 h loss of MMP may be a consequence or in parallel to the loss of cell viability, thus, there were no signs of a strong signalling effect, indicating that the loss of MMP was associated with an intrinsic induction of apoptosis.

Figure 4. Change of MMP

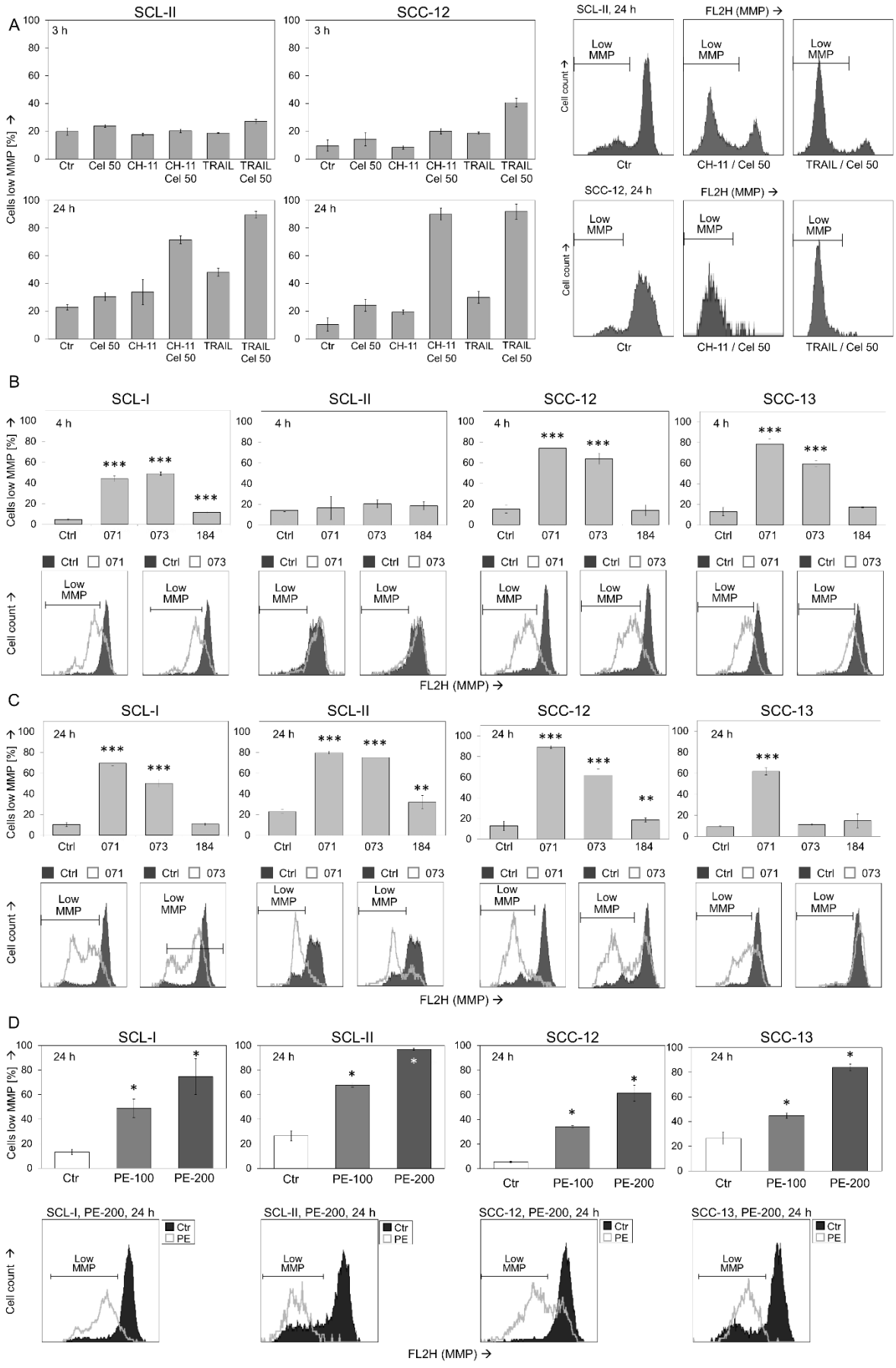

Figure 4. Loss of mitochondrial membrane potential (MMP). (A) Cells were treated with celecoxib (50 μM), CH-11 (100 ng/mL), TRAIL (50 ng/mL) or combinations for 3 h and 24 h, respectively. (B-C) Cells were treated with DKP-071, -073 and -184 at 10 μM at 4 h and 24 h. (D) Cells were treated with PE (100, 200 μg/ml) for 24 h.

4. 4 Caspase Activation in Course of Treatment

When cells were treated with celecoxib (50 μM) alone, caspase activation remained completely unaffected. However, the activation of caspase-8 and caspase-3 were strongly enhanced when combined with celecoxib (50 μM) /TRAIL (50 ng/mL). The activation of caspase-6, -7 and -9 were enhanced as well (Figure 5A). With these data, it was shown that combination therapy fully activated the pro-apoptotic caspase cascade.

As for indirubin derivatives, treatment with indirubin derivatives (10 μM) showed effects on caspase processing. The strongest caspase activation was obtained in the combination of indirubin derivatives (10 μM)/TRAIL (50 ng/mL), which was consistent with the apoptotic rates shown above. Response to DKP-071/TRAIL and DKP-073/TRAIL, the proform of caspase-4 (86 kDa), -6, -7, -8 and -9 were nearly completely degraded within 24 h. Also, characteristic processing products were obtained including caspase-3, -7, -8 and -9 (Figure 5B). For these data, the indirubin derivative/TRAIL combination fully activated the caspase cascade.

As for PE, some induction of caspase-3 activation was obtained after PE treatment. However, the activation of caspase-3 was still at a relatively low level, which can be seen from a comparison with positive control SCC-12 cells, which were treated with DKP-071 (10 μM) /TRAIL (50 ng/ml). Similarly, only weak activation of the initiator caspases of the pro-apoptotic extrinsic and intrinsic pathways was observed. Caspase-8 proform was downregulated only in SCL-II (200 μg/ml PE; downregulated to 64%). Caspase-9 cleavage products were slightly increased in SCL-I (1.7-fold, 200 μg/ml) and SCC-12 (3.7-fold, 200 μg/ml) (Figure 5C). The weak caspase treatment was consistent with only moderate induction of apoptosis as described above.

Figure 5 Activation of caspase cascade

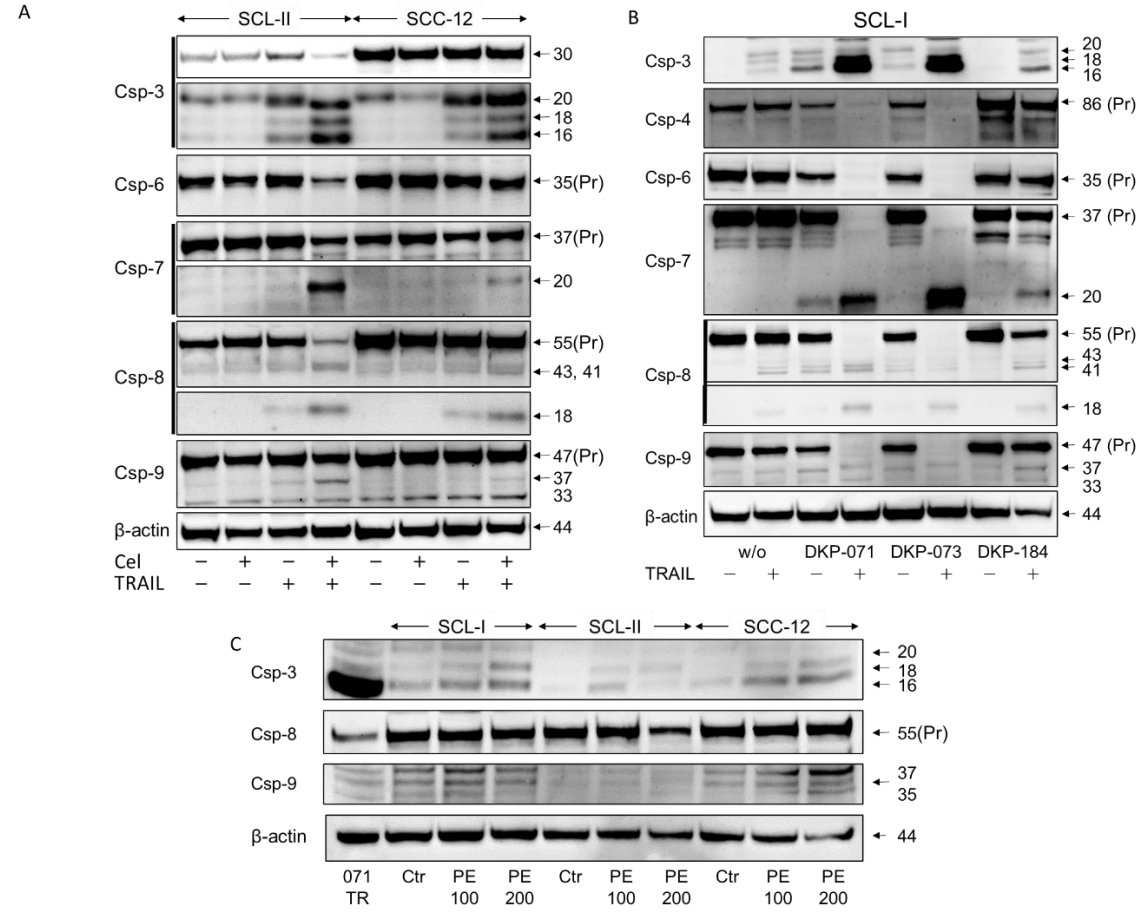

Figure 5. Enhanced caspase activation in course of combined treatment. (A) Cells were treated for 24 h with celecoxib (50 μM) and/or TRAIL (50 ng/ml). (B) Cells were treated for 24 h with indirubin derivatives (DKP-071, -073 and -184, 10 μM), TRAIL (50 ng/mL) or the combinations. (C) Cells were treated for 24 h with PE (100, 200 μg/ml). For demonstrating full caspase-3 activation, a positive control is shown, (+) Ctr, consisting of SCC-12 cells treated with an indirubin derivative (DKP-071, 10 μM) / TRAIL (50 ng/mL). Proforms (P) as well as caspase cleavage products (C) of caspases were identified.

4. 5 Regulation of apoptosis and cell proliferation by characteristic mediators

To further investigate the mechanisms of the anti-tumor effects mediated by the three treatments in cSCC cells, the expression of several apoptotic and cell proliferation regulators was investigated.

Celecoxib can upregulate p21, the cell cycle inhibitor, in SCL-II and SCC-12 cell lines, indirubin derivatives in SCL-I and PE in SCL-I, SCL-II and SCC-12 cell lines (Figure 6A-C),

suggesting that celecoxib, indirubin derivatives and PE-mediated up-regulation of p21 exerts a specific effect in inhibiting cell proliferation.

Mcl-1, as the anti-apoptotic family members, was down-regulated by celecoxib alone in SCC-12, whereas in SCL-II both Mcl-1 and Bcl-w were down-regulated by combination treatment. The pro-apoptotic protein Puma and Bad were upregulated in both cell lines by celecoxib (Figure 6A). However, there was no significant change in the expression of Bcl-2, Bax and Bak proteins (data not shown).

As for indirubin derivatives, we found upregulation of the pro-apoptotic protein Puma in SCL-II and SCC-12, whereas, in SCC-12, anti-apoptotic Bcl-2 was downregulated (Figure 6B). In opposite, no significant changes were detected for Mcl-1 and Bcl-w or the Bax and Bak (for which the data not shown). As for PE, no significant changes were obtained for the Bcl-2 family members (data not shown).

As other anti-apoptotic factors, celecoxib downregulated cIAPs (survivin and XIAP) and cFLIP; indirubin derivatives downregulated the caspase-3 antagonist XIAP (Figure 6A-B). Additionally, survivin was downregulated by the combinations (data not shown)

The pan-caspase inhibitor QVD-Oph was applied to demonstrate the significance of caspase activation for the anti-tumor effects. In SCL-II and SCC-12, after treatment with celecoxib and TRAIL, QVD-Oph completely abrogated any caspase processing (Figure 8A) and apoptosis induction (Figure 8C), indicating the significant role of caspases in this setting.

As for indirubin derivatives, the effects mediated by the indirubin derivatives /TRAIL combination on cell viability and apoptosis were attenuated by QVD-Oph (Figure 8C). Meanwhile, the processing/activation of effector caspases-3, -6 and -7 by DKP-071/TRAIL treatment was abrogated by the pan-caspase inhibitor QVD-Oph (Figure 8B). However, QVD-Oph had no effects on the indirubin derivatives-mediated change of MMP and ROS (data not shown). These data suggested that caspases seem to contribute significantly to the indirubin

derivatives-mediated effects on apoptosis and cell viability, but they are not upstream of mitochondrial activation and ROS production.

Figure 6 Regulation of characteristic mediators of apoptosis and cell proliferation

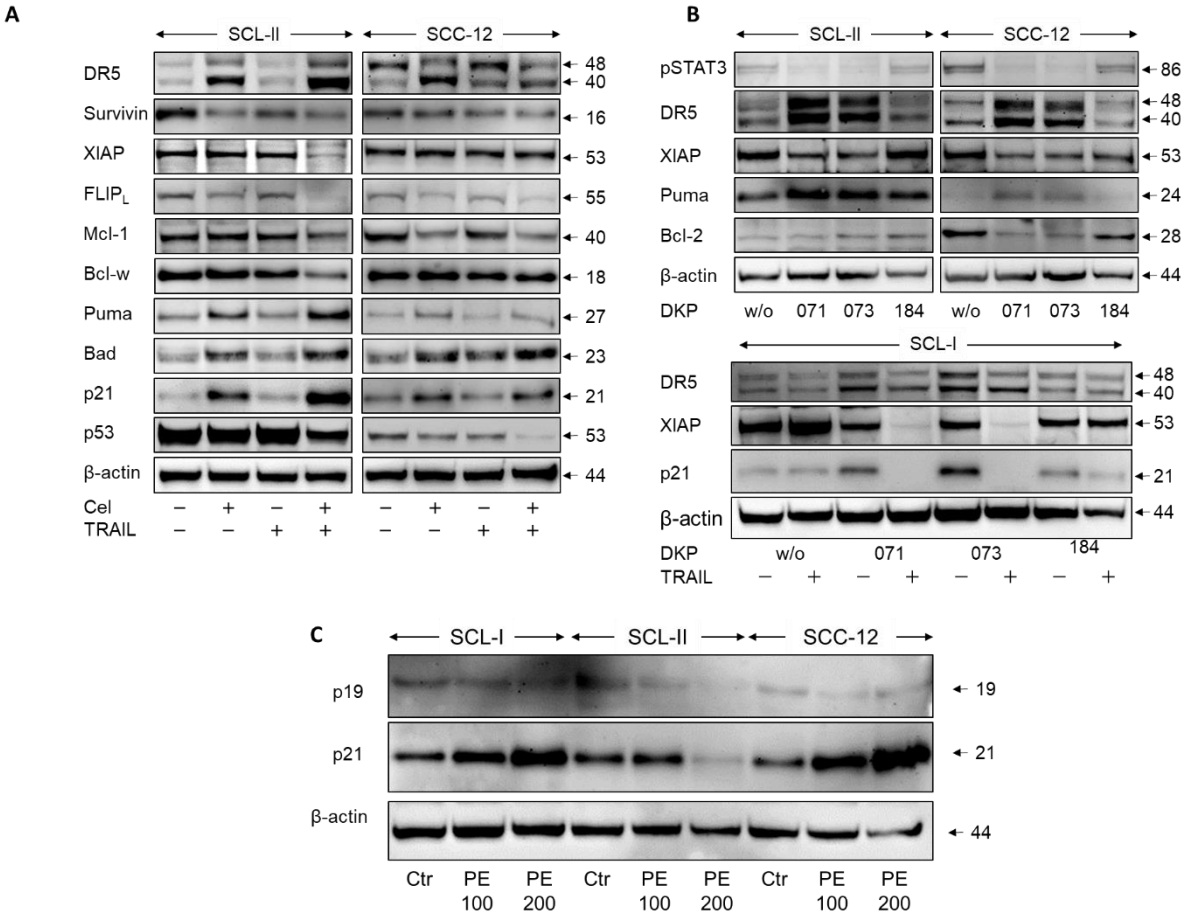

Figure 6. Regulation of characteristic mediators of apoptosis and cell proliferation. (A) Cell were treated for 24 h with celecoxib (50 μM), TRAIL (50 ng/ml) or the combination. (B) Cell were treated for 24 h with DKP-071, -073 and -184 at 10 μM, TRAIL (50 ng/mL) or the combinations. (C) Cell were treated for 24 h with PE (100, 200 μg/ml). Size of proteins (in kDa) is indicated on the right side, as determined in comparison to a protein size marker run in parallel. Analysis of β-actin served as loading control.

4. 6 Roles of ROS

In three treatments, the generation of ROS occurred at early or late phase, implying that ROS was related to the therapeutic mechanism of three drugs. Celecoxib induced ROS production at early time, for the lowest celecoxib concentration, the results were equivalent to H_2O_2, as a positive control (Figure 7A). The generation of high ROS seems to be a classic result of celecoxib. For indirubin derivatives, the induction of ROS production in cSCC cells was a very

common early effect. The percentage of cells with high ROS levels generally ranged from 60% to 90% after 4 h of indirubin derivatives treatment (Figure 7B).

It is well known that EGCG (a major component of polyphenol E) has antioxidant activity and is also frequently used as an antioxidant in clinical applications (56). In four cell lines, the reduction in ROS levels was an early response to PE treatment (100/200 μg/ml). The situation, however, reversed at 24 h, in response to PE, ROS levels were enhanced in SCL-II, SCC-12 and SCC-13 (Figure 7C).

In our previous work, antioxidant treatment can prevent ROS production, such as NAC or vitamin E, which could demonstrate the important role of ROS in apoptosis. However, this method failed in celecoxib-treated cells, neither NAC nor tocopherol or several other antioxidant treatments prevented celecoxib-induced ROS production. As a contrast, NAC reduce H_2O_2-induced ROS production (Figure 9A). Meanwhile, celecoxib-induced apoptosis could not be stopped by antioxidant pre-treatment, indicating that the ROS production induced by celecoxib was too strong to be inhibited.

As for indirubin derivatives, the strategy of applying antioxidants to inhibit ROS was successful in the treatment of indirubin derivatives. Pre-treatment with NAC (1 mM) for 1 h nearly abolished ROS production in all cell lines (Figure 9B), caused an almost complete restoration of cell viability and cell proliferation (Figure 9D) as well as abolished apoptosis (Figure 9C). Inhibition of ROS production also strongly affected the loss of MMP (Figure 9E). The activation of caspase cascade was completely abolished by NAC as well as pan-caspase inhibitor QVD-Oph. Interestingly, activation of caspase-8 was attenuated by NAC but not QVD-Oph (Figure 8B), indicating that activation of the promoter caspase-8 is downstream of ROS induction as well.

In addition, most of the other activation steps were found in reaction to indirubin derivatives treatment, such as downregulation of XIAP, survivin, appear to be downstream of ROS, as they

were also reversed by NAC pre-treatment (Figure 8B). It indicated that ROS is a major regulator of the role of indirubin derivatives in cSCC cells.

The same strategy was applied to evaluate the relationship between ROS and cell viability in response to PE, while NAC by itself had no effects on cell viability. Compared to PE treatment alone, it significantly enhanced the PE-mediated reduction in cell viability, when cells were treated with the combination of PE (100 μg/ml) and NAC (1 mM) (Figure 9F). A similar trend was observed in 24 h WST-1 (Figure 9G). It suggested that PE-mediated ROS imbalance contributes to its inhibitory effects.

Figure 7 – Variant regulation of ROS by different antagonists

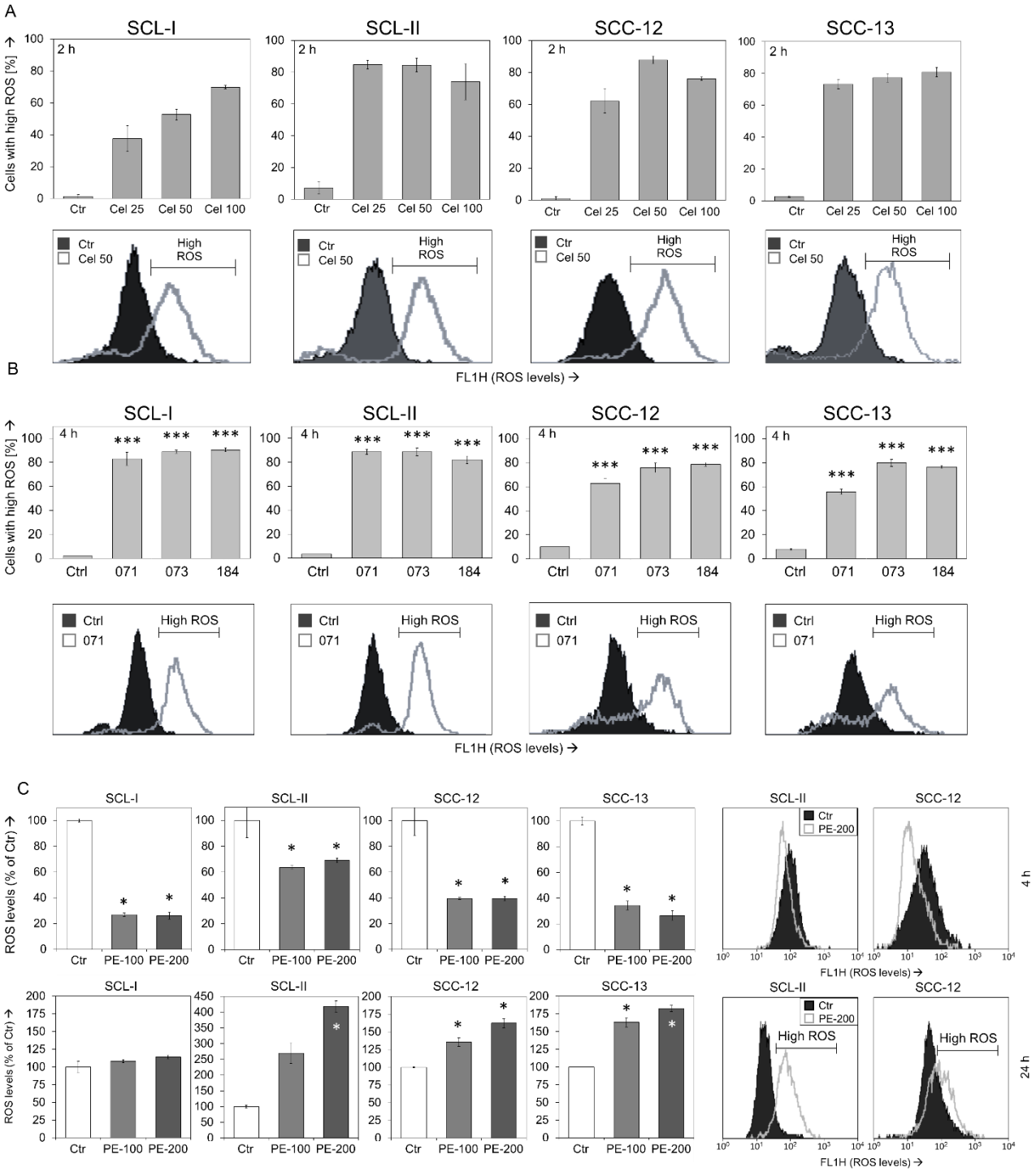

Figure 7. Variant regulation of ROS by different antagonists. (A) Cells were treated for 2 h with increasing dose of celecoxib (25-100 µM). (B) Cells were treated for 4 h with DKP-071, -073 and -184 at 10 µM. (C) Cells were treated for 4 h and 24 h with PE (100, 200 µg/ml).

Figure 8 – Effects of caspase inhibition

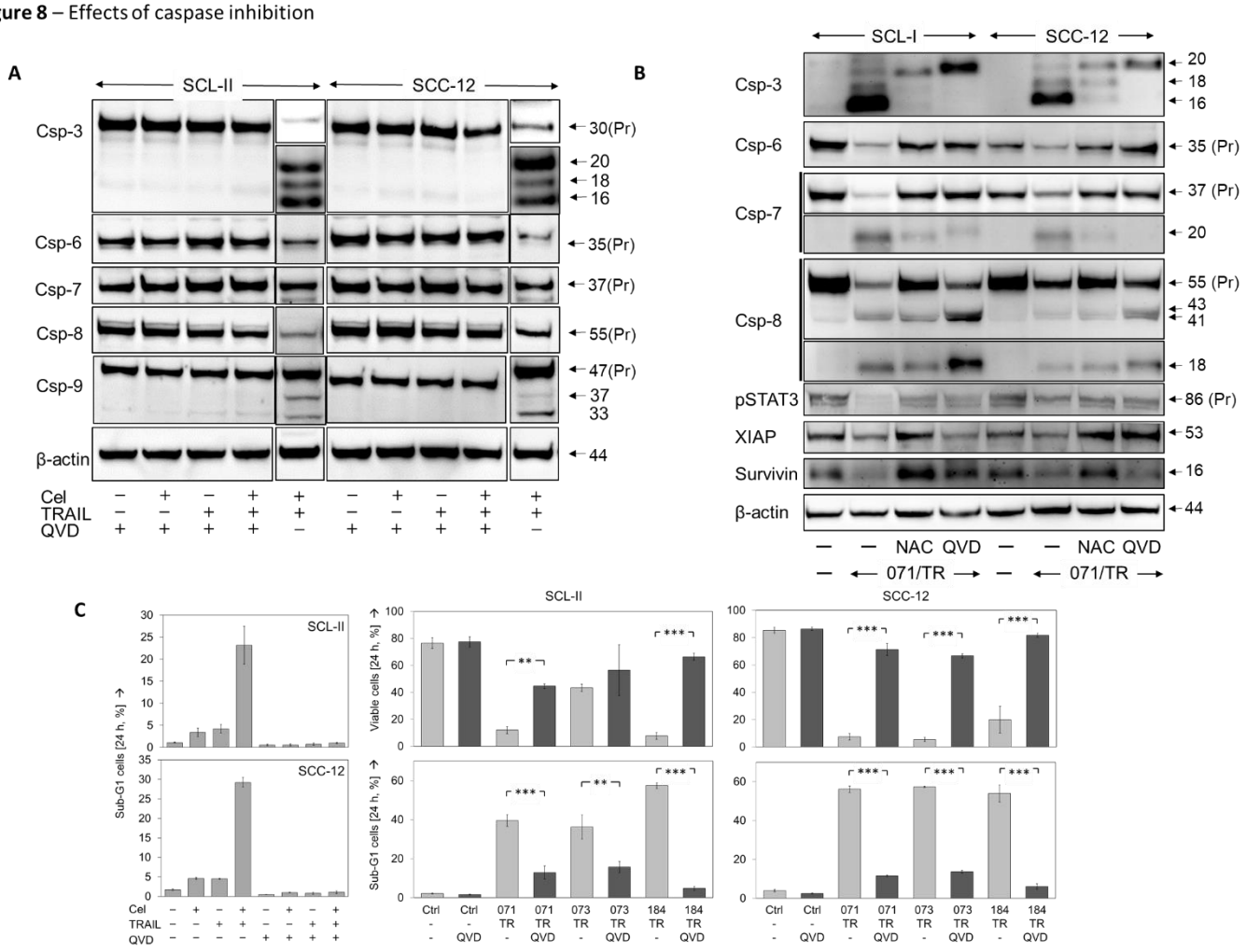

Figure 8. – Effects of caspase inhibition. (A) Cells were treated for 24 h with celecoxib (50 μM), TRAIL (50 ng/ml) or the combination. In addition, cells received the QVD (10 μM) at 1 h before other treatments started. (B) Cells received pretreatment for 1 h with NAC (1 mM) or QVD (10 μM), followed by combination of DKP-071 (071; 10 μM) and TRAIL (TR; 50 ng/mL). Proteins had been extracted at 24 h of treatment. Size of proteins (in kDa) is indicated on the right side. Expression of β-actin is shown as loading control. (C) Apoptosis was determined at 24 h by cell cycle analysis Cell viability was determined by calcein-AM staining. As for celecoxib, cells were treated for 24 h with celecoxib (50 μM), TRAIL (50 ng/ml) or the combination. As for indirubin derivatives, cells were treated with combinations of 071/TRAIL, 073/TRAIL and 184/TRAIL.

Figure 9 Antagonistic effects of NAC .

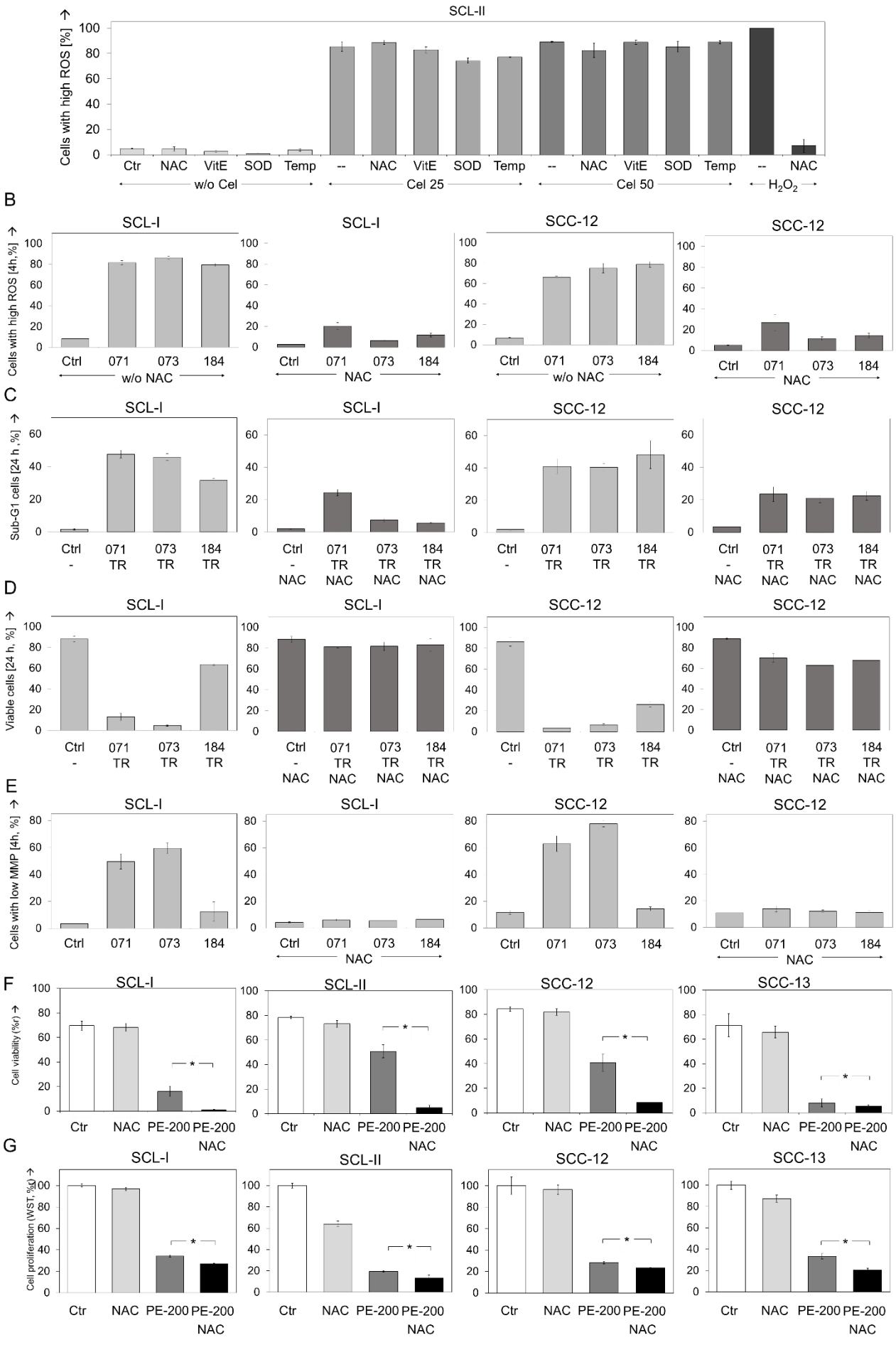

Figure 9. Antagonistic effects of NAC. (A) ROS levels were determined by H_2DCFDA staining. Treatment with different antioxydative strategies was shown in SCL-II in addition to celecoxib treatment (25 and 50 µM): NAC, Nacetyl cysteine [1 mM]; VitE, tocopherol [1 mM]; Glut, glutathion, [1 mM]; Temp, Tempol [1 mM]. Antioxydants were generally applied at 1 h before celecoxib. (B) ROS production, cells were treated with indirubin derivatives (DKP-071, -073 and -184; 10 µM). (C) Apoptosis was determined at 24 h by cell cycle analysis Cells were treated with combinations of indirubin derivatives (DKP-071, -073 and -184 at 10 µM) and TRAIL (TR; 50 ng/mL) (D) Cell viability was determined by calcein-AM staining in cell lines at 24 h in response to the combinations of indirubin derivatives (DKP-071, -073 and -184 at 10 µM) and TRAIL (TR; 50 ng/mL). (E) Loss of MMP was investigated at 4 h in response to indirubin derivatives (DKP-071, -073 and -184 at 10 µM). (F) Cells were treated with PE (200 µg/ml) +/- NAC (1 mM), as indicated. Cell viability was determined at 24 h of treatment by calcein-AM staining. Values represent the percentage of cells with high calcein staining (viable cells). (G) Cells were treated with PE (100 µg/ml) +/- 1 mM NAC, as indicated. Cell proliferation rates were determined by WST-1 assay.

5. Discussion

Among skin cancers, cSCC has the second highest incidence. The incidence of carcinoma in situ of cSCC, AK, is even higher. However, conventional treatment of AK is not sufficient to stop its progression (57), which makes the treatment of cSCC and AK more difficult and thus represents serious health problems worldwide.

5. 1 Celecoxib

Celecoxib has been use as an anti-inflammatory, antipyretic and analgesic drug in clinical (58). In recent years, its anti-tumor potential has been investigated and its anti-cancer cell growth and metastasis inhibitory effects have been validated both *in vitro* and *in vivo* experiments (59-62). It was suggested that celecoxib may prevent the progression from AK to cSCC progression (63).

5. 2 Indirubin derivatives and Sinecatechins

Natural compounds have been considered as a rich source of biologically active principles that may target abnormally activated signalling pathways and other modalities of cancer cells. Because natural compounds often have few or no side effects, they may be often involved in first- and second-line chemotherapy through limiting painful side effects. Therefore, natural compounds or plant extracts have received attention in the development of new drugs for treatment of cancer (64). Hence, we investigated the mechanisms of two natural compounds and plant extracts in treatment of cSCC cells, indirubin derivatives and sinecatechins. Indirubin derivatives' anti-tumor activity was also verified by clinical trials in chronic myeloid leukaemia, chronic granulocytic leukaemia, head and neck cancer, without serious toxic side effects (29, 30, 65). Sinecatechins has long been used in clinical applications and it has also been suggested for the treatment of AK (34).

5. 3 Enhanced anti-tumor effects in combinations with TRAIL

Traditional single-drug and single-target therapies often have limited efficacy due to the presence of adverse effects and drug resistance (66). Combination therapies, however, can counteract bio buffering, overcome limited efficacy, drug resistance and reduce unwanted off-target effects (67, 68). In combinations, the efficiency of celecoxib can be improved, as in the combination with histone deacetylase inhibitors and Plumbagin in non-Hodgkin's lymphoma and melanoma cells, respectively (69, 70). Improved response to chemotherapy was also obtained in combinations with celecoxib (71, 72). In this research, it was shown that the use of celecoxib alone leads to a limited effect on apoptosis and cell viability. However, when combined with death ligands, apoptosis was enhanced and cell viability was decreased. Compared to celecoxib, indirubin derivatives were able to induce partial apoptosis and loss of activity. But the effect of indirubin derivatives was strongly enhanced when they were combined with the death ligand TRAIL. Enhancing death ligand-induced apoptosis by celecoxib and indirubin derivatives enhance the immune response of patients to cSCC. This combination has also been shown to be effective in other tumour cells. For example, the combination of celecoxib and TRAIL has shown promising therapeutic results in non-small cell lung cancer, colon cancer and glioblastoma (73-75). Indirubin derivatives and TRAIL in melanoma (53), breast and bladder cancer cell lines (76). Thus, the combination with TRAIL or TRAIL receptor agonists may greatly improve the efficiency of celecoxib and indirubin derivatives.

5. 4 Caspase activation

Celecoxib alone did not affect apoptosis, whereas indirubin derivatives could induce weak activation of caspase-cascade. Interestingly, both drugs have a stronger activation of the pro-apoptotic caspase cascade when used in combination with TRAIL. Because of the strong activation of caspase cascade by celecoxib/TRAIL and indirubin derivatives/TRAIL, we

applied caspase inhibitors to assess the extent of caspase cascade involvement, which nearly completely abrogated apoptosis induced by indirubin derivatives and two combinations.

Pro-apoptotic caspase cascade can also be blocked by cIAPs and c-FLIP (77, 78). We showed that celecoxib downregulates c-FLIP and survivin in cSCC cells, while XIAP was downregulated by the combination treatment in one cell line. Indirubin derivatives showed significant downregulation of XIAP and survivin as well. PE, however, had no significant regulatory effect on cIAPs. Thus, the downregulation of XIAP and survivin seen in cSCC cells may contribute to a strongly activated caspase cascade. The downregulation of caspase antagonists by indirubin derivatives and celecoxib has been observed in other different cancers, such as celecoxib in leukaemia, myeloma and non-small cell lung cancer cells (79-81). Indirubin derivatives are observed in melanoma, breast cancer, and CTCL cells (52, 53, 82).

However, in PE-treated cSCC cells, there was a significant inhibitory effect only at the level of cell proliferation and viability, and no significant effect on the induction of apoptosis. The same was seen in MCF-7 (37), which has a strong anti-proliferative effect but exhibited a weak effect on the induction of apoptosis. Contrary to our studies, however, the green tea component EGCG strongly induced apoptosis (40-70%) in lung cancer cells (H1299, A549)(36), gastric cancer cells (SGC7901) (35) and colorectal cancer cells (SW480, SW620, LS411N)(83). Thus, while green tea components strongly induced apoptosis in other cell types, this effect could be masked in cSCC cells by strongly decreased cell proliferation and cell viability. Only weak activation/processing of caspases (-3, -8 and -9) was seen with high concentrations of PE, which is consistent with their lower levels of apoptosis. Thus, the part of activation of caspases is involved in the mechanism of PE treatment of cSCC may not be critical. The delayed effect of the loss of MMP supports this interpretation.

5. 5 Upregulation of p21 and TRAIL receptor

The effects of the three drugs showed a high degree of polymorphism, with some of the investigated proteins being either up- or down-regulated. Treatment with three drugs showed a strong effects on the cell proliferation. The p21 is well known as a CDK inhibitor. The upregulation of p21 was found after treatment with three drugs, which explains the strong inhibition of proliferation, especially in PE, whose main feature is to affect cSCC cells by inhibiting cell activity and proliferative capacity rather than inducing apoptosis. In addition, similar reports on the same mechanism of PE have been reported in MCF-7 breast cancer cells, prostate cancer cells, and SCC-13 (84-86).

When celecoxib and indirubin derivatives were combined with TRAIL respectively, their anti-tumor effects were significantly enhanced. This may be due to celecoxib and indirubin derivatives could enhance the effectiveness of TRAIL. Therefore, the receptors of TRAIL were investigated as well. We found celecoxib and indirubin derivatives could upregulated TRAIL receptor-2 (DR5), which can increase the sensitivity of TRAIL and contributed to the combined anti-tumor effect. In non-small cell lung and hepatocellular carcinoma, the same mechanism was seen in the upregulation of DR5 by celecoxib, (81, 87). Indirubin derivatives in hepatoma, cervical, colon cancer and melanoma cells (53, 88, 89).

5. 6 Different roles of ROS

In this study, ROS played a specific role in the mechanism of each drug for cSCC. This study suggests that celecoxib and indirubin derivatives may affect both intrinsic and extrinsic apoptotic pathways in cSCC cells. How they regulate different regulators, of which ROS may serve as an explanation. Elevated ROS production in cancer has been shown to play a role in pro- and anti-tumor signalling. Increased levels of ROS promote sustained cell survival and proliferation through many pathways as well as inactivation of their downstream targets including Bad, Bax, Bim, Foxo and PTEN. Also elevated ROS production was associated with

inhibition of the JNK pathway (90). However, toxic levels of ROS in cells are known to cause cell death, as intrinsic apoptosis caused by the mitochondrial pathway and extrinsic apoptosis directed by activation of the death receptor pathway. Toxic levels of ROS lead to the release and translocation of cytochrome c into the cytoplasm, formed the complex of Apaf-1 and pro-caspase-9 that induces the activation of caspase-3 and 7, leading to apoptosis (46). On the other hand, high levels of ROS activates death ligands. Binding of TNFα ligands to the TNFR1 death receptor triggers activation of the promoter caspase-8. The promoter caspase-8 leads to the cleavage of caspase- 3. Activation of caspase-8 also induces cleavage of the Bcl-1 protein Bid to tBid and feeds back into the apoptotic pathway inherent in the release of cytochrome c (91). Here, we demonstrate that celecoxib produces large amounts of ROS in cSCC cells. The early appearance of ROS, even at moderate concentrations of celecoxib, at that time the apoptosis and loss of viability are not evident, indicating that ROS are upstream of other effects. Although ROS by themselves are not enough to trigger apoptosis, they, via death ligands, prepare cSCC cells for apoptosis induction. In melanoma and breast cancer cells, the induction of ROS during celecoxib treatment has been observed as well (92), and related studies have shown that celecoxib combined with 5-fluorouracil (5-FU) can inhibit AKT phosphorylation and reduce SCC cell proliferation in a dose-dependent manner by generating large amounts of ROS (93). Similarly, cSCC cells also produced large amounts of ROS after 4 h of treatment with the indirubin derivatives. ROS production appears to be a common mechanism for indirubin derivatives in skin cancer cells. We could found similar results from our previous projects (52, 53). In cSCC cells, indirubin derivatives-mediated highly polymorphic effects, including caspases, mitochondrial membrane potential, PKC, STAT3, p21, DR5 and Bcl-2 proteins. The important role of ROS in apoptosis could be demonstrated by antioxidant methods in the past (53, 94). The antioxidant NAC abrogated the pro-apoptotic effect of indirubin derivatives, restored cell viability and proliferation, and blocked the regulation of all protein expression induced by the indirubin derivatives, as well as all other effects. Our data suggested that ROS

is a key regulator of these pathways. Indeed, ROS production is upstream of other identified influence, but, in cSCC cells, celecoxib-induced ROS appears to be strong, and shows several features that cannot be prevented by several antioxidants. Therefore, a key role of ROS on celecoxib-induced apoptosis in cSCC cells has been proposed, which could not be conclusively proven. The effects of celecoxib and indirubin derivatives on ROS were significantly upregulated and subsequently exerted an anti-tumor effect, which was consistent with the ROS mechanism identified by previous work in our laboratory.

However, the effect of PE on cSCC cells was biphasic. In HepG2 hepatocellular carcinoma cells (95), primary lymphoma cells (96) and malignant mesothelioma cells (97) have also been reported in response to EGCG increased ROS levels. In all three reports, the induction of ROS was obtained later, within 24 hours. EGCG may exert both antioxidant and pro-oxidant activities. We hypothesise that PE inhibits cell proliferation and viability by decreasing ROS early. This hypothesis was supported by an additional antioxidant, N-acetylcysteine (NAC). Although NAC alone had no significant effect on cSCC viability, the combination of PE and NAC led to a further decrease in ROS and subsequent a strong further decrease in cell proliferation and viability. Inhibition of ROS production in tumor cells is likely to lead to inhibition of pro-tumorigenic signalling, resulting in reduced cell survival and proliferation, reduced metabolic adaptations and reduced levels of DNA damage and genetic instability (90). Manipulation of ROS levels can be used as a therapeutic target for cancer by increasing ROS production, leading to programmed cell death, or inhibiting ROS to suppress cell proliferation. The same mechanism of inhibition of cell proliferation through inhibition of ROS is also seen in Metformin, metformin causes apoptosis in pancreatic cancer by increasing protein expression of MnSOD/SOD2 and decreasing protein expression of NOX2 and NOX4 (98), which in turn inhibits NOX4-directed ROS production and leads to apoptosis via the AKT/apoptosis signal-regulated kinase 1 (ASK1) pathway (99). Studies in J. Stanicka's laboratory have shown that inhibition of the protein tyrosine kinase FLT3-ITD and inhibition of p22phox and NOX4

activity in AML cells, followed by inhibition of NOX4-directed ROS production, subsequently led to decreased cell survival and reduced DNA damage and genomic instability (43). These experiments inhibited tumor cell activity by suppressing ROS levels. Meanwhile, antioxidants inhibit tumor metastasis by scavenging ROS production in cancer. For example, overexpression of the antioxidant SOD3 reduced breast cancer metastasis *in vivo* (100). However, the application of antioxidants in cancer treatment is complicated, because some antioxidants including vitamins A, E and carotenoids are associated with an increased incidence of cancer. (101, 102).

5. 7 Conclusion

In conclusion, this study suggests that celecoxib, indirubin derivatives and PE might be promising candidates for the treatment of cSCC, provided they are also tolerated in vivo and clinically. In this study, ROS plays a crucial role in three treatments and we discussed two mechanisms for targeting ROS as a treatment for cSCC, although most of the ROS-induced signalling targets remain unknown. Enhancing ROS production to induce tumor cell death and inhibiting ROS levels or enhancing antioxidant capacity to supress pro-tumor signalling pathways. Building on these experiments, we can better understand the role of ROS production in cancer and identify specific ROS-targeted pathways that may help find more effective ways to treat cSCC in the future.

Reference list

1. Reinehr CPH, Bakos RM. Actinic keratoses: review of clinical, dermoscopic, and therapeutic aspects. An Bras Dermatol. 2019;94(6):637-57.
2. Stockfleth E. The importance of treating the field in actinic keratosis. J Eur Acad Dermatol Venereol. 2017;31 Suppl 2:8-11.
3. Cramer P, Stockfleth E. Actinic keratosis: where do we stand and where is the future going to take us? Expert Opin Emerg Dr. 2020;25(1):49-58.
4. Que SKT, Zwald FO, Schmults CD. Cutaneous squamous cell carcinoma: Incidence, risk factors, diagnosis, and staging. J Am Acad Dermatol. 2018;78(2):237-47.
5. Szewczyk M, Pazdrowski J, Golusinski P, Danczak-Pazdrowska A, Marszalek S, Golusinski W. Analysis of selected risk factors for nodal metastases in head and neck cutaneous squamous cell carcinoma. Eur Arch Otorhinolaryngol. 2015;272(10):3007-12.
6. Work G, Invited R, Kim JYS, Kozlow JH, Mittal B, Moyer J, Olenecki T, Rodgers P. Guidelines of care for the management of cutaneous squamous cell carcinoma. J Am Acad Dermatol. 2018;78(3):560-78.
7. Corchado-Cobos R, Garcia-Sancha N, Gonzalez-Sarmiento R, Perez-Losada J, Canueto J. Cutaneous Squamous Cell Carcinoma: From Biology to Therapy. Int J Mol Sci. 2020;21(8).
8. Eberle J. Countering TRAIL Resistance in Melanoma. Cancers (Basel). 2019;11(5).
9. Hanahan D, Weinberg RA. Hallmarks of cancer: the next generation. Cell. 2011;144(5):646-74.
10. Ashkenazi A, Holland P, Eckhardt SG. Ligand-based targeting of apoptosis in cancer: the potential of recombinant human apoptosis ligand 2/Tumor necrosis factor-related apoptosis-inducing ligand (rhApo2L/TRAIL). J Clin Oncol. 2008;26(21):3621-30.
11. Walczak H, Miller RE, Ariail K, Gliniak B, Griffith TS, Kubin M, Chin W, Jones J, Woodward A, Le T, Smith C, Smolak P, Goodwin RG, Rauch CT, Schuh JC, Lynch DH. Tumoricidal activity of tumor necrosis factor-related apoptosis-inducing ligand in vivo. Nat Med. 1999;5(2):157-63.
12. Krammer PH, Arnold R, Lavrik IN. Life and death in peripheral T cells. Nat Rev Immunol. 2007;7(7):532-42.
13. Fischer U, Janicke RU, Schulze-Osthoff K. Many cuts to ruin: a comprehensive update of caspase substrates. Cell Death Differ. 2003;10(1):76-100.
14. Chipuk JE, Moldoveanu T, Llambi F, Parsons MJ, Green DR. The BCL-2 family reunion. Mol Cell. 2010;37(3):299-310.
15. Galluzzi L, Vitale I, Aaronson SA, Abrams JM, Adam D, Agostinis P, Alnemri ES, Altucci L, Amelio I, Andrews DW, Annicchiarico-Petruzzelli M, Antonov AV, Arama E, Baehrecke EH, Barlev NA, Bazan NG, Bernassola F, Bertrand MJM, Bianchi K, Blagosklonny MV, Blomgren K, Borner C, Boya P, Brenner C, Campanella M, Candi E, Carmona-Gutierrez D, Cecconi F, Chan FK, Chandel NS, Cheng EH, Chipuk JE, Cidlowski JA, Ciechanover A, Cohen GM, Conrad M, Cubillos-Ruiz JR, Czabotar PE, D'Angiolella V, Dawson TM, Dawson VL, De Laurenzi V, De Maria R, Debatin KM, DeBerardinis RJ, Deshmukh M, Di Daniele N, Di Virgilio F, Dixit VM, Dixon SJ, Duckett CS, Dynlacht BD, El-Deiry WS, Elrod JW, Fimia GM, Fulda S, Garcia-Saez AJ, Garg AD, Garrido C, Gavathiotis E, Golstein P, Gottlieb E, Green DR, Greene LA, Gronemeyer H, Gross A, Hajnoczky G, Hardwick JM, Harris IS, Hengartner MO, Hetz C, Ichijo H, Jaattela M, Joseph B, Jost PJ, Juin PP, Kaiser WJ, Karin M, Kaufmann T, Kepp O, Kimchi A, Kitsis RN, Klionsky DJ, Knight RA, Kumar S, Lee SW, Lemasters JJ, Levine B, Linkermann A, Lipton SA, Lockshin RA, Lopez-Otin C, Lowe SW, Luedde T, Lugli E, MacFarlane M, Madeo F, Malewicz M, Malorni W, Manic G, Marine JC, Martin SJ, Martinou JC, Medema JP, Mehlen P, Meier P, Melino S, Miao EA, Molkentin JD, Moll UM, Munoz-Pinedo C, Nagata S, Nunez G, Oberst A, Oren M, Overholtzer M, Pagano M, Panaretakis T, Pasparakis M, Penninger JM, Pereira DM, Pervaiz S, Peter ME, Piacentini M, Pinton P, Prehn JHM, Puthalakath H, Rabinovich GA, Rehm M, Rizzuto R, Rodrigues CMP, Rubinsztein DC, Rudel T, Ryan KM, Sayan E, Scorrano L, Shao F, Shi Y, Silke J, Simon HU, Sistigu

A, Stockwell BR, Strasser A, Szabadkai G, Tait SWG, Tang D, Tavernarakis N, Thorburn A, Tsujimoto Y, Turk B, Vanden Berghe T, Vandenabeele P, Vander Heiden MG, Villunger A, Virgin HW, Vousden KH, Vucic D, Wagner EF, Walczak H, Wallach D, Wang Y, Wells JA, Wood W, Yuan J, Zakeri Z, Zhivotovsky B, Zitvogel L, Melino G, Kroemer G. Molecular mechanisms of cell death: recommendations of the Nomenclature Committee on Cell Death 2018. Cell Death Differ. 2018;25(3):486-541.
16. Roufayel R, Mezher R, Storey KB. The Role of Retinoblastoma Protein in Cell Cycle Regulation: An Updated Review. Curr Mol Med. 2021;21(8):620-9.
17. Roy A, Banerjee S. p27 and leukemia: cell cycle and beyond. J Cell Physiol. 2015;230(3):504-9.
18. Li J, Poi MJ, Tsai MD. Regulatory mechanisms of tumor suppressor P16(INK4A) and their relevance to cancer. Biochemistry. 2011;50(25):5566-82.
19. Varra V, Woody NM, Reddy C, Joshi NP, Geiger J, Adelstein DJ, Burkey BB, Scharpf J, Prendes B, Lamarre ED, Lorenz R, Gastman B, Manyam BV, Koyfman SA. Suboptimal Outcomes in Cutaneous Squamous Cell Cancer of the Head and Neck with Nodal Metastases. Anticancer Res. 2018;38(10):5825-30.
20. Schmults CD, Karia PS, Carter JB, Han J, Qureshi AA. Factors predictive of recurrence and death from cutaneous squamous cell carcinoma: a 10-year, single-institution cohort study. JAMA Dermatol. 2013;149(5):541-7.
21. Rong Y, Zuo L, Shang L, Bazan JG. Radiotherapy treatment for nonmelanoma skin cancer. Expert Rev Anticancer Ther. 2015;15(7):765-76.
22. Gurram B, Zhang S, Li M, Li H, Xie Y, Cui H, Du J, Fan J, Wang J, Peng X. Celecoxib Conjugated Fluorescent Probe for Identification and Discrimination of Cyclooxygenase-2 Enzyme in Cancer Cells. Anal Chem. 2018;90(8):5187-93.
23. Grosch S, Maier TJ, Schiffmann S, Geisslinger G. Cyclooxygenase-2 (COX-2)-independent anticarcinogenic effects of selective COX-2 inhibitors. J Natl Cancer Inst. 2006;98(11):736-47.
24. Arber N, Eagle CJ, Spicak J, Racz I, Dite P, Hajer J, Zavoral M, Lechuga MJ, Gerletti P, Tang J, Rosenstein RB, Macdonald K, Bhadra P, Fowler R, Wittes J, Zauber AG, Solomon SD, Levin B, Pre SAPTI. Celecoxib for the prevention of colorectal adenomatous polyps. N Engl J Med. 2006;355(9):885-95.
25. Thompson PA, Ashbeck EL, Roe DJ, Fales L, Buckmeier J, Wang F, Bhattacharyya A, Hsu CH, Chow SH, Ahnen DJ, Boland CR, Heigh RI, Fay DE, Hamilton SR, Jacobs ET, Martinez EM, Alberts DS, Lance P. Celecoxib for the Prevention of Colorectal Adenomas: Results of a Suspended Randomized Controlled Trial. J Natl Cancer Inst. 2016;108(12).
26. Gallouet AS, Travert M, Bresson-Bepoldin L, Guilloton F, Pangault C, Caulet-Maugendre S, Lamy T, Tarte K, Guillaudeux T. COX-2-independent effects of celecoxib sensitize lymphoma B cells to TRAIL-mediated apoptosis. Clin Cancer Res. 2014;20(10):2663-73.
27. Xu XT, Hu WT, Zhou JY, Tu Y. Celecoxib enhances the radiosensitivity of HCT116 cells in a COX-2 independent manner by up-regulating BCCIP. Am J Transl Res. 2017;9(3):1088-100.
28. Grosch S, Tegeder I, Niederberger E, Brautigam L, Geisslinger G. COX-2 independent induction of cell cycle arrest and apoptosis in colon cancer cells by the selective COX-2 inhibitor celecoxib. FASEB J. 2001;15(14):2742-4.
29. Blazevic T, Heiss EH, Atanasov AG, Breuss JM, Dirsch VM, Uhrin P. Indirubin and Indirubin Derivatives for Counteracting Proliferative Diseases. Evid Based Complement Alternat Med. 2015;2015:654098.
30. Xiao Z, Hao Y, Liu B, Qian L. Indirubin and meisoindigo in the treatment of chronic myelogenous leukemia in China. Leuk Lymphoma. 2002;43(9):1763-8.
31. Sun B, Wang J, Liu L, Mao L, Peng L, Wang Y. Synthesis and activity of novel indirubin derivatives. Chem Biol Drug Des. 2021;97(3):565-71.
32. Libnow S, Methling K, Hein M, Michalik D, Harms M, Wende K, Flemming A, Kockerling M, Reinke H, Bednarski PJ, Lalk M, Langer P. Synthesis of indirubin-N'-glycosides and their anti-proliferative activity against human cancer cell lines. Bioorg Med Chem. 2008;16(10):5570-83.

33. Erben F, Kleeblatt D, Sonneck M, Hein M, Feist H, Fahrenwaldt T, Fischer C, Matin A, Iqbal J, Plotz M, Eberle J, Langer P. Synthesis and antiproliferative activity of selenoindirubins and selenoindirubin-N-glycosides. Org Biomol Chem. 2013;11(24):3963-78.
34. Stockfleth E, Meyer T. Sinecatechins (Polyphenon E) ointment for treatment of external genital warts and possible future indications. Expert Opin Biol Ther. 2014;14(7):1033-43.
35. Fu JD, Yao JJ, Wang H, Cui WG, Leng J, Ding LY, Fan KY. Effects of EGCG on proliferation and apoptosis of gastric cancer SGC7901 cells via down-regulation of HIF-1alpha and VEGF under a hypoxic state. Eur Rev Med Pharmacol Sci. 2019;23(1):155-61.
36. Gu JJ, Qiao KS, Sun P, Chen P, Li Q. Study of EGCG induced apoptosis in lung cancer cells by inhibiting PI3K/Akt signaling pathway. Eur Rev Med Pharmacol Sci. 2018;22(14):4557-63.
37. Huang CY, Han Z, Li X, Xie HH, Zhu SS. Mechanism of EGCG promoting apoptosis of MCF-7 cell line in human breast cancer. Oncol Lett. 2017;14(3):3623-7.
38. Giorgio M, Trinei M, Migliaccio E, Pelicci PG. Hydrogen peroxide: a metabolic by-product or a common mediator of ageing signals? Nat Rev Mol Cell Bio. 2007;8(9):722a-8.
39. Zorov DB, Juhaszova M, Sollott SJ. Mitochondrial reactive oxygen species (ROS) and ROS-induced ROS release. Physiol Rev. 2014;94(3):909-50.
40. Park WH. Effects of antioxidants and MAPK inhibitors on cell death and reactive oxygen species levels in H2O2-treated human pulmonary fibroblasts. Oncol Lett. 2013;5(5):1633-8.
41. Liou GY, Storz P. Reactive oxygen species in cancer. Free Radic Res. 2010;44(5):479-96.
42. Roy K, Wu Y, Meitzler JL, Juhasz A, Liu H, Jiang G, Lu J, Antony S, Doroshow JH. NADPH oxidases and cancer. Clin Sci (Lond). 2015;128(12):863-75.
43. Stanicka J, Russell EG, Woolley JF, Cotter TG. NADPH oxidase-generated hydrogen peroxide induces DNA damage in mutant FLT3-expressing leukemia cells. J Biol Chem. 2015;290(15):9348-61.
44. Ames BN, Shigenaga MK, Hagen TM. Oxidants, antioxidants, and the degenerative diseases of aging. Proc Natl Acad Sci U S A. 1993;90(17):7915-22.
45. Szatrowski TP, Nathan CF. Production of large amounts of hydrogen peroxide by human tumor cells. Cancer Res. 1991;51(3):794-8.
46. Sabharwal SS, Schumacker PT. Mitochondrial ROS in cancer: initiators, amplifiers or an Achilles' heel? Nat Rev Cancer. 2014;14(11):709-21.
47. Moloney JN, Stanicka J, Cotter TG. Subcellular localization of the FLT3-ITD oncogene plays a significant role in the production of NOX- and p22(phox)-derived reactive oxygen species in acute myeloid leukemia. Leuk Res. 2017;52:34-42.
48. Gorrini C, Harris IS, Mak TW. Modulation of oxidative stress as an anticancer strategy. Nat Rev Drug Discov. 2013;12(12):931-47.
49. Ichijo H, Nishida E, Irie K, ten Dijke P, Saitoh M, Moriguchi T, Takagi M, Matsumoto K, Miyazono K, Gotoh Y. Induction of apoptosis by ASK1, a mammalian MAPKKK that activates SAPK/JNK and p38 signaling pathways. Science. 1997;275(5296):90-4.
50. Moon DO, Kim MO, Choi YH, Hyun JW, Chang WY, Kim GY. Butein induces G(2)/M phase arrest and apoptosis in human hepatoma cancer cells through ROS generation. Cancer Letters. 2010;288(2):204-13.
51. Pelicano H, Carney D, Huang P. ROS stress in cancer cells and therapeutic implications. Drug Resist Updat. 2004;7(2):97-110.
52. Soltan MY, Sumarni U, Assaf C, Langer P, Reidel U, Eberle J. Key Role of Reactive Oxygen Species (ROS) in Indirubin Derivative-Induced Cell Death in Cutaneous T-Cell Lymphoma Cells. Int J Mol Sci. 2019;20(5).
53. Zhivkova V, Kiecker F, Langer P, Eberle J. Crucial role of reactive oxygen species (ROS) for the proapoptotic effects of indirubin derivative DKP-073 in melanoma cells. Mol Carcinog. 2019;58(2):258-69.
54. Quast SA, Berger A, Eberle J. ROS-dependent phosphorylation of Bax by wortmannin sensitizes melanoma cells for TRAIL-induced apoptosis. Cell Death Dis. 2013;4:e839.

55. Kleeblatt D, Becker M, Plotz M, Schonherr M, Villinger A, Hein M, Eberle J, Kunz M, Rahman Q, Langer P. Synthesis and bioactivity of N-glycosylated 3-(2-oxo-2-arylethylidene)-indolin-2-ones. Rsc Adv. 2015;5(27):20769-82.
56. Khan N, Mukhtar H. Tea Polyphenols in Promotion of Human Health. Nutrients. 2018;11(1).
57. Rosenberg AR, Tabacchi M, Ngo KH, Wallendorf M, Rosman IS, Cornelius LA, Demehri S. Skin cancer precursor immunotherapy for squamous cell carcinoma prevention. JCI Insight. 2019;4(6).
58. Toloczko-Iwaniuk N, Dziemianczyk-Pakiela D, Nowaszewska BK, Celinska-Janowicz K, Miltyk W. Celecoxib in Cancer Therapy and Prevention - Review. Curr Drug Targets. 2019;20(3):302-15.
59. Rosas C, Sinning M, Ferreira A, Fuenzalida M, Lemus D. Celecoxib decreases growth and angiogenesis and promotes apoptosis in a tumor cell line resistant to chemotherapy. Biol Res. 2014;47:27.
60. Ghanghas P, Jain S, Rana C, Sanyal SN. Chemoprevention of Colon Cancer through Inhibition of Angiogenesis and Induction of Apoptosis by Nonsteroidal Anti-Inflammatory Drugs. J Environ Pathol Toxicol Oncol. 2016;35(3):273-89.
61. Li WW, Long GX, Liu DB, Mei Q, Wang JF, Hu GY, Jiang JZ, Sun W, Gan L, Hu GQ. Cyclooxygenase-2 inhibitor celecoxib suppresses invasion and migration of nasopharyngeal carcinoma cell lines through a decrease in matrix metalloproteinase-2 and -9 activity. Pharmazie. 2014;69(2):132-7.
62. Wang LW, Hsiao CF, Chen WT, Lee HH, Lin TC, Chen HC, Chen HH, Chien CR, Lin TY, Liu TW. Celecoxib plus chemoradiotherapy for locally advanced rectal cancer: a phase II TCOG study. J Surg Oncol. 2014;109(6):580-5.
63. Elmets CA, Viner JL, Pentland AP, Cantrell W, Lin HY, Bailey H, Kang S, Linden KG, Heffernan M, Duvic M, Richmond E, Elewski BE, Umar A, Bell W, Gordon GB. Chemoprevention of nonmelanoma skin cancer with celecoxib: a randomized, double-blind, placebo-controlled trial. J Natl Cancer Inst. 2010;102(24):1835-44.
64. Das PK, Zahan T, Abdur Rakib M, Khanam JA, Pillai S, Islam F. Natural Compounds Targeting Cancer Stem Cells: A Promising Resource for Chemotherapy. Anticancer Agents Med Chem. 2019;19(15):1796-808.
65. You WC, Hsieh CC, Huang JT. Effect of extracts from indigowood root (Isatis indigotica Fort.) on immune responses in radiation-induced mucositis. J Altern Complement Med. 2009;15(7):771-8.
66. Spiro Z, Kovacs IA, Csermely P. Drug-therapy networks and the prediction of novel drug targets. J Biol. 2008;7(6):20.
67. Lecca P, Priami C. Biological network inference for drug discovery. Drug Discov Today. 2013;18(5-6):256-64.
68. Lotsch J, Geisslinger G. Low-dose drug combinations along molecular pathways could maximize therapeutic effectiveness while minimizing collateral adverse effects. Drug Discov Today. 2011;16(23-24):1001-6.
69. Torres-Collado AX, Jazirehi AR. Overcoming Resistance of Human Non-Hodgkin's Lymphoma to CD19-CAR CTL Therapy by Celecoxib and Histone Deacetylase Inhibitors. Cancers (Basel). 2018;10(6).
70. Gowda R, Sharma A, Robertson GP. Synergistic inhibitory effects of Celecoxib and Plumbagin on melanoma tumor growth. Cancer Lett. 2017;385:243-50.
71. Guo Q, Li Q, Wang J, Liu M, Wang Y, Chen Z, Ye Y, Guan Q, Zhou Y. A comprehensive evaluation of clinical efficacy and safety of celecoxib in combination with chemotherapy in metastatic or postoperative recurrent gastric cancer patients: A preliminary, three-center, clinical trial study. Medicine (Baltimore). 2019;98(27):e16234.
72. Perroud HA, Rico MJ, Alasino CM, Queralt F, Mainetti LE, Pezzotto SM, Rozados VR, Scharovsky OG. Safety and therapeutic effect of metronomic chemotherapy with cyclophosphamide and celecoxib in advanced breast cancer patients. Future Oncol. 2013;9(3):451-62.
73. Liu X, Yue P, Zhou Z, Khuri FR, Sun SY. Death receptor regulation and celecoxib-induced apoptosis in human lung cancer cells. J Natl Cancer Inst. 2004;96(23):1769-80.

74. Edagawa M, Kawauchi J, Hirata M, Goshima H, Inoue M, Okamoto T, Murakami A, Maehara Y, Kitajima S. Role of activating transcription factor 3 (ATF3) in endoplasmic reticulum (ER) stress-induced sensitization of p53-deficient human colon cancer cells to tumor necrosis factor (TNF)-related apoptosis-inducing ligand (TRAIL)-mediated apoptosis through up-regulation of death receptor 5 (DR5) by zerumbone and celecoxib. J Biol Chem. 2014;289(31):21544-61.
75. van Roosmalen IAM, Reis CR, Setroikromo R, Yuvaraj S, Joseph JV, Tepper PG, Kruyt FAE, Quax WJ. The ER stress inducer DMC enhances TRAIL-induced apoptosis in glioblastoma. Springerplus. 2014;3:495.
76. Braig S, Bischoff F, Abhari BA, Meijer L, Fulda S, Skaltsounis L, Vollmar AM. The pleiotropic profile of the indirubin derivative 6BIO overcomes TRAIL resistance in cancer. Biochem Pharmacol. 2014;91(2):157-67.
77. Irmler M, Thome M, Hahne M, Schneider P, Hofmann K, Steiner V, Bodmer JL, Schroter M, Burns K, Mattmann C, Rimoldi D, French LE, Tschopp J. Inhibition of death receptor signals by cellular FLIP. Nature. 1997;388(6638):190-5.
78. Deveraux QL, Takahashi R, Salvesen GS, Reed JC. X-linked IAP is a direct inhibitor of cell-death proteases. Nature. 1997;388(6639):300-4.
79. Xu Y, Zhao YM, Huang H. [Celecoxib-induced apoptosis in acute promyelocytic leukemia cell line MR2 and its mechanism]. Zhejiang Da Xue Xue Bao Yi Xue Ban. 2007;36(4):319-24.
80. Zhang S, Suvannasankha A, Crean CD, White VL, Johnson A, Chen CS, Farag SS. OSU-03012, a novel celecoxib derivative, is cytotoxic to myeloma cells and acts through multiple mechanisms. Clin Cancer Res. 2007;13(16):4750-8.
81. Liu X, Yue P, Schonthal AH, Khuri FR, Sun SY. Cellular FLICE-inhibitory protein down-regulation contributes to celecoxib-induced apoptosis in human lung cancer cells. Cancer Res. 2006;66(23):11115-9.
82. Nam S, Buettner R, Turkson J, Kim D, Cheng JQ, Muehlbeyer S, Hippe F, Vatter S, Merz KH, Eisenbrand G, Jove R. Indirubin derivatives inhibit Stat3 signaling and induce apoptosis in human cancer cells. Proc Natl Acad Sci U S A. 2005;102(17):5998-6003.
83. Luo KW, Xia J, Cheng BH, Gao HC, Fu LW, Luo XL. Tea polyphenol EGCG inhibited colorectal-cancer-cell proliferation and migration via downregulation of STAT3. Gastroenterol Rep (Oxf). 2021;9(1):59-70.
84. Balasubramanian S, Adhikary G, Eckert RL. The Bmi-1 polycomb protein antagonizes the (-)-epigallocatechin-3-gallate-dependent suppression of skin cancer cell survival. Carcinogenesis. 2010;31(3):496-503.
85. Gupta S, Hussain T, Mukhtar H. Molecular pathway for (-)-epigallocatechin-3-gallate-induced cell cycle arrest and apoptosis of human prostate carcinoma cells. Arch Biochem Biophys. 2003;410(1):177-85.
86. Suganuma M, Okabe S, Kai Y, Sueoka N, Sueoka E, Fujiki H. Synergistic effects of (-)-epigallocatechin gallate with (-)-epicatechin, sulindac, or tamoxifen on cancer-preventive activity in the human lung cancer cell line PC-9. Cancer Res. 1999;59(1):44-7.
87. Yamanaka Y, Shiraki K, Inoue T, Miyashita K, Fuke H, Yamaguchi Y, Yamamoto N, Ito K, Sugimoto K, Nakano T. COX-2 inhibitors sensitize human hepatocellular carcinoma cells to TRAIL-induced apoptosis. Int J Mol Med. 2006;18(1):41-7.
88. Shi J, Shen HM. Critical role of Bid and Bax in indirubin-3'-monoxime-induced apoptosis in human cancer cells. Biochem Pharmacol. 2008;75(9):1729-42.
89. Berger A, Quast SA, Plotz M, Hein M, Kunz M, Langer P, Eberle J. Sensitization of melanoma cells for death ligand-induced apoptosis by an indirubin derivative--Enhancement of both extrinsic and intrinsic apoptosis pathways. Biochem Pharmacol. 2011;81(1):71-81.
90. Moloney JN, Cotter TG. ROS signalling in the biology of cancer. Semin Cell Dev Biol. 2018;80:50-64.
91. Fulda S, Debatin KM. Extrinsic versus intrinsic apoptosis pathways in anticancer chemotherapy. Oncogene. 2006;25(34):4798-811.

92. Pritchard R, Rodriguez-Enriquez S, Pacheco-Velazquez SC, Bortnik V, Moreno-Sanchez R, Ralph S. Celecoxib inhibits mitochondrial O2 consumption, promoting ROS dependent death of murine and human metastatic cancer cells via the apoptotic signalling pathway. Biochem Pharmacol. 2018;154:318-34.
93. Sung MW, Lee DY, Park SW, Oh SM, Choi JJ, Shin ES, Kwon SK, Ahn SH, Kim YH. Celecoxib enhances the inhibitory effect of 5-FU on human squamous cell carcinoma proliferation by ROS production. Laryngoscope. 2017;127(4):E117-E23.
94. Bauer D, Werth F, Nguyen HA, Kiecker F, Eberle J. Critical role of reactive oxygen species (ROS) for synergistic enhancement of apoptosis by vemurafenib and the potassium channel inhibitor TRAM-34 in melanoma cells. Cell Death Dis. 2017;8(2):e2594.
95. Khiewkamrop P, Phunsomboon P, Richert L, Pekthong D, Srisawang P. Epistructured catechins, EGCG and EC facilitate apoptosis induction through targeting de novo lipogenesis pathway in HepG2 cells. Cancer Cell Int. 2018;18:46.
96. Tsai CY, Chen CY, Chiou YH, Shyu HW, Lin KH, Chou MC, Huang MH, Wang YF. Epigallocatechin-3-Gallate Suppresses Human Herpesvirus 8 Replication and Induces ROS Leading to Apoptosis and Autophagy in Primary Effusion Lymphoma Cells. Int J Mol Sci. 2017;19(1).
97. Ranzato E, Martinotti S, Magnelli V, Murer B, Biffo S, Mutti L, Burlando B. Epigallocatechin-3-gallate induces mesothelioma cell death via H2 O2 -dependent T-type Ca2+ channel opening. J Cell Mol Med. 2012;16(11):2667-78.
98. Cheng G, Lanza-Jacoby S. Metformin decreases growth of pancreatic cancer cells by decreasing reactive oxygen species: Role of NOX4. Biochem Biophys Res Commun. 2015;465(1):41-6.
99. Mochizuki T, Furuta S, Mitsushita J, Shang WH, Ito M, Yokoo Y, Yamaura M, Ishizone S, Nakayama J, Konagai A, Hirose K, Kiyosawa K, Kamata T. Inhibition of NADPH oxidase 4 activates apoptosis via the AKT/apoptosis signal-regulating kinase 1 pathway in pancreatic cancer PANC-1 cells. Oncogene. 2006;25(26):3699-707.
100. Teoh-Fitzgerald ML, Fitzgerald MP, Zhong W, Askeland RW, Domann FE. Epigenetic reprogramming governs EcSOD expression during human mammary epithelial cell differentiation, tumorigenesis and metastasis. Oncogene. 2014;33(3):358-68.
101. Omenn GS, Goodman GE, Thornquist MD, Balmes J, Cullen MR, Glass A, Keogh JP, Meyskens FL, Valanis B, Williams JH, Barnhart S, Hammar S. Effects of a combination of beta carotene and vitamin A on lung cancer and cardiovascular disease. N Engl J Med. 1996;334(18):1150-5.
102. Klein EA, Thompson IM, Jr., Tangen CM, Crowley JJ, Lucia MS, Goodman PJ, Minasian LM, Ford LG, Parnes HL, Gaziano JM, Karp DD, Lieber MM, Walther PJ, Klotz L, Parsons JK, Chin JL, Darke AK, Lippman SM, Goodman GE, Meyskens FL, Jr., Baker LH. Vitamin E and the risk of prostate cancer: the Selenium and Vitamin E Cancer Prevention Trial (SELECT). JAMA. 2011;306(14):1549-56.

Statutory Declaration

“I, Jiaqi-Zhu, by personally signing this document in lieu of an oath, hereby affirm that I prepared the submitted dissertation on the topic: **Crucial Role of Reactive Oxygen Species for targeting of Cutaneous SCC Cells （Entscheidende Rolle Reaktiver Sauerstoffspezies für die bekämpfung von Kutanen SCC-Zellen）**, independently and without the support of third parties, and that I used no other sources and aids than those stated.
All parts which are based on the publications or presentations of other authors, either in letter or in spirit, are specified as such in accordance with the citing guidelines. The sections on methodology (in particular regarding practical work, laboratory regulations, statistical processing) and results (in particular regarding figures, charts and tables) are exclusively my responsibility.

Furthermore, I declare that I have correctly marked all of the data, the analyses, and the conclusions generated from data obtained in collaboration with other persons, and that I have correctly marked my own contribution and the contributions of other persons (cf. declaration of contribution). I have correctly marked all texts or parts of texts that were generated in collaboration with other persons.

My contributions to any publications to this dissertation correspond to those stated in the below joint declaration made together with the supervisor. All publications created within the scope of the dissertation comply with the guidelines of the ICMJE (International Committee of Medical Journal Editors; www.icmje.org) on authorship. In addition, I declare that I shall comply with the regulations of Charité – Universitätsmedizin Berlin on ensuring good scientific practice.

I declare that I have not yet submitted this dissertation in identical or similar form to another Faculty.

The significance of this statutory declaration and the consequences of a false statutory declaration under criminal law (Sections 156, 161 of the German Criminal Code) are known to me.”

Date Signature

Declaration of your own contribution to the publications

Jiaqi Zhu contributed the following to the below listed publications:

Publication 1: Zhu, J., May, S., Ulrich, C., Stockfleth, E., & Eberle, J, High ROS Production by Celecoxib and Enhanced Sensitivity for Death Ligand-Induced Apoptosis in Cutaneous SCC Cell Lines, International Journal of Molecular Sciences, 2021
Contribution:
This study was designed by Jürgen Eberle. Jiaqi Zhu investigated the changes of ROS, apoptosis, cell viability, mitochondrial membrane potential and performed the Western blotting. Jiaqi Zhu collected and analyzed the data, prepared the figures 5, 6 and 7. With the help of Jürgen Eberle, Jiaqi Zhu wrote the original draft. Finally, Jürgen Eberle and Jiaqi Zhu made the critical revisions of the manuscript.

Publication 2: Zhu, J., Langer, P., Ulrich, C., & Eberle, J., Crucial Role of Reactive Oxygen Species (ROS) for the Proapoptotic Effects of Indirubin Derivatives in Cutaneous SCC Cells, Antioxidants, 2021
Contribution:
This study was designed together by Jürgen Eberle and Jiaqi Zhu. Jiaqi Zhu investigated the changes of cell proliferation, ROS, apoptosis, cell viability, mitochondrial membrane potential and performed the Western blotting. Jiaqi Zhu collected and analyzed the data, prepared all the figures according to Jürgen Eberle's comments. With the help of Jürgen Eberle, Jiaqi Zhu wrote the original draft. Jürgen Eberle and Jiaqi Zhu made the critical revisions of the manuscript.

Publication 3: Zhu, J.; Gillissen, B.; Dang Tran, D.L.; May, S.; Ulrich, C.; Stockfleth, E.; Eberle, J, Inhibition of Cell Proliferation and Cell Viability by Sinecatechins in Cutaneous SCC Cells Is Related to an Imbalance of ROS and Loss of Mitochondrial Membrane Potential., Antioxidants, 2022
Contribution:
This study was designed by Jürgen Eberle. Jiaqi Zhu investigated the changes of cell proliferation, ROS, apoptosis, cell viability and performed the Western blotting. Jürgen Eberle and Jiaqi Zhu collected and analyzed the data. Jiaqi Zhu prepared figures 5, 6C and 6D according to Jürgen Eberle's comments. Jürgen Eberle, Bernd Gillissen and Jiaqi Zhu wrote the original draft. Jürgen Eberle and Jiaqi Zhu made the critical revisions of the manuscript.

_____
Signature, date and stamp of first supervising university professor / lecturer

_____
Signature of doctoral candidate

Auszug aus der Journal Summary List (1)

Journal Data Filtered By: **Selected JCR Year: 2019** Selected Editions: SCIE,SSCI Selected Categories: **"BIOCHEMISTRY and MOLECULAR BIOLOGY"** Selected Category Scheme: WoS

Gesamtanzahl: 297 Journale

Rank	Full Journal Title	Total Cites	Journal Impact Factor	Eigenfactor Score
1	CELL	258,178	38.637	0.564970
2	NATURE MEDICINE	85,220	36.130	0.168730
3	Annual Review of Biochemistry	20,499	25.787	0.024820
4	MOLECULAR CELL	69,148	15.584	0.166260
5	Molecular Cancer	15,448	15.302	0.023990
6	PROGRESS IN LIPID RESEARCH	6,139	15.083	0.005730
7	TRENDS IN BIOCHEMICAL SCIENCES	18,416	14.732	0.032060
8	TRENDS IN MICROBIOLOGY	13,604	13.546	0.022780
9	Signal Transduction and Targeted Therapy	1,182	13.493	0.003380
10	Nature Chemical Biology	22,084	12.587	0.060130
11	MOLECULAR PSYCHIATRY	22,227	12.384	0.054730
12	Molecular Plant	11,432	12.084	0.028530
13	NATURAL PRODUCT REPORTS	11,239	12.000	0.013610
14	NATURE STRUCTURAL & MOLECULAR BIOLOGY	27,178	11.980	0.056800
15	NUCLEIC ACIDS RESEARCH	201,649	11.501	0.403470
16	TRENDS IN MOLECULAR MEDICINE	10,618	11.099	0.018720
17	GENOME RESEARCH	41,755	11.093	0.076940
18	MOLECULAR BIOLOGY AND EVOLUTION	50,486	11.062	0.084810
19	CELL DEATH AND DIFFERENTIATION	21,095	10.717	0.029600
20	Redox Biology	10,157	9.986	0.023810

Rank	Full Journal Title	Total Cites	Journal Impact Factor	Eigenfactor Score
21	EMBO JOURNAL	64,724	9.889	0.059690
22	CURRENT OPINION IN CHEMICAL BIOLOGY	10,968	9.689	0.017770
23	PLANT CELL	54,927	9.618	0.048640
24	CURRENT BIOLOGY	63,256	9.601	0.133170
25	MOLECULAR ASPECTS OF MEDICINE	6,207	9.577	0.005750
26	Molecular Systems Biology	8,914	8.991	0.017390
27	Cell Systems	3,822	8.673	0.029290
28	MATRIX BIOLOGY	6,878	8.572	0.011920
29	ONCOGENE	66,303	7.971	0.068320
30	Cell Chemical Biology	3,326	7.739	0.015770
31	CRITICAL REVIEWS IN BIOCHEMISTRY AND MOLECULAR BIOLOGY	3,675	7.634	0.006380
32	EMBO REPORTS	14,976	7.497	0.030290
33	BIOCHIMICA ET BIOPHYSICA ACTA-REVIEWS ON CANCER	5,650	7.365	0.007800
34	PLOS BIOLOGY	31,650	7.076	0.060300
35	Essays in Biochemistry	2,383	6.966	0.005060
36	CURRENT OPINION IN STRUCTURAL BIOLOGY	11,035	6.908	0.021890
37	CELLULAR AND MOLECULAR LIFE SCIENCES	26,128	6.496	0.037010
38	Science Signaling	12,736	6.467	0.026590
39	ANTIOXIDANTS & REDOX SIGNALING	21,119	6.323	0.024660
40	Molecular Ecology Resources	10,868	6.286	0.019630
41	FREE RADICAL BIOLOGY AND MEDICINE	42,665	6.170	0.036960
42	BIOMACROMOLECULES	38,863	6.092	0.031320

Selected JCR Year: 2019; Selected Categories: "BIOCHEMISTRY and MOLECULAR BIOLOGY"

Rank	Full Journal Title	Total Cites	Journal Impact Factor	Eigenfactor Score
43	Computational and Structural Biotechnology Journal	1,954	6.018	0.004980
44	CYTOKINE & GROWTH FACTOR REVIEWS	5,935	5.982	0.007380
45	Advances in Carbohydrate Chemistry and Biochemistry	634	5.800	0.000340
46	EXPERIMENTAL AND MOLECULAR MEDICINE	5,536	5.418	0.010300
47	AMERICAN JOURNAL OF RESPIRATORY CELL AND MOLECULAR BIOLOGY	12,243	5.373	0.016040
48	RNA Biology	6,589	5.350	0.015820
49	Acta Crystallographica Section D-Structural Biology	21,750	5.266	0.018220
50	MOLECULAR ECOLOGY	38,951	5.163	0.050800
51	INTERNATIONAL JOURNAL OF BIOLOGICAL MACROMOLECULES	47,121	5.162	0.057240
52	BIOCHEMICAL SOCIETY TRANSACTIONS	12,651	5.160	0.016140
53	HUMAN MOLECULAR GENETICS	39,652	5.100	0.064170
54	Journal of Genetics and Genomics	2,271	5.065	0.004310
55	Cell and Bioscience	1,898	5.026	0.004210
56	Antioxidants	2,568	5.014	0.004170
57	FASEB JOURNAL	43,126	4.966	0.043730
58	International Review of Cell and Molecular Biology	2,167	4.934	0.004350
59	Open Biology	2,886	4.931	0.009590
60	Journal of Integrative Plant Biology	5,005	4.885	0.006830
61	Advances in Microbial Physiology	1,227	4.875	0.000960
61	Nucleic Acid Therapeutics	1,030	4.875	0.003610

Selected JCR Year: 2019; Selected Categories: "BIOCHEMISTRY and MOLECULAR BIOLOGY"

Rank	Full Journal Title	Total Cites	Journal Impact Factor	Eigenfactor Score
63	JOURNAL OF NUTRITIONAL BIOCHEMISTRY	11,460	4.873	0.011150
64	STRUCTURE	15,145	4.862	0.026940
65	International Journal of Biological Sciences	6,262	4.858	0.009710
66	BIOORGANIC CHEMISTRY	5,712	4.831	0.006730
67	Genes & Diseases	1,081	4.803	0.003310
68	JOURNAL OF MOLECULAR BIOLOGY	56,952	4.760	0.040330
69	BIOFACTORS	3,769	4.734	0.002930
70	BIOELECTROCHEMISTRY	4,944	4.722	0.004950
71	Reviews of Physiology Biochemistry and Pharmacology	805	4.700	0.000670
72	JOURNAL OF ENZYME INHIBITION AND MEDICINAL CHEMISTRY	5,415	4.673	0.005420
73	BIOESSAYS	10,189	4.627	0.016560
74	INTERNATIONAL JOURNAL OF MOLECULAR SCIENCES	77,286	4.556	0.143760
75	APOPTOSIS	6,339	4.545	0.005660
76	BIOCHIMICA ET BIOPHYSICA ACTA-MOLECULAR AND CELL BIOLOGY OF LIPIDS	10,266	4.519	0.016350
77	ACS Chemical Neuroscience	6,881	4.486	0.015300
78	JOURNAL OF LIPID RESEARCH	24,223	4.483	0.022420
79	ACS Chemical Biology	12,884	4.434	0.035490
80	FEBS Journal	18,845	4.392	0.025250
81	JOURNAL OF PHOTOCHEMISTRY AND PHOTOBIOLOGY B-BIOLOGY	12,794	4.383	0.013640
82	BIOCHIMICA ET BIOPHYSICA ACTA-MOLECULAR BASIS OF DISEASE	15,965	4.352	0.024200

Selected JCR Year: 2019; Selected Categories: "BIOCHEMISTRY and MOLECULAR BIOLOGY"

Publication 1

International Journal of *Molecular Sciences*

MDPI

Article

High ROS Production by Celecoxib and Enhanced Sensitivity for Death Ligand-Induced Apoptosis in Cutaneous SCC Cell Lines

Jiaqi Zhu [1,2], Stefanie May [1], Claas Ulrich [1], Eggert Stockfleth [3] and Jürgen Eberle [1,*]

[1] Department of Dermatology, Venerology and Allergology, Skin Cancer Center, Charité Universitätsmedizin Berlin, 10117 Berlin, Germany; zhujiaqijiaqi@gmail.com (J.Z.); stefanie.may@charite.de (S.M.); Claas.Ulrich@charite.de (C.U.)
[2] Department of Gynecology and Obstetrics, Jilin University, Changchun 130012, China
[3] Department of Dermatologie, Venerologie und Allergologie, Klinikum Bochum, Ruhr-Universität Bochum, 44791 Bochum, Germany; e.stockfleth@klinikum-bochum.de
* Correspondence: juergen.eberle@charite.de; Tel.: +49-30-450-518-383

Abstract: Incidence of cutaneous squamous cell carcinoma (cSCC) and actinic keratosis has increased worldwide, and non-steroidal anti-inflammatory drugs as celecoxib are considered for treatment. We show here strong anti-proliferative effects of celecoxib in four cSCC cell lines, while apoptosis and cell viability largely remained unaffected. Impeded apoptosis was overcome in combinations with agonistic CD95 antibody or TNF-related apoptosis-inducing ligand (TRAIL), resulting in up to 60% apoptosis and almost complete loss of cell viability. Proapoptotic caspase cascades were activated, and apoptosis was suppressed by caspase inhibition. TRAIL receptor (DR5) and proapoptotic Bcl-2 proteins (Puma and Bad) were upregulated, while anti-apoptotic factors (survivin, XIAP, cFLIP, Mcl-1, and Bcl-w) were downregulated. Strongly elevated levels of reactive oxygen species (ROS) turned out as particularly characteristic for celecoxib, appearing already after 2 h. ROS production alone was not sufficient for apoptosis induction but may play a critical role in sensitizing cancer cells for apoptosis and therapy. Thus, the full therapeutic potential of celecoxib may be better used in combinations with death ligands. Furthermore, the immune response against cSCC/AK may be improved by celecoxib, and combinations with checkpoint inhibitors, recently approved for the treatment of cSCC, may be considered.

Keywords: cutaneous SCC; celecoxib; apoptosis; reactive oxygen species; TRAIL; death ligands

Citation: Zhu, J.; May, S.; Ulrich, C.; Stockfleth, E.; Eberle, J. High ROS Production by Celecoxib and Enhanced Sensitivity for Death Ligand-Induced Apoptosis in Cutaneous SCC Cell Lines. *Int. J. Mol. Sci.* **2021**, *22*, 3622. https://doi.org/10.3390/ijms22073622

Academic Editor: Sergio Di Meo

Received: 24 February 2021
Accepted: 26 March 2021
Published: 31 March 2021

1. Introduction

Actinic keratosis (AK) is derived from neoplastic epidermal keratinocytes and is characterized by high prevalence and the risk to proceed into invasive cutaneous squamous cell carcinoma (cSCC). About 20% of skin cancer deaths worldwide are related to cSCC [1]. Thus, it is the second most common skin cancer in Caucasians and East Asians (including Japanese and Chinese) and even the most common skin cancer in African Americans [2,3].

The effects of anticancer drugs are strongly related to the induction of apoptosis, a mechanism basic for the control of tissue homeostasis [4]. Thus, resistance to apoptosis represents a crucial step in oncogenesis and drug resistance [5]. Intrinsic proapoptotic pathways are activated in response to cellular stress situations as well as by anticancer treatment, e.g., by chemotherapy. This relies on a loss of mitochondrial membrane potential and the release of mitochondrial factors such as cytochrome c, which triggers activation of initiator caspase-9 [6].

On the other hand, extrinsic induction of apoptosis is initiated by death ligands such as CD95L/FasL and TRAIL (TNF-related apoptosis-inducing ligand). Upon death receptor activation, death-inducing signaling complexes are formed, resulting in activation of initiator caspases, such as caspase-8 and caspase-10 [7]. Initiator caspases may cleave

and thus activate effector caspases as -3, -6, and -7, which cleave a large number of death substrates with the final result of DNA fragmentation and apoptosis induction [8]. In particular, the death ligand TRAIL has attracted much consideration due to its anticancer activity, while normal cells are largely spared [9,10]. However, cancer cells may also develop TRAIL resistance, limiting its clinical applicability [11].

Besides the well-established pathways, there is increasing evidence for a particular role of reactive oxygen species (ROS) in the control of apoptosis. In melanoma as well as in cutaneous T-cell lymphoma cells, we have previously described enhanced ROS levels after inhibition of phosphoinositol-3 kinase and BRAF as well as in response to indirubin derivatives [12–15]. However, the relation of ROS to previously described apoptosis pathways remained largely fragmentary so far.

Cyclooxygenase-2 (COX-2) represents the primary cancer target of NSAIDs (nonsteroidal anti-inflammatory drugs) [16]. The NSAID and COX-2 inhibitor celecoxib has attracted broad attention because of its antitumor activities. Thus, clinical trials have shown efficiency in colorectal adenoma, leading to FDA approval of celecoxib for patients with familial adenomatous polyposis [17–19]. Concerning COX-2, however, increasing evidence in the last years has shown that the anticancer activity of celecoxib may be more related to COX-2-independent effects [20–22].

Drug combinations may overcome the problems of limited efficiency and resistance, but the combination of celecoxib and TRAIL was not investigated in cSCC so far. Celecoxib's mode of action in cSCC also remained largely elusive. Here, we show in cSCC cells that apoptosis by celecoxib can be strongly enhanced in combinations with TRAIL or with CD95 agonistic antibodies. This was related to caspase activation as well as to the regulation of apoptosis-related proteins. Finally, enhanced levels of reactive oxygen species (ROS) appeared as highly characteristic for celecoxib, although ROS levels alone were not sufficient for apoptosis induction. The results may be considered for improving cSCC/AK therapy.

2. Results

2.1. Decreased Cell Proliferation by Celecoxib Despite Little Effect on Apoptosis

We evaluated the therapeutic potential of celecoxib in four representative cSCC cell lines (SCL-I, SCL-II, SCC-12, and SCC-13). Real-time cell analysis (RTCA) showed a dose-dependent decrease in cell proliferation in response to celecoxib (20, 50, and 100 μM), which started almost immediately after the onset of treatment (time: 0; Figure 1a,b). In SCL-II and SCC-12, an additional WST-1 assay was performed at 24 h and proved dose-dependent anti-proliferative effects with revealed values of 35% (SCL-II) and 10% (SCC-12) for 50 μM celecoxib (Figure 1c). Anti-proliferative effects were not based on direct cell cytotoxicity, as determined by lactate dehydrogenase (LDH) release assays in SCL-II and SCC-12 at 2 h after the start of celecoxib treatment (Figure 1d).

In contrast, apoptosis induction was much less pronounced and below 5% for treatments with 25 and 50 μM celecoxib at 24 and 48 h (Figure 1e). Similarly, only little effects were obtained at the level of cell viability for 25 and 50 μM (9–16% reduction, as compared to controls). Somewhat stronger effects were seen only for 100 μM celecoxib (73–84% reduction, as compared to controls; Figure 1f). Thus, while cell proliferation was clearly affected also by moderate celecoxib concentrations (25 and 50 μM), direct effects on apoptosis and cell viability were limited.

2.2. Strongly Enhanced Apoptosis in Combinations with Death Ligands

In order to identify conditions that may increase the proapoptotic effects of celecoxib, it was combined with TRAIL and CD95 agonistic antibody CH-11. This revealed strongly enhanced apoptosis in all cell lines. Thus, the combination of celecoxib (50 μM) with TRAIL (50 ng/mL) for 48 h resulted in apoptosis rates of 64%, 29%, 38%, and 25% in SCL-I, SCL-II, SCC-12, and SCC-13, respectively. Similarly, the combination with CH-11 (100 ng/mL) resulted in apoptosis rates of 17%, 24%, 32%, and 19% (Figure 2).

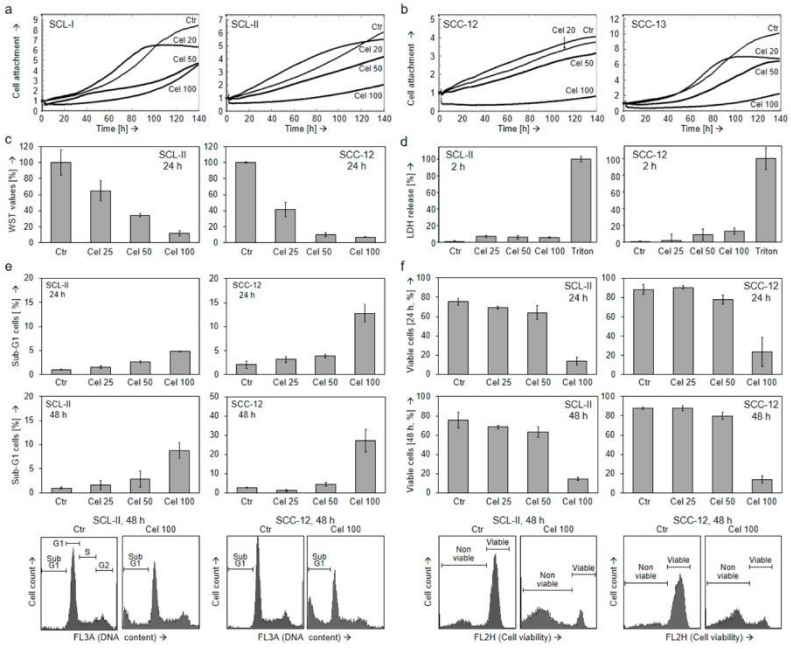

Figure 1. Decreased cell proliferation by celecoxib despite little effects on apoptosis. (**a**,**b**) Real-time cell analysis (RTCA) of (**a**) squamous cell carcinoma cell lines SCL-I and SCL-II as well as (**b**) of squamous cell carcinoma cell lines SCC-12 and SCC-13 treated with 20, 50, and 100 µM celecoxib (time 0 h = start of treatment). The determined cell index gives a relative measurement of cell attachment. The experiment was performed twice with triple values, which revealed highly comparable results. (**c**) Cell proliferation was quantified by WST-1 assay in SCL-II and SCC-12 at 24 h of celecoxib treatment (25, 50, 100 µM). (**d**) Direct cytotoxicity was determined in SCL-II and SCC-12 at 2 h of treatment by quantification of lactate dehydrogenase (LDH)-release (fold change of non-treated controls, set to 1). Cells treated with triton x100 (0.7%) were used as positive controls. (**e**,**f**) Apoptosis (**e**) and cell viability (**f**) were determined in SCL-II and SCC-12 at 24 h and at 48 h in response to 25, 50, and 100 µM celecoxib. Apoptotic cells were identified in cell cycle analyses as sub-G1 cells characterized by DNA fragmentation, whereas cell viability was determined by calcein-AM staining. Examples of flow cytometry measurements are given below. (**c**–**f**) Mean values are shown in representative experiments. At least two independent experiments, each one with triplicates, revealed highly comparable results.

Enhanced apoptosis came along with a reciprocal loss of cell viability. Thus, in combinations of celecoxib with TRAIL, cell viability at 48 h was decreased to 9%, 32%, 13%, and 10% in SCL-I, SCL-II, SCC-12, and SCC-13, respectively. In combination with CH-11, it was decreased to 50%, 30%, 13%, and 36%, respectively (Figure 3). Thus, death ligands and celecoxib appeared as highly effective combination partners.

2.3. Changes of Mitochondrial Membrane Potential

Addressing the mechanisms of celecoxib-mediated effects in cSCC cells, we determined changes in the mitochondrial membrane potential (MMP). No major changes of MMP were seen at early times (3 h) in response to celecoxib or combination treatment, clearly not suggestive for the initial activation of intrinsic apoptosis pathways. At 24 h, celecoxib treatment alone also did not result in strong effects at the level of MMP (<30% cells with low MMP). Significant loss of MMP (up to 90%) was seen only in combination when apoptosis was also strongly induced (Figure 4). Thus, loss of MMP appeared in parallel with induced apoptosis or as a result of it.

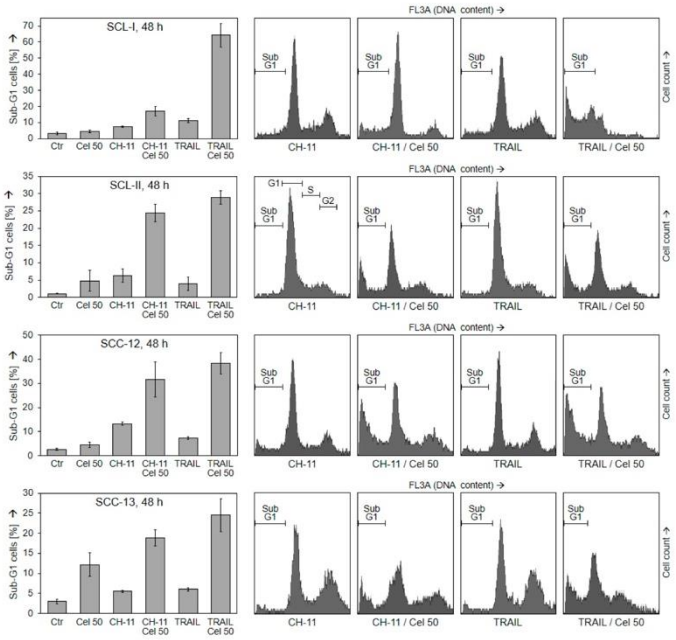

Figure 2. Induction of apoptosis in combinations with death ligands. Cell lines SCL-I, SCL-II, SCC-12 and SCC-13 were treated with celecoxib (50 μM), CH-11 (100 ng/mL), TRAIL (50 ng/mL) or combinations. Apoptosis was determined at 48 h by propidium iodide staining and cell cycle analysis. Left, results of representative experiments are shown. At least two independent experiments, each one with triplicate values, revealed highly comparable results. Right side, examples of flow cytometry measurements are shown (CH-11, TRAIL and combination treatments); apoptotic cell populations (sub-G1) are indicated.

2.4. Enhanced Caspase Activation in Course of Combined Treatment

To distinguish between caspase-dependent and independent mechanisms, caspase activation in response to celecoxib and TRAIL was investigated in SCL-II and SCC-12 by Western blotting. This included effector caspases -3, -6, and -7, as well as caspase-8 and caspase-9, the major initiator caspases of the extrinsic and intrinsic apoptosis pathways. While TRAIL alone resulted in some caspase processing, in particular of caspase-8 (43, 41, and 18 kDa) and caspase-3 (20, 18, and 16 kDa), celecoxib alone remained completely without effect on caspase activation (no processing) (Figure 5).

Activation of caspase-8 and caspase-3 were strongly enhanced in the combination of celecoxib/TRAIL. Similarly enhanced was the activation of caspase-6 (reduction in the 35 kDa proform), caspase-7 (reduction in the 37 kDa proform and cleavage products at 20 kDa), and caspase-9 (cleavage products of 37 kDa) (Figure 5). Collectively, these data indicate a complete activation of proapoptotic caspase cascades by combination treatment.

The pan-caspase inhibitor QVD-Oph was applied to prove the decisive role of caspases. In SCL-II and SCC-12, QVD-Oph completely abrogated any caspase processing (Figure 6a) as well as apoptosis induction (Figure 6b), thus proving the significant role of caspases in this setting.

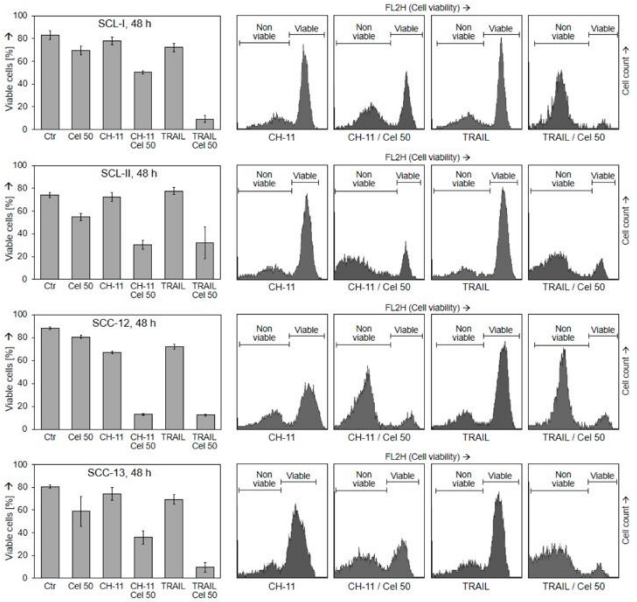

Figure 3. Loss of cell viability in combinations with death ligands. Cell lines SCL-I, SCL-II, SCC-12 and SCC-13 were treated with celecoxib (50 μM), CH-11 (100 ng/mL), TRAIL (50 ng/mL) or combinations. Cell viability was determined at 48 h by calcein staining and flow cytometry. Left, results of representative experiments are shown. At least two independent experiments, each one with triplicate values, revealed highly comparable results. Right side, examples of flow cytometry measurements (CH-11, TRAIL and combination treatments) are shown; viable and non-viable cell populations are indicated.

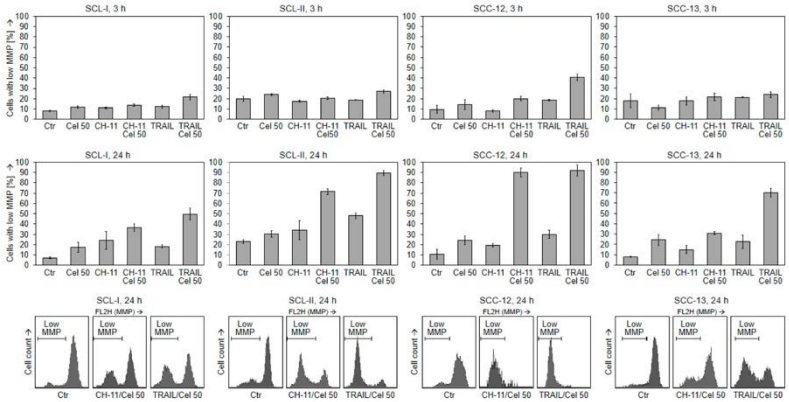

Figure 4. Changes of mitochondrial membrane potential (MMP). Four cSCC cell lines were treated with celecoxib (50 μM), CH-11 (100 ng/mL), TRAIL (50 ng/mL) or combinations for 3 h and 24 h, respectively. Percent of cells with low MMP were determined by $TMRM^+$ staining. Mean values and SDs of representative experiments are shown. At least two independent experiments, each one consisting of triplicate values, revealed highly comparable results. Example cytometry measurements of controls and combination treatments are given below; cell fractions with low MMP are indicated.

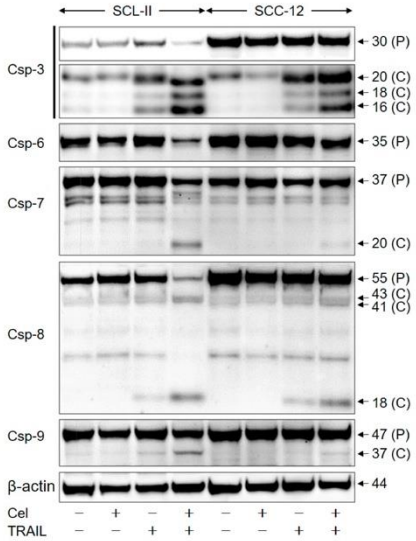

Figure 5. Enhanced caspase activation in the course of combination treatment. SCL-II and SCC-12 cells were treated for 24 h with celecoxib (50 μM) and/or TRAIL (50 ng/mL). Protein extracts were analyzed by Western blotting for expression of caspase-3, caspase-6, caspase-7, caspase-8 and caspase-9. Equal protein amounts (30 μg per lane) were separated by SDS-PAGE, and consistent blotting was proven by Ponceau staining as well as by evaluation of expression of β-actin. Proforms (P) as well as caspase cleavage products (C) were identified. Two independent series of protein extracts and independent Western blots revealed highly comparable results.

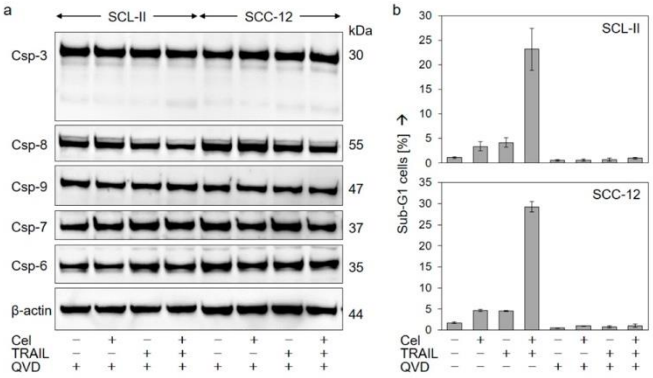

Figure 6. Inhibition of apoptosis by a caspase inhibitor. SCL-II and SCC-12 were treated for 24 h with celecoxib (50 μM), TRAIL (50 ng/mL), or the combination. In addition, cells received the pan-caspase inhibitor QVD-Oph (10 μM) at 1 h before other treatments started. (**a**) Protein extracts were analyzed by Western blotting for caspase activation (processing). Equal protein amounts (30 μg per lane) were separated by SDS-PAGE, and consistent blotting was proven by Ponceau staining as well as by evaluation of β-actin expression. Molecular weights (in kDa) of caspase proforms are indicated. Two independent series of protein extracts and independent Western blots revealed highly comparable results. (**b**) Apoptosis was determined at 24 h of treatment by cell cycle analysis and quantification of sub-G1 cells (mean values +/− SDs of representative experiments). Two independent experiments, each one with triplicate values, showed the same result.

2.5. Regulation of Mediators of Apoptosis and Cell Proliferation

For illuminating celecoxib's effects in cSCC cells, proteins involved in the control of apoptosis and cell proliferation were investigated in SCL-II and SCC-12 at 24 h of treatment by Western blotting. Suggesting a particular role in celecoxib-mediated inhibition of cell proliferation, the cell cycle inhibitor p21 was strongly upregulated by celecoxib in both cell lines. Further suggesting a particular role for TRAIL sensitivity, the major TRAIL receptor, DR5 (40 kDa), was significantly upregulated by celecoxib (Figure 7).

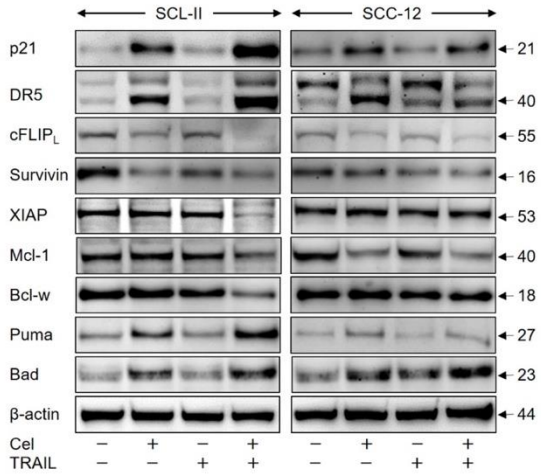

Figure 7. Regulation of characteristic mediators of apoptosis and cell proliferation. Cell lines SCL-II and SCC-12 were treated for 24 h with celecoxib (50 μM), TRAIL (50 ng/mL) or the combination. Expression levels of p21 (21 kDa), TRAIL-R2/DR5 (40 kDa), cFLIP (long isoform, 55 kDa), survivin (16 kDa), XIAP (53 kDa), Mcl-1 (40 kDa), Bcl-w (18 kDa), Puma (27 kDa) and Bad (23 kDa) were analysed by Western blotting. Analysis of β-actin (44 kDa) served as loading control. Largely similar results were obtained in three independent Western blot experiments using three independent series of cell extracts.

Several other proteins were suggestive for an enhancement of proapoptotic pathways by celecoxib. Thus, effector caspases may be blocked by cellular inhibitor of apoptosis proteins (cIAPs, e.g., survivin and chromosome X-linked inhibitor of apoptosis protein (XIAP)), whereas caspase-8 activity is suppressed by its competitive inhibitor cFLIP (cellular FLICE-like inhibitory protein). The long isoform of cFLIP (FLIP$_L$, 55 kDa) was downregulated by celecoxib in both cell lines, and in SCL-II, also survivin and XIAP were downregulated either by celecoxib alone or by combination treatment (Figure 7).

The family of pro- and anti-apoptotic Bcl-2 proteins are critically involved in the control of intrinsic apoptosis pathways. Of the anti-apoptotic family members, Mcl-1 was downregulated in SCC-12 by celecoxib alone, whereas in SCL-II, both Mcl-1 and Bcl-w were downregulated by combination treatment. Also, the proapoptotic BH3-only family members, Puma and Bad, were upregulated in both cell lines by celecoxib alone (Figure 7), while for the anti-apoptotic Bcl-2 as well as for the proapoptotic Bax and Bak proteins, no significant changes in expression were seen (data not show). These findings underlined that celecoxib resulted in multiple effects on cell proliferation- and apoptosis-related proteins involved both in intrinsic and extrinsic apoptosis pathways.

2.6. Massive ROS Production by Celecoxib

Most impressive was the massive production of reactive oxygen species (ROS) in response to celecoxib, which appeared as an early effect already at 2 h in all cSCC cell lines.

The vast majority of cells were responsive (54–75%) seen by an almost complete shift of the cells´ peak in flow cytometry. The full ROS shift was already obtained for the lowest celecoxib concentration of 25 µM, and the effects were even comparable to H_2O_2, used as a positive control (Figure 8a). Thus, high ROS production appeared as a typical result of celecoxib.

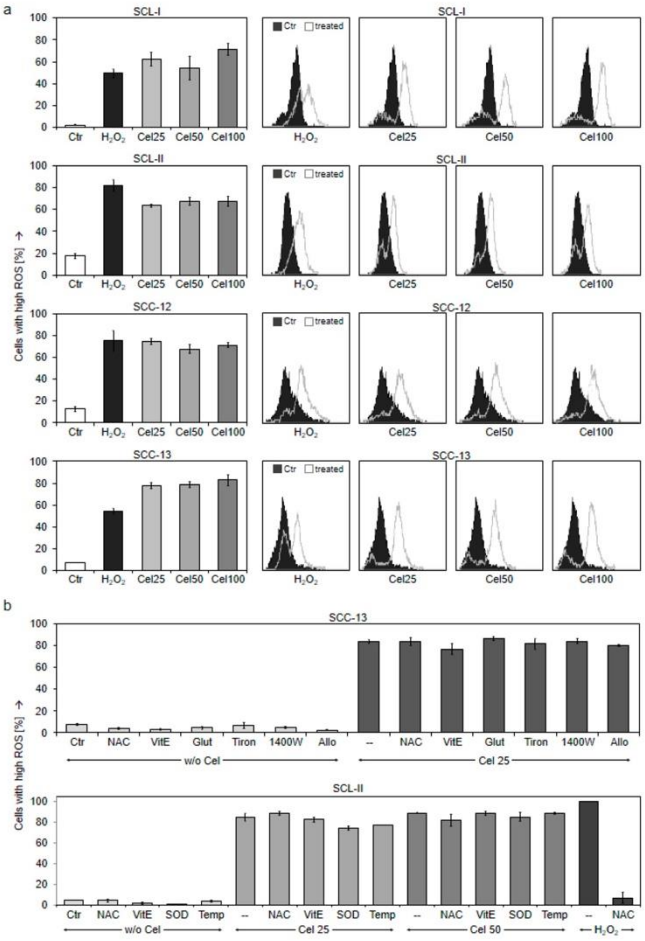

Figure 8. Strongly enhanced ROS levels by celecoxib. (**a**) Four cSCC cell lines were treated for 2 h with increasing concentrations of celecoxib (25, 50, and 100 µM), whereas H_2O_2 (1 mM, 1 h) was used as a positive control. ROS levels were determined by H_2DCFDA staining and flow cytometry. Mean values +/− SDs of representative experiments are shown; at least two independent experiments, each one consisting of triplicate values, revealed highly comparable results. Example cytometry measurements (overlays vs. controls) are shown on the right side. (**b**) Treatment with different antioxidative strategies is shown in SCC-13 and SCL-II in addition to celecoxib treatment (25 and 50 µM): NAC, N-acetyl cysteine (1 mM); VitE, tocopherol (1 mM); Glut, glutathione (1 mM); Tiron (1 mM); 1400W (100 µM); Allo, Allopurinol (1 mM); Temp, Tempol (1 mM). Antioxydants were generally applied at 1 h before celecoxib.

Increasing evidence in recent years has proven that ROS plays a vital role in the regulation of apoptosis. In previous work, in melanoma and cutaneous T-cell lymphoma cells, ROS production could often be prevented by antioxidant treatment as by N-acetyl cysteine (NAC) or by vitamin E (tocopherol), which thus allowed to prove the significant role of ROS in apoptosis [14,15]. This strategy, however, failed here for the high ROS levels produced in cSCC cells in response to celecoxib. Neither NAC nor tocopherol or several other antioxidative treatments tested were able to significantly prevent celecoxib-induced ROS production, as demonstrated for SCC-13 and SCL-II. In contrast, H_2O_2-induced ROS was decreased by NAC (Figure 8b). In agreement, apoptosis induced by celecoxib could not be reduced significantly by antioxidative pre-treatment (data not shown), suggesting that celecoxib-induced ROS was too strong.

3. Discussion

Cutaneous SCC and AK are characterized by high incidence and provoke severe health problems worldwide [1]. While many cSCCs can be treated by surgical excision and chemotherapy, a subset of patients develops therapy resistance, recurrence, and metastasis [23]. Furthermore, topical treatments of AK are often non-sufficient and cannot prevent tumor progression [24]. Thus, new and efficient treatments are needed for cSCC and AK.

The anti-inflammatory, analgesic, and anti-pyretic drug celecoxib has been in clinical use for many years [25]. Anti-neoplastic effects as inhibition of cancer cell growth and suppression of metastases have also been reported in vitro and in mouse models of colorectal, nasopharyngeal, and mammary carcinoma [26–28]. In clinical trials, celecoxib revealed positive results for colorectal and breast cancer [29], and it was approved for adjuvant treatment of familial adenomatous polyposis [17]. Another clinical trial suggested that progression from AK to cSCC may be diminished [30].

The efficiency of celecoxib may be improved in combinations, as shown, e.g., in non-Hodgkin lymphoma and melanoma cells with histone deacetylase inhibitors and plumbagin, respectively [31,32]. In clinical trials, improved response to chemotherapy was also obtained in combinations with celecoxib [33,34]. In the present study, celecoxib alone showed only little effects on apoptosis and cell viability in cultured cSCC cells, but apoptosis was strongly enhanced, and cell viability was decreased in combinations with death ligands. TRAIL represents a promising antitumor strategy due to its selective activity in cancer cells [9–11]. Thus, the efficiency of celecoxib may be crucially improved by combination with TRAIL or TRAIL receptor agonists.

Death ligands furthermore represent basic elements of an antitumor immune response driven by cytotoxic T-lymphocytes and natural killer cells [11]. Thus, enhancing death ligand-induced apoptosis by celecoxib may improve the immune response against cSCC. Positive combination effects of celecoxib and TRAIL were also found in other tumor cells, e.g., of non-small-cell lung carcinoma, colon cancer, and glioblastoma [35–37]. In contrast, in cSCC, the effects of TRAIL were not sufficiently investigated so far. Only for a combination of diclofenac and TRAIL an enhanced apoptotic response was shown [38].

A better understanding of the mechanisms of induced apoptosis can provide insights, which may be used for translational strategies. While not affected by celecoxib alone, proapoptotic caspase cascades were fully activated in combination with TRAIL, and their essential role was proven by a caspase inhibitor. Caspase dependency of celecoxib-induced apoptosis was also found in gastric cancer and non-small-cell lung cancer cells [39,40].

For demonstrating the decisive role of certain caspases, siRNA strategies may also apply. Thus, the role of caspase 8 in celecoxib-induced apoptosis in human lung cancer cells was shown [35], whereas apoptosis induced by another NSAID (FR122047) in MCF-7 breast cancer cells was even enhanced by siRNA knockdown of caspase-9 [41]. Due to the massive activation of caspases-3, -6, -7, -8, and -9 by celecoxib/TRAIL, we aimed to investigate the principle involvement of the caspase cascade, for which the used pan-caspase inhibitor appeared as particularly suitable.

Caspase-8 is antagonized by its competitive inhibitor cFLIP (cellular FLICE-like inhibitory protein), while cIAPs (cellular inhibitor of apoptosis proteins) as XIAP and survivin inhibit effector caspases and caspase-9 [42,43]. We show here the downregulation of cFLIP and survivin in cSCC cells in response to celecoxib, while XIAP was downregulated by the combination treatment in one cell line. Downregulation of cFLIP by celecoxib was also found in non-small-cell lung cancer cells [40], and it was downregulated in cSCC cells in response to diclofenac [38]. Roles of survivin and XIAP in celecoxib-mediated effects were also seen in leukemia and myeloma cells [44,45]. Downregulation of caspase antagonists thus appears as a frequent effect of celecoxib and may critically contribute to caspase activation in combinations.

In this study, highly pleiotropic effects of celecoxib were shown; namely, a number of investigated proteins were either upregulated or downregulated. Good examples in this context are upregulation of the cell cycle inhibitor p21 [46] and of the TRAIL receptor DR5, which may significantly affect inhibition of cell proliferation in cSCC cells and enhancement of TRAIL sensitivity, respectively. In colorectal cancer cells, p21 was also upregulated by celecoxib [47], and upregulation of DR5 by celecoxib was reported in non-small-cell lung cancer as well as in hepatocellular carcinoma cells [40,48].

Intrinsic, mitochondrial apoptosis pathways are critically controlled by Bcl-2 family proteins comprising of anti-apoptotic (e.g., Bcl-2, Mcl-1, and Bcl-w), proapoptotic multidomain (Bax and Bak) as well as proapoptotic BH3-only proteins (e.g., Puma and Bad) [6]. Suggesting an activation of intrinsic apoptosis pathways, Mcl-1 and Bcl-w were downregulated, while Puma and Bad were upregulated by celecoxib in cSCC cells. Mcl-1 is considered an important factor for the control of apoptosis in keratinocytes [49]. Its downregulation by celecoxib was also reported in hepatocellular carcinoma cells [50], and Bcl-w was downregulated in cSCC cells by diclofenac [51].

We have already previously shown the upregulation of Bad by celecoxib in the cell line SCL-II [51], and upregulation of Bad is shown here also in SCC-12. Upregulation of Puma by celecoxib was also found in stomach cancer cells, and its functional role in the activation of intrinsic apoptosis pathways was suggested [52]. In contrast, Puma was even downregulated by diclofenac in cSCC cells [51], thus suggesting a different mode of action in this setting.

The data of the present study suggest that celecoxib affects both intrinsic and extrinsic apoptosis pathways in cSCC cells. The question remains, how it can regulate so many different proteins. Here, reactive oxygen species (ROS) may serve as an explanation. ROS play important roles in tissue damage and aging, but in recent years an increasing body of evidence has also shown critical roles of ROS in apoptosis regulation in cancer cells. Thus in melanoma cells, apoptosis induction by different agents as an iron-substituted nucleoside analog, indirubin derivatives as well as by protein kinase B or BRAF inhibition was shown to be largely ROS-dependent [12–14,53]. Also in cutaneous T-cell lymphoma cells, apoptosis induction by indirubin derivatives was ROS-dependent [15]. Induction of ROS in the course of celecoxib treatment has already been reported in melanoma and breast cancer cells [54], and ROS production was suggested as a key mechanism for celecoxib's anticancer activity in combination with 5-FU in head and neck cancer cells [55].

Here, we demonstrate massive ROS production by celecoxib in cSCC cells. ROS appeared very early and even at moderate celecoxib concentrations, suggesting ROS as upstream of other effects. While ROS were not sufficient to induce apoptosis themselves, they may prepare cSCC cells for apoptosis induction through death ligands. In previous studies, the significant role of ROS in apoptosis could be proven by antioxidative strategies, e.g., by N-acetyl cysteine or by tocopherol/vitamin E [12–14,53]. However, celecoxib-induced ROS in cSCC cells appeared as very strong and revealed characteristics, which could not be inhibited by different antioxidative strategies. Thus, the decisive role of ROS for celecoxib-induced apoptosis in cSCC cells is suggested here but could not be finally proven so far.

ROS levels in cells may also be regulated by antioxidative enzymes such as catalase and superoxide dismutase (SOD). For colon cancer, inhibition of tumor growth by celecoxib-loaded liposomes was accompanied by activation of SOD, which was further related to an antioxidative activity [56]. Celecoxib also increased SOD activity in rat stomach and colon mucosa [57]. In cSCC, however, the situation was clearly different, as ROS production by celecoxib in cSCC cells was strong, rapid, and long-lasting. We thus may not expect that CAT or SOD may be directly involved.

ROS induction appears as a promising anticancer strategy. Although the clinical effects of some ROS-inducing drugs were limited, as sulphasalazine in gastric cancer patients [58], other strategies have been favorably tested, e.g., the glutathione disulfide mimetic NOV-002 in patients with HER2-negative breast cancer [59]. Lack of efficiency may have many different causes, e.g., drug uptake, delivery, stability, and resistance mechanisms. Thus, limited efficiency of some strategies may not necessarily mean that ROS induction is not suitable for anticancer therapy.

At present, immune checkpoint inhibitors represent highly promising therapeutic strategies, also for cSCC. They may, however, not apply for all patients due to limitations because of side effects as well as therapy resistance [60]. Thus, new and additional anticancer strategies are still needed, which may also be used in combinations to improve efficiency. As shown here, celecoxib enhanced apoptosis sensitivity of cSCC cells for TRAIL. As TRAIL serves as an important factor of the immune system, it is suggestive that celecoxib in this way may also support an antitumor immune response. However, this effect could not be directly proven in the present study. Suitable animal experiments for investigating the function of the human immune response are rare and constitute a major challenge. Nevertheless, the antineoplastic effects of celecoxib have been shown in animal models of colorectal and mammary carcinoma [26,27].

In conclusion, lack of apoptosis induction by celecoxib alone suggests that its full therapeutic potential may be achieved only in combinations, and TRAIL appears as particularly suitable. As death ligands represent characteristic effectors of the immune system, celecoxib may also support an immune response against cSCC/AK, and combinations with immune checkpoint inhibitors recently approved for the treatment of cSCC may be considered. As concerning the mode of action in cSCC cells, highly pleiotropic effects on apoptosis regulators were found for celecoxib, which affects both intrinsic and extrinsic apoptosis pathways. ROS production by celecoxib appeared as most pronounced and may serve as a master regulator.

4. Materials and Methods

4.1. Cell Culture and Treatment

Four representative cSCC cell lines (SCL-I, SCL-II, SCC-12, and SCC-13) were used, which were derived from human facial skin lesions [38]. They were maintained at 5% CO_2 in RPMI 1640 growth medium (Life Technologies, Darmstadt, Germany) supplemented with 10% FCS, 2 mM glutamine, non-essential amino acids, and antibiotics. Most assays were performed in 24-well plates after seeding 5×10^4 cells per well. Treatments: celecoxib (BioMol, Hamburg, Germany; 1000-8672, 25–100 µM), agonistic anti-CD95 antibody (CH-11, IgM mouse; Beckman Coulter, Krefeld, Germany; 100 ng/mL), and Killer TRAIL™ (Adipogen, San Diego USA, AG-40T-0001; 50 ng/mL). Control cells received the celecoxib´s solvent DMSO. For caspase inhibition, the pan-caspase inhibitor QVD-Oph (Abcam, Cambridge, UK; 10 µM) was given at 1 h before agonists were applied.

4.2. Cell Proliferation Assays

Growth rates were determined by real-time cell analysis (RTCA, xCELLigence; Agilent, Santa Clara, CA, USA). A number of 10,000 cells were seeded per well in special 96-well E-plates equipped with electrodes in the bottom of wells, and treatments started after 24 h. Electric resistance was continuously determined up to 140 h, which served as a

measurement of cell confluence. A second cell proliferation assay was based on WST-1 staining (Water soluble tetrazolium-1, Roche Diagnostics), further analyzed by ELISA.

4.3. Determination of Apoptosis, Cytotoxicity and Cell Viability

Quantification of apoptosis was performed by cell cycle analysis. Cells were harvested by trypsinization and lysed in hypotonic buffer. Isolated nuclei were stained for 1 h with 40 mg/mL propidium iodide (Sigma-Aldrich, St. Louis, MO, USA). Cells in G1, G2, and S-phase, as well as sub-G1 cells, were quantified by flow cytometry at FL3A using a FACS Calibur (BD Bioscience, Bedford, MA, USA). Due to the washing out of small DNA fragments, nuclei with less DNA than G1 (sub-G1) correspond to apoptotic cells.

Cytotoxicity was determined in cell culture supernatants by quantification of released lactate dehydrogenase (LDH) activity. Cells were stained by a cytotoxicity detection assay (Roche Diagnostics, Penzberg, Germany) and analyzed by an ELISA reader. Triton x100-treated cells (0.7%) were used as a positive control.

Cell viability was determined by staining cells with calcein-AM (PromoCell, Heidelberg, Germany; AM = acetoxymethylester), which is converted in viable cells through intracellular esterase activity to green-fluorescent calcein. Cells, grown and treated in 24-well plates, were harvested by trypsinization and stained for 1 h with 2.5 µg/mL calcein-AM at 37 °C. After labeling, cells were washed with PBS and measured by flow cytometry (FL2H).

4.4. Mitochondrial Membrane Potential

Mitochondrial membrane potential ($\Delta\Psi m$) was determined by staining cells with the fluorescent dye $TMRM^+$ (Tetramethylrhodamin-methylester, Sigma-Aldrich). Cells, grown and treated in 24-well plates, were harvested by trypsinization and stained for 20 min at 37 °C with 1 µM $TMRM^+$. After 2-times washing with PBS, staining of cells was quantified by flow cytometry (FL2H).

4.5. Analysis of Reactive Oxygen Species (ROS)

For determination of intracellular ROS levels, cells grown in 24-well plates were pre-incubated for 1 h with the fluorescent dye H_2DCFDA (2′,7′-dichlorodihydrofluorescein diacetate, D-399, Thermo Fisher Scientific, Hennigsdorf, Germany, 10 µM), before starting treatment with effectors. After 2–24 h treatment, cells were harvested by trypsinization, washed several times with PBS, and analyzed by flow cytometry (FL1H). As a positive control, treatment with H_2O_2 (1 mM, 1 h) was applied. Different antioxidative treatments were used aiming at the suppression of celecoxib-induced ROS levels, including N-acetyl cysteine (NAC, Sigma-Aldrich, Taufkirchen, Germany, up to 4 mM), tocopherol (vitamin E, Fluka, Steinheim, Germany, up to 4 mM), glutathione (Sigma-Aldrich, 1 mM); Tiron (Sigma-Aldrich, 1 mM); 1400 W Sigma-Aldrich, 100 µM); Allopurinol (Sigma-Aldrich, 1 mM); TEMPOL (1-Oxyl-2,2,6,6-tetramethyl-4-hydroxypiperidine, Santa Cruz; 1 mM). Antioxidants were generally applied at 1 h before starting celecoxib treatment.

4.6. Western Blotting

For Western blotting, total protein extracts were obtained by cell lysis buffer containing 150 mM NaCl, EDTA (1 mM), 1% NP-40; 50 mM Tris (pH 8.0), as well as phosphatase and protease inhibitors. Following SDS polyacrylamide gel electrophoresis, proteins were blotted on nitrocellulose membranes.

Primary antibodies of Cell Signaling (Danvers, MA, USA): Caspase-3 (9662, rabbit, 1:1000), Cleaved caspase-3 (9664, rabbit, 1:1000), Caspase-8 (9746, mouse, 1:1000), Caspase-9 (9502, rabbit, 1:1000), Caspase-6 (9762, rabbit, 1:1000), Caspase-7 (9492, rabbit, 1:1000), XIAP (2042, rabbit, 1:1000), Mcl-1 (4572, rabbit, 1:1000), Bad (9292, rabbit, 1:1000), and Bcl-w (2724, rabbit, 1:1000). Primary antibodies of Santa Cruz Biotech (Dallas, TX, USA): c-FILP (sc-5276, mouse, 1:500), survivin (sc-177779, mouse, 1:500), p21(sc-6246, mouse, 1:500), p53 (sc-126, mouse, 1:500), β-actin (sc-47778, mouse, 1:1000), Puma (sc-374223, mouse, 1:500),

Bax (sc-7480, mouse, 1:500), and Bak (sc-832, mouse, 1:500). Primary antibody of Abcam (Cambridge, UK): DR5 (ab8416, rabbit, 1:1000). Secondary antibodies: peroxidase-labelled goat anti-rabbit and goat anti-mouse (Dako, Hamburg, Germany; 1:5000).

4.7. Statistical Analyses

All assays were done in triplicate determinations, and at least two independent experiments were performed. Presented Western blot data were verified by at least two independent series of cellular extracts. Statistical significance was proven by Student's *t*-test (two-tailed, heteroscedastic) using all data of independent experiments (at least six individual measurements); *p*-values < 0.05 were considered as statistically significant.

Author Contributions: Conceptualization, J.E., E.S. and C.U.; methodology, J.E., J.Z. and S.M.; validation, J.Z., J.E.; formal analysis, J.E.; investigation, J.Z., S.M. and J.E.; resources, J.E. and C.U.; data curation, J.Z., S.M. and J.E.; writing—original draft preparation, J.E. and J.Z.; writing—review and editing, J.E., J.Z.; C.U. and E.S.; supervision, J.E.; funding acquisition, J.E. and E.S. All authors have read and agreed to the published version of the manuscript.

Funding: This research was funded by the European skin cancer foundation (ESCF), project S0251/100 10/2015.

Institutional Review Board Statement: Not applicable. Study did not involve humans or animals.

Acknowledgments: We acknowledge support from the German Research Foundation (DFG) and the Open Access Publication Fund of Charité—Universitätsmedizin Berlin.

Conflicts of Interest: E.S. has been working as a consultant for the company Pfizer. Other authors declare no conflict of interest. The funders had no role in the design of the study; in the collection, analyses, or interpretation of data; in the writing of the manuscript, or in the decision to publish the results.

References

1. Szewczyk, M.; Pazdrowski, J.; Golusiński, P.; Dańczak-Pazdrowska, A.; Marszałek, S.; Golusiński, W. Analysis of selected risk factors for nodal metastases in head and neck cutaneous squamous cell carcinoma. *Eur. Arch. Otorhinolaryngol.* **2015**, *272*, 3007–3012. [CrossRef] [PubMed]
2. Amaral, T.; Osewold, M.; Presser, D.; Meiwes, A.; Garbe, C.; Leiter, U. Advanced cutaneous squamous cell carcinoma: Real world data of patient profiles and treatment patterns. *J. Eur. Acad. Dermatol. Venereol.* **2019**, *33*, 44–51. [CrossRef]
3. Halder, R.M.; Bridgeman-Shah, S. Skin cancer in African Americans. *Cancer* **1995**, *75*, 667–673. [CrossRef]
4. Kerr, J.F.; Wyllie, A.H.; Currie, A.R. Apoptosis: A basic biological phenomenon with wide-ranging implications in tissue kinetics. *Br. J. Cancer* **1972**, *26*, 239–257. [CrossRef] [PubMed]
5. Hanahan, D.; Weinberg, R.A. Hallmarks of cancer: The next generation. *Cell* **2011**, *144*, 646–674. [CrossRef] [PubMed]
6. Chipuk, J.E.; Moldoveanu, T.; Llambi, F.; Parsons, M.J.; Green, D.R. The BCL-2 family reunion. *Mol. Cell* **2010**, *37*, 299–310. [CrossRef]
7. Krammer, P.H.; Arnold, R.; Lavrik, I.N. Life and death in peripheral T cells. *Nat. Rev. Immunol.* **2007**, *7*, 532–542. [CrossRef]
8. Fischer, U.; Janicke, R.U.; Schulze-Osthoff, K. Many cuts to ruin: A comprehensive update of caspase substrates. *Cell Death Differ.* **2003**, *10*, 76–100. [CrossRef]
9. Ashkenazi, A.; Holland, P.; Eckhardt, S.G. Ligand-based targeting of apoptosis in cancer: The potential of recombinant human apoptosis ligand 2/Tumor necrosis factor-related apoptosis-inducing ligand (rhApo2L/TRAIL). *J. Clin. Oncol.* **2008**, *26*, 3621–3630. [CrossRef] [PubMed]
10. Walczak, H.; Miller, R.E.; Ariail, K.; Gliniak, B.; Griffith, T.S.; Kubin, M.; Chin, W.; Jones, J.; Woodward, A.; Le, T.; et al. Tumoricidal activity of tumor necrosis factor-related apoptosis-inducing ligand in vivo. *Nat. Med.* **1999**, *5*, 157–163. [CrossRef]
11. Eberle, J. Countering TRAIL Resistance in Melanoma. *Cancers* **2019**, *11*, 656. [CrossRef]
12. Bauer, D.; Werth, F.; Nguyen, H.A.; Kiecker, F.; Eberle, J. Critical role of reactive oxygen species (ROS) for synergistic enhancement of apoptosis by vemurafenib and the potassium channel inhibitor TRAM-34 in melanoma cells. *Cell Death Dis.* **2017**, *8*, e2594. [CrossRef]
13. Quast, S.A.; Berger, A.; Eberle, J. ROS-dependent phosphorylation of Bax by wortmannin sensitizes melanoma cells for TRAIL-induced apoptosis. *Cell Death Dis.* **2013**, *4*, e839. [CrossRef] [PubMed]
14. Zhivkova, V.; Kiecker, F.; Langer, P.; Eberle, J. Crucial role of reactive oxygen species (ROS) for the proapoptotic effects of indirubin derivative DKP-073 in melanoma cells. *Mol. Carcinog.* **2019**, *58*, 258–269. [CrossRef]
15. Soltan, M.Y.; Sumarni, U.; Assaf, C.; Langer, P.; Reidel, U.; Eberle, J. Key Role of Reactive Oxygen Species (ROS) in Indirubin Derivative-Induced Cell Death in Cutaneous T-Cell Lymphoma Cells. *Int. J. Mol. Sci.* **2019**, *20*, 1158. [CrossRef] [PubMed]

16. Gurram, B.; Zhang, S.; Li, M.; Li, H.; Xie, Y.; Cui, H.; Du, J.; Fan, J.; Wang, J.; Peng, X. Celecoxib Conjugated Fluorescent Probe for Identification and Discrimination of Cyclooxygenase-2 Enzyme in Cancer Cells. *Anal. Chem.* **2018**, *90*, 5187–5193. [CrossRef] [PubMed]
17. Grosch, S.; Maier, T.J.; Schiffmann, S.; Geisslinger, G. Cyclooxygenase-2 (COX-2)-independent anticarcinogenic effects of selective COX-2 inhibitors. *J. Natl. Cancer Inst.* **2006**, *98*, 736–747. [CrossRef]
18. Arber, N.; Eagle, C.J.; Spicak, J.; Racz, I.; Dite, P.; Hajer, J.; Zavoral, M.; Lechuga, M.J.; Gerletti, P.; Tang, J.; et al. Celecoxib for the prevention of colorectal adenomatous polyps. *N. Engl. J. Med.* **2006**, *355*, 885–895. [CrossRef] [PubMed]
19. Thompson, P.A.; Ashbeck, E.L.; Roe, D.J.; Fales, L.; Buckmeier, J.; Wang, F.; Bhattacharyya, A.; Hsu, C.H.; Chow, S.H.; Ahnen, D.J.; et al. Celecoxib for the Prevention of Colorectal Adenomas: Results of a Suspended Randomized Controlled Trial. *J. Natl. Cancer Inst.* **2016**, *108*, djw151. [CrossRef] [PubMed]
20. Gallouet, A.S.; Travert, M.; Bresson-Bepoldin, L.; Guilloton, F.; Pangault, C.; Caulet-Maugendre, S.; Lamy, T.; Tarte, K.; Guillaudeux, T. COX-2-independent effects of celecoxib sensitize lymphoma B cells to TRAIL-mediated apoptosis. *Clin. Cancer Res.* **2014**, *20*, 2663–2673. [CrossRef]
21. Xu, X.T.; Hu, W.T.; Zhou, J.Y.; Tu, Y. Celecoxib enhances the radiosensitivity of HCT116 cells in a COX-2 independent manner by up-regulating BCCIP. *Am. J. Transl. Res.* **2017**, *9*, 1088–1100. [PubMed]
22. Grosch, S.; Tegeder, I.; Niederberger, E.; Brautigam, L.; Geisslinger, G. COX-2 independent induction of cell cycle arrest and apoptosis in colon cancer cells by the selective COX-2 inhibitor celecoxib. *FASEB J.* **2001**, *15*, 2742–2744. [CrossRef] [PubMed]
23. Que, S.K.T.; Zwald, F.O.; Schmults, C.D. Cutaneous squamous cell carcinoma: Incidence, risk factors, diagnosis, and staging. *J. Am. Acad. Dermatol.* **2018**, *78*, 237–247. [CrossRef] [PubMed]
24. Rosenberg, A.R.; Tabacchi, M.; Ngo, K.H.; Wallendorf, M.; Rosman, I.S.; Cornelius, L.A.; Demehri, S. Skin cancer precursor immunotherapy for squamous cell carcinoma prevention. *JCI Insight* **2019**, *4*, e125476. [CrossRef]
25. Toloczko-Iwaniuk, N.; Dziemianczyk-Pakiela, D.; Nowaszewska, B.K.; Celinska-Janowicz, K.; Miltyk, W. Celecoxib in Cancer Therapy and Prevention—Review. *Curr. Drug Targets* **2019**, *20*, 302–315. [CrossRef]
26. Rosas, C.; Sinning, M.; Ferreira, A.; Fuenzalida, M.; Lemus, D. Celecoxib decreases growth and angiogenesis and promotes apoptosis in a tumor cell line resistant to chemotherapy. *Biol. Res.* **2014**, *47*, 27. [CrossRef] [PubMed]
27. Ghanghas, P.; Jain, S.; Rana, C.; Sanyal, S.N. Chemoprevention of Colon Cancer through Inhibition of Angiogenesis and Induction of Apoptosis by Nonsteroidal Anti-Inflammatory Drugs. *J. Environ. Pathol. Toxicol. Oncol.* **2016**, *35*, 273–289. [CrossRef]
28. Li, W.W.; Long, G.X.; Liu, D.B.; Mei, Q.; Wang, J.F.; Hu, G.Y.; Jiang, J.Z.; Sun, W.; Gan, L.; Hu, G.Q. Cyclooxygenase-2 inhibitor celecoxib suppresses invasion and migration of nasopharyngeal carcinoma cell lines through a decrease in matrix metalloproteinase-2 and -9 activity. *Pharmazie* **2014**, *69*, 132–137.
29. Wang, L.W.; Hsiao, C.F.; Chen, W.T.; Lee, H.H.; Lin, T.C.; Chen, H.C.; Chen, H.H.; Chien, C.R.; Lin, T.Y.; Liu, T.W. Celecoxib plus chemoradiotherapy for locally advanced rectal cancer: A phase II TCOG study. *J. Surg. Oncol.* **2014**, *109*, 580–585. [CrossRef]
30. Elmets, C.A.; Viner, J.L.; Pentland, A.P.; Cantrell, W.; Lin, H.Y.; Bailey, H.; Kang, S.; Linden, K.G.; Heffernan, M.; Duvic, M.; et al. Chemoprevention of nonmelanoma skin cancer with celecoxib: A randomized, double-blind, placebo-controlled trial. *J. Natl. Cancer Inst.* **2010**, *102*, 1835–1844. [CrossRef]
31. Torres-Collado, A.X.; Jazirehi, A.R. Overcoming Resistance of Human Non-Hodgkin's Lymphoma to CD19-CAR CTL Therapy by Celecoxib and Histone Deacetylase Inhibitors. *Cancers* **2018**, *10*, 200. [CrossRef]
32. Gowda, R.; Sharma, A.; Robertson, G.P. Synergistic inhibitory effects of Celecoxib and Plumbagin on melanoma tumor growth. *Cancer Lett.* **2017**, *385*, 243–250. [CrossRef]
33. Guo, Q.; Liu, X.; Lu, L.; Yuan, H.; Wang, Y.; Chen, Z.; Ji, R.; Zhou, Y. Comprehensive evaluation of clinical efficacy and safety of celecoxib combined with chemotherapy in management of gastric cancer. *Medicine* **2017**, *96*, e8857. [CrossRef] [PubMed]
34. Perroud, H.A.; Rico, M.J.; Alasino, C.M.; Queralt, F.; Mainetti, L.E.; Pezzotto, S.M.; Rozados, V.R.; Scharovsky, O.G. Safety and therapeutic effect of metronomic chemotherapy with cyclophosphamide and celecoxib in advanced breast cancer patients. *Future Oncol.* **2013**, *9*, 451–462. [CrossRef] [PubMed]
35. Liu, X.; Yue, P.; Zhou, Z.; Khuri, F.R.; Sun, S.Y. Death receptor regulation and celecoxib-induced apoptosis in human lung cancer cells. *J. Natl. Cancer Inst.* **2004**, *96*, 1769–1780. [CrossRef]
36. Edagawa, M.; Kawauchi, J.; Hirata, M.; Goshima, H.; Inoue, M.; Okamoto, T.; Murakami, A.; Maehara, Y.; Kitajima, S. Role of activating transcription factor 3 (ATF3) in endoplasmic reticulum (ER) stress-induced sensitization of p53-deficient human colon cancer cells to tumor necrosis factor (TNF)-related apoptosis-inducing ligand (TRAIL)-mediated apoptosis through up-regulation of death receptor 5 (DR5) by zerumbone and celecoxib. *J. Biol. Chem.* **2014**, *289*, 21544–21561.
37. van Roosmalen, I.A.M.; Reis, C.R.; Setroikromo, R.; Yuvaraj, S.; Joseph, J.V.; Tepper, P.G.; Kruyt, F.A.E.; Quax, W.J. The ER stress inducer DMC enhances TRAIL-induced apoptosis in glioblastoma. *Springerplus* **2014**, *3*, 495. [CrossRef]
38. Fecker, L.F.; Stockfleth, E.; Braun, F.K.; Rodust, P.M.; Schwarz, C.; Kohler, A.; Leverkus, M.; Eberle, J. Enhanced death ligand-induced apoptosis in cutaneous SCC cells by treatment with diclofenac/hyaluronic acid correlates with downregulation of c-FLIP. *J. Investig. Dermatol.* **2010**, *130*, 2098–2109. [CrossRef]
39. Pang, R.P.; Zhou, J.G.; Zeng, Z.R.; Li, X.Y.; Chen, W.; Chen, M.H.; Hu, P.J. Celecoxib induces apoptosis in COX-2 deficient human gastric cancer cells through Akt/GSK3beta/NAG-1 pathway. *Cancer Lett.* **2007**, *251*, 268–277. [CrossRef]
40. Liu, X.; Yue, P.; Schonthal, A.H.; Khuri, F.R.; Sun, S.Y. Cellular FLICE-inhibitory protein down-regulation contributes to celecoxib-induced apoptosis in human lung cancer cells. *Cancer Res.* **2006**, *66*, 11115–11119. [CrossRef]

41. Jeong, H.S.; Choi, H.Y.; Lee, E.R.; Kim, J.H.; Jeon, K.; Lee, H.J.; Cho, S.G. Involvement of caspase-9 in autophagy-mediated cell survival pathway. *Biochim. Biophys. Acta* **2011**, *1813*, 80–90. [CrossRef]
42. Irmler, M.; Thome, M.; Hahne, M.; Schneider, P.; Hofmann, K.; Steiner, V.; Bodmer, J.L.; Schroter, M.; Burns, K.; Mattmann, C.; et al. Inhibition of death receptor signals by cellular FLIP. *Nature* **1997**, *388*, 190–195. [CrossRef]
43. Deveraux, Q.L.; Takahashi, R.; Salvesen, G.S.; Reed, J.C. X-linked IAP is a direct inhibitor of cell-death proteases. *Nature* **1997**, *388*, 300–304. [CrossRef]
44. Zhang, S.; Suvannasankha, A.; Crean, C.D.; White, V.L.; Johnson, A.; Chen, C.S.; Farag, S.S. OSU-03012, a novel celecoxib derivative, is cytotoxic to myeloma cells and acts through multiple mechanisms. *Clin. Cancer Res.* **2007**, *13*, 4750–4758. [CrossRef] [PubMed]
45. Xu, Y.; Zhao, Y.M.; Huang, H. Celecoxib-induced apoptosis in acute promyelocytic leukemia cell line MR2 and its mechanism. *J. Zhejiang Univ. Med. Sci.* **2007**, *36*, 319–324. [PubMed]
46. Karimian, A.; Ahmadi, Y.; Yousefi, B. Multiple functions of p21 in cell cycle, apoptosis and transcriptional regulation after DNA damage. *DNA Repair* **2016**, *42*, 63–71. [CrossRef]
47. Dvory-Sobol, H.; Cohen-Noyman, E.; Kazanov, D.; Figer, A.; Birkenfeld, S.; Madar-Shapiro, L.; Benamouzig, R.; Arber, N. Celecoxib leads to G2/M arrest by induction of p21 and down-regulation of cyclin B1 expression in a p53-independent manner. *Eur. J. Cancer* **2006**, *42*, 422–426. [CrossRef] [PubMed]
48. Yamanaka, Y.; Shiraki, K.; Inoue, T.; Miyashita, K.; Fuke, H.; Yamaguchi, Y.; Yamamoto, N.; Ito, K.; Sugimoto, K.; Nakano, T. COX-2 inhibitors sensitize human hepatocellular carcinoma cells to TRAIL-induced apoptosis. *Int. J. Mol. Med.* **2006**, *18*, 41–47. [CrossRef]
49. Sitailo, L.A.; Jerome-Morais, A.; Denning, M.F. Mcl-1 functions as major epidermal survival protein required for proper keratinocyte differentiation. *J. Investig. Dermatol.* **2009**, *129*, 1351–1360. [CrossRef]
50. Kern, M.A.; Haugg, A.M.; Koch, A.F.; Schilling, T.; Breuhahn, K.; Walczak, H.; Fleischer, B.; Trautwein, C.; Michalski, C.; Schulze-Bergkamen, H.; et al. Cyclooxygenase-2 inhibition induces apoptosis signaling via death receptors and mitochondria in hepatocellular carcinoma. *Cancer Res.* **2006**, *66*, 7059–7066. [CrossRef]
51. Rodust, P.M.; Fecker, L.F.; Stockfleth, E.; Eberle, J. Activation of mitochondrial apoptosis pathways in cutaneous squamous cell carcinoma cells by diclofenac/hyaluronic acid is related to upregulation of Bad as well as downregulation of Mcl-1 and Bcl-w. *Exp. Dermatol.* **2012**, *21*, 520–525. [CrossRef]
52. Ishihara, T.; Hoshino, T.; Namba, T.; Tanaka, K.; Mizushima, T. Involvement of up-regulation of PUMA in non-steroidal anti-inflammatory drug-induced apoptosis. *Biochem. Biophys. Res. Commun.* **2007**, *356*, 711–717. [CrossRef]
53. Franke, J.C.; Plötz, M.; Prokop, A.; Geilen, C.C.; Schmalz, H.G.; Eberle, J. New caspase-independent but ROS-dependent apoptosis pathways are targeted in melanoma cells by an iron-containing cytosine analogue. *Biochem. Pharmacol.* **2010**, *79*, 575–586. [CrossRef]
54. Pritchard, R.; Rodriguez-Enriquez, S.; Pacheco-Velazquez, S.C.; Bortnik, V.; Moreno-Sanchez, R.; Ralph, S. Celecoxib inhibits mitochondrial O_2 consumption, promoting ROS dependent death of murine and human metastatic cancer cells via the apoptotic signalling pathway. *Biochem. Pharmacol.* **2018**, *154*, 318–334. [CrossRef]
55. Sung, M.W.; Lee, D.Y.; Park, S.W.; Oh, S.M.; Choi, J.J.; Shin, E.S.; Kwon, S.K.; Ahn, S.H.; Kim, Y.H. Celecoxib enhances the inhibitory effect of 5-FU on human squamous cell carcinoma proliferation by ROS production. *Laryngoscope* **2017**, *127*, E117–E123. [CrossRef] [PubMed]
56. Perumal, V.; Banerjee, S.; Das, S.; Sen, R.K.; Mandal, M. Effect of liposomal celecoxib on proliferation of colon cancer cell and inhibition of DMBA-induced tumor in rat model. *Cancer Nanotechnol.* **2011**, *2*, 67–79. [CrossRef] [PubMed]
57. Kirkova, M.; Alexandova, A.; Kesiova, M.; Tsvetanova, E.; Georgieva, A.; Todorov, S. Potential antioxidant activity of celecoxib and amtolmetin guacyl: In vitro studies. *Auton. Autacoid Pharmacol.* **2007**, *27*, 13–18. [CrossRef] [PubMed]
58. Shitara, K.; Doi, T.; Nagano, O.; Fukutani, M.; Hasegawa, H.; Nomura, S.; Sato, A.; Kuwata, T.; Asai, K.; Einaga, Y.; et al. Phase 1 study of sulfasalazine and cisplatin for patients with CD44v-positive gastric cancer refractory to cisplatin (EPOC1407). *Gastric Cancer* **2017**, *20*, 1004–1009. [CrossRef]
59. Perillo, B.; Di Donato, M.; Pezone, A.; Di Zazzo, E.; Giovannelli, P.; Galasso, G.; Castoria, G.; Migliaccio, A. ROS in cancer therapy: The bright side of the moon. *Exp. Mol. Med.* **2020**, *52*, 192–203. [CrossRef]
60. Bukamur, H.; Katz, H.; Alsharedi, M.; Alkrekshi, A.; Shweihat, Y.R.; Munn, N.J. Immune Checkpoint Inhibitor-Related Pulmonary Toxicity: Focus on Nivolumab. *South Med. J.* **2020**, *113*, 600–605. [CrossRef] [PubMed]

Auszug aus der Journal Summary List (2)

Journal Data Filtered By: **Selected JCR Year: 2019** Selected Editions: SCIE,SSCI Selected Categories: **"BIOCHEMISTRY and MOLECULAR BIOLOGY"** Selected Category Scheme: WoS

Gesamtanzahl: 297 Journale

Rank	Full Journal Title	Total Cites	Journal Impact Factor	Eigenfactor Score
1	CELL	258,178	38.637	0.564970
2	NATURE MEDICINE	85,220	36.130	0.168730
3	Annual Review of Biochemistry	20,499	25.787	0.024820
4	MOLECULAR CELL	69,148	15.584	0.166260
5	Molecular Cancer	15,448	15.302	0.023990
6	PROGRESS IN LIPID RESEARCH	6,139	15.083	0.005730
7	TRENDS IN BIOCHEMICAL SCIENCES	18,416	14.732	0.032060
8	TRENDS IN MICROBIOLOGY	13,604	13.546	0.022780
9	Signal Transduction and Targeted Therapy	1,182	13.493	0.003380
10	Nature Chemical Biology	22,084	12.587	0.060130
11	MOLECULAR PSYCHIATRY	22,227	12.384	0.054730
12	Molecular Plant	11,432	12.084	0.028530
13	NATURAL PRODUCT REPORTS	11,239	12.000	0.013610
14	NATURE STRUCTURAL & MOLECULAR BIOLOGY	27,178	11.980	0.056800
15	NUCLEIC ACIDS RESEARCH	201,649	11.501	0.403470
16	TRENDS IN MOLECULAR MEDICINE	10,618	11.099	0.018720
17	GENOME RESEARCH	41,755	11.093	0.076940
18	MOLECULAR BIOLOGY AND EVOLUTION	50,486	11.062	0.084810
19	CELL DEATH AND DIFFERENTIATION	21,095	10.717	0.029600
20	Redox Biology	10,157	9.986	0.023810

Rank	Full Journal Title	Total Cites	Journal Impact Factor	Eigenfactor Score
21	EMBO JOURNAL	64,724	9.889	0.059690
22	CURRENT OPINION IN CHEMICAL BIOLOGY	10,968	9.689	0.017770
23	PLANT CELL	54,927	9.618	0.048640
24	CURRENT BIOLOGY	63,256	9.601	0.133170
25	MOLECULAR ASPECTS OF MEDICINE	6,207	9.577	0.005750
26	Molecular Systems Biology	8,914	8.991	0.017390
27	Cell Systems	3,822	8.673	0.029290
28	MATRIX BIOLOGY	6,878	8.572	0.011920
29	ONCOGENE	66,303	7.971	0.068320
30	Cell Chemical Biology	3,326	7.739	0.015770
31	CRITICAL REVIEWS IN BIOCHEMISTRY AND MOLECULAR BIOLOGY	3,675	7.634	0.006380
32	EMBO REPORTS	14,976	7.497	0.030290
33	BIOCHIMICA ET BIOPHYSICA ACTA-REVIEWS ON CANCER	5,650	7.365	0.007800
34	PLOS BIOLOGY	31,650	7.076	0.060300
35	Essays in Biochemistry	2,383	6.966	0.005060
36	CURRENT OPINION IN STRUCTURAL BIOLOGY	11,035	6.908	0.021890
37	CELLULAR AND MOLECULAR LIFE SCIENCES	26,128	6.496	0.037010
38	Science Signaling	12,736	6.467	0.026590
39	ANTIOXIDANTS & REDOX SIGNALING	21,119	6.323	0.024660
40	Molecular Ecology Resources	10,868	6.286	0.019630
41	FREE RADICAL BIOLOGY AND MEDICINE	42,665	6.170	0.036960
42	BIOMACROMOLECULES	38,863	6.092	0.031320

Selected JCR Year: 2019; Selected Categories: "BIOCHEMISTRY and MOLECULAR BIOLOGY"

Rank	Full Journal Title	Total Cites	Journal Impact Factor	Eigenfactor Score
43	Computational and Structural Biotechnology Journal	1,954	6.018	0.004980
44	CYTOKINE & GROWTH FACTOR REVIEWS	5,935	5.982	0.007380
45	Advances in Carbohydrate Chemistry and Biochemistry	634	5.800	0.000340
46	EXPERIMENTAL AND MOLECULAR MEDICINE	5,536	5.418	0.010300
47	AMERICAN JOURNAL OF RESPIRATORY CELL AND MOLECULAR BIOLOGY	12,243	5.373	0.016040
48	RNA Biology	6,589	5.350	0.015820
49	Acta Crystallographica Section D-Structural Biology	21,750	5.266	0.018220
50	MOLECULAR ECOLOGY	38,951	5.163	0.050800
51	INTERNATIONAL JOURNAL OF BIOLOGICAL MACROMOLECULES	47,121	5.162	0.057240
52	BIOCHEMICAL SOCIETY TRANSACTIONS	12,651	5.160	0.016140
53	HUMAN MOLECULAR GENETICS	39,652	5.100	0.064170
54	Journal of Genetics and Genomics	2,271	5.065	0.004310
55	Cell and Bioscience	1,898	5.026	0.004210
56	Antioxidants	2,568	5.014	0.004170
57	FASEB JOURNAL	43,426	4.966	0.043730
58	International Review of Cell and Molecular Biology	2,167	4.934	0.004350
59	Open Biology	2,886	4.931	0.009590
60	Journal of Integrative Plant Biology	5,005	4.885	0.006830
61	Advances in Microbial Physiology	1,227	4.875	0.000960
61	Nucleic Acid Therapeutics	1,030	4.875	0.003610

Selected JCR Year: 2019; Selected Categories: "BIOCHEMISTRY and MOLECULAR BIOLOGY"

Publication 2

antioxidants

MDPI

Article

Crucial Role of Reactive Oxygen Species (ROS) for the Proapoptotic Effects of Indirubin Derivatives in Cutaneous SCC Cells

Jiaqi Zhu [1,2], Peter Langer [3,4], Claas Ulrich [1] and Jürgen Eberle [1,*]

[1] Skin Cancer Center, Department of Dermatology, Venerology and Allergology, Charité Universitätsmedizin Berlin, 10117 Berlin, Germany; zhujiaqijiaqi@gmail.com (J.Z.); claas.ulrich@charite.de (C.U.)
[2] Department of Gynecology and Obstetrics, Jilin University, Changchun 130000, China
[3] Institute of Chemistry, University of Rostock, 18051 Rostock, Germany; peter.langer@uni-rostock.de
[4] Leibniz Institute of Catalysis, University of Rostock, 18051 Rostock, Germany
* Correspondence: juergen.eberle@charite.de; Tel.: +49-30-450-518-383

Abstract: Efficient drugs are needed for countering the worldwide high incidence of cutaneous squamous cell carcinoma (cSCC) and actinic keratosis. Indirubin derivatives represent promising candidates, but their effects in cSCC cells have not been reported before. Here, we investigated the efficacy of three indirubin derivatives (DKP-071, -073 and -184) in four cSCC cell lines. High efficacy was seen in SCL-I, SCL-II, SCC-12 and SCC-13, resulting in up to 80% loss of cell proliferation, 60% loss of cell viability and 30% induced apoptosis (10 μM). Apoptosis was further enhanced in combinations with TNF-related apoptosis-inducing ligand (TRAIL). Induction of reactive oxygen species (ROS) appeared as critical for these effects. Thus, antioxidative pretreatment completely abolished apoptosis as well as restored cell proliferation and viability. Concerning the pathways, complete activation of caspases cascades (caspases-3, -4, -6, -7, -8 and -9), loss of mitochondrial membrane potential, activation of proapoptotic PKCδ (protein kinase C delta), inhibition of STAT3 (signal transducer and activator of transcription 3), downregulation of antiapoptotic XIAP (X-linked inhibitor of apoptosis protein) and survivin as well as upregulation of the proapoptotic Bcl-2 protein Puma and the cell cycle inhibitor p21 were obtained. Importantly, all activation steps were prevented by antioxidants, thus proving ROS as a master regulator of indirubins' antitumor effects. ROS induction presently develops as an important issue in anticancer therapy.

Keywords: cutaneous SCC; indirubin; apoptosis; reactive oxygen species (ROS); antioxidants

Citation: Zhu, J.; Langer, P.; Ulrich, C.; Eberle, J. Crucial Role of Reactive Oxygen Species (ROS) for the Proapoptotic Effects of Indirubin Derivatives in Cutaneous SCC Cells. *Antioxidants* **2021**, *10*, 1514. https://doi.org/10.3390/antiox10101514

Academic Editors: Stefania Filosa and Tadeusz Sarna

Received: 20 June 2021
Accepted: 13 September 2021
Published: 24 September 2021

1. Introduction

Actinic keratosis (AK) derives from neoplastic epidermal keratinocytes and is characterized by high prevalence and the risk to proceed into invasive cutaneous squamous cell carcinoma (cSCC). Cutaneous SCC accounts for about 20% of skin malignancies and about 20% of skin cancer deaths worldwide [1,2]. For Caucasians and East Asian populations (including Japanese and Chinese), cSCC is the second most commonly diagnosed skin cancer, following basal cell carcinoma [3,4], whereas for black people, it is the most commonly diagnosed skin cancer [5]. New and alternative therapeutic options are needed for early and late disease.

The elimination of tumor cells by the induction of apoptosis represents a principal goal in cancer therapy, while therapy resistance is frequently explained by apoptosis deficiency [6]. Thus, resistance to apoptosis represents a crucial step in oncogenesis and drug resistance [7]. Three mayor types of cell death have been distinguished, namely type I (apoptosis), type II (autophagy) and type III (necrosis) [8]. Intrinsic proapoptotic pathways can be activated in response to cellular stress situations, including high levels of reactive oxygen species (ROS) as well as by anticancer treatment, e.g., by chemotherapy. This relies

on mitochondrial outer membrane permeability (MOMP), loss of mitochondrial membrane potential and release of mitochondrial factors such as cytochrome c, which may trigger activation of initiator caspase-9 [9]. This step is critically controlled by the family of pro- and anti-apoptotic Bcl-2 proteins. Thus, Bcl-2 exerts its antiapoptotic function through binding and inhibition of the proapoptotic family member Bax [8,9]. Often, activation of apoptosis and inhibition of cell proliferation are regulated in parallel. Thus, the cyclin-dependent kinase inhibitor p21 (Cip1/Waf1) represents a major target of p53, which also drives the expression of several proapoptotic factors [10].

On the other hand, extrinsic induction of apoptosis is initiated by death ligands such as CD95L/FasL and TRAIL (TNF-related apoptosis-inducing ligand). Upon death receptor activation, cell membrane-bound death-inducing signaling complexes are formed, resulting in activation of initiator caspases, such as caspase-8 and caspase-10 [11]. In particular, the death ligand TRAIL has attracted much consideration due to its anticancer activity, while normal cells are largely spared [12,13]. Furthermore, caspase-4 may be involved in endoplasmic reticulum stress-induced apoptosis, besides its roles in inflammation [14,15]. Initiator caspases may cleave and thus activate effector caspases such as caspases-3, -6 and -7, which themselves cleave a large number of death substrates with the final result of DNA fragmentation and apoptosis induction [16].

Additionally, several signaling pathways contribute to the regulation of apoptosis. Thus, the STAT3 pathway can be activated in response to cytokines and growth factors. STAT3 then translocates to the cell nucleus and acts as a transcription activator for a variety of genes that mediate cell growth and inhibition of apoptosis [17]. The protein kinase C (PKC) family of isoenzymes encloses several serine-threonine kinases, which are involved in the regulation of different cellular processes, including cell proliferation, cell differentiation and apoptosis [18]. While PKCα and PKCβ in particular support cell proliferation and cell invasion [19], PKCδ was reported as proapoptotic. Following phosphorylation and translocation steps, PKCδ can be activated through processing, which releases the active catalytic domain (41 kDa) from its 78 kDa proform. Activated PKCδ was related to the induction of apoptosis through tyrosine phosphorylation and thus activation of caspase-3 [20,21].

Reactive oxygen species (ROS) are involved in several signaling pathways. The formation of different kinds of ROS can result in molecular damage and increased oxidative activity. Thus, ROS play important roles in different kinds of diseases of the neuronal, cardiovascular and nervous systems, as well as in aging [22]. Furthermore, ROS may contribute to the regulation of apoptosis, as shown in melanoma cells by an iron-substituted nucleoside analogue [23], in cSCC cells for celecoxib [24] and in cutaneous T-cell lymphoma cells (CTCL) for an indirubin derivative [25]. ROS may derive from mitochondrial leakage or other sources [26], but their relation to the described apoptosis pathways is less clear to date.

Indirubin has been identified as the active ingredient of a traditional Chinese herbal medicine (Danggui Longhui Wan), used for treatment of chronic and inflammatory diseases. Clinical results from the 1980s, which have been obtained in chronic myelocytic leukemia patients treated with indirubin, stimulated several studies on this compound [27,28]. Due to the only limited antitumor activity of the native form, the structure of indirubin is presently employed in several laboratories as a skeleton for the synthesis of new derivatives to increase its antitumor effects [29–31].

We have previously reported the synthesis of a new series of indirubin derivatives based on N-glycosylated 3-alkylideneoxindoles containing halogen substituents [32]. Here, we investigated the proapoptotic effects of DKP-071, DKP-073 and DKP-184 in cSCC cells and unraveled the downstream signaling pathways. These appeared as essentially based on the production of reactive oxygen species, which opens new perceptions in the proapoptotic targeting of cSCC cells.

2. Materials and Methods

2.1. Cell Culture and Treatment

For investigating the effects of indirubin derivatives DKP-071, DKP-073 and DKP-184, we investigated four cSCC cell lines (SCL-I, SCL-II, SCC-12 and SCC-13). There is not much information in the literature to distinguish these cell lines by their origin, as all four derive from human facial skin. Only in terms of sensitivity, we found in previous studies that SCL-I is resistant to diclofenac/hyaluronic acid, while others were sensitive [33]. The HaCaT cell line was reported to derive from spontaneously immortalized keratinocytes [34]. Cells were maintained at 5% CO_2 in RPMI 1640 growth medium (Life Technologies, Darmstadt, Germany) supplemented with 10% FCS, 2 mM glutamine and non-essential amino acids. Most assays were performed in 24-well plates, and 4×10^4 cells were seeded per well.

Cells were treated with KillerTRAIL™ (Adipogen, San Diego, CA, USA; AG-40T-0001; 50 ng/mL) and with the indirubin derivatives DKP-071, DKP-073 and DKP-184 (2.5–20 μM) [32], whereas control cells received only the solvent DMSO. Cells were also treated with non-substituted indirubin (BioMol, Hamburg, Germany; TGM-T6169) at equimolar concentrations. For caspase inhibition, cells were treated with the pan-caspase inhibitor QVD-Oph (Abcam, Cambridge, UK; 10 μM), which was applied 1 h before cells were treated with agonists. For inhibition of PKCδ, bisindolylmaleimide I (Cayman Chemical, Ann Arbor, MI, USA) was used at 1 μM.

2.2. Cell Proliferation Assays

Cell proliferation was determined by WST-1 assay (Roche Diagnostics, Penzberg, Germany), which depends on the cleavage of the water-soluble tetrazolium salt by mitochondrial dehydrogenases in metabolically active cells. WST-1 detects live cells and can thus by used for counting only viable cells. The read-out is thus complex and reflects both cell number and viability of quantified cells.

2.3. Determination of Apoptosis, Cell Viability and Cytotoxicity

Quantification of apoptosis was performed by cell cycle analysis. Cells were harvested by trypsinization, and all cells were lysed in hypotonic buffer. In this way, cells' nuclei were isolated and were further stained for 1 h with 40 mg/mL of propidium iodide (Sigma-Aldrich, St. Louis, MO, USA). Cells in G1, G2 and S-phase, as well as sub-G1 cells, were depicted by flow cytometry at FL3A using a FACS Calibur (BD Bioscience, Bedford, MA, USA). Due to the washing out of small DNA fragments, nuclei with less DNA than G1 (sub-G1) correspond to apoptotic cells. Thus, the increase of the sub-G1 fraction indicates the percentage of cells with DNA fragmentation (apoptotic cells).

Cell viability was determined by staining cells with calcein-AM (PromoCell, Heidelberg, Germany), which is converted in viable cells by intracellular esterases to green fluorescent calcein. Cells, grown and treated in 24-well plates, were harvested by trypsinization and stained with 2.5 μg/mL of calcein-AM at 37 °C for 1 h. Labeled cells were washed with PBS and measured by flow cytometry (FL2H).

Possible cytotoxic effects were determined at 4 and at 24 h of treatment by quantification of lactate dehydrogenase (LDH) activity in cell culture supernatants. Released LDH is indicative for damaged and cytotoxic cells. LDH activity was determined in an ELISA reader after applying a WST-1 cytotoxicity detection assay (Roche Diagnostics, Penzberg, Germany).

2.4. Mitochondrial Membrane Potential

Mitochondrial membrane potential ($\Delta\psi m$) was determined by staining cells with the fluorescent dye $TMRM^+$ (Sigma-Aldrich, Darmstadt, Germany). Cells, grown and treated in 24-well plates, were harvested by trypsinization and stained for 20 min at 37 °C with 1 μM of $TMRM^+$. After 2-times washing with PBS, cells were measured by flow cytometry (FL2H).

2.5. Analysis of Reactive Oxygen Species (ROS)

For determination of intracellular ROS levels, cells grown in 24-well plates were pre-incubated for 1 h with the fluorescent dye H_2DCF-DA (D-399, Thermo Fisher Scientific, Hennigsdorf, Germany, 10 µM), before starting treatment with effectors. After 2–24 h of treatment, cells were harvested by trypsinization, washed several times with PBS and analyzed by flow cytometry (FL1H). As a positive control, treatment with H_2O_2 (1 mM, 1 h) was applied. Antioxidative treatments were used, aiming at the suppression of indirubin-induced ROS levels. Thus, N-acetylcysteine (NAC, Sigma-Aldrich, Taufkirchen, Germany) was used in concentrations of up to 1 mM and was generally applied 1 h before starting indirubin treatments.

2.6. Western Blotting

For Western blotting, total protein extracts were obtained by a cell lysis buffer containing 150 mM NaCl, EDTA (1 mM), 1% NP-40, 50 mM Tris (pH 8.0) as well as phosphatase and protease inhibitors. Following SDS polyacrylamide gel electrophoresis, proteins were blotted on nitrocellulose membranes.

Primary antibodies of Cell Signaling (Danvers, MA, USA) were: Caspase-3 (9662, rabbit, 1:1000), Cleaved caspase-3 (9664, rabbit, 1:1000), Caspase-8 (9746, mouse, 1:1000), Caspase-9 (9502, rabbit, 1:1000), Caspase-6 (9762, rabbit, 1:1000), Caspase-7 (9492, rabbit, 1:1000), XIAP (2042, rabbit, 1:1000), Mcl-1 (4572, rabbit, 1:1000), Bad (9292, rabbit, 1:1000), Bcl-w (2724, rabbit, 1:1000), Bcl-2 (2872, rabbit, 1:1000). Primary antibodies of Santa Cruz Biotech (Dallas, TX, USA) were: Caspase-4 (sc-1229, goat, 1:500), c-FILP (sc-5276, mouse, 1:500), survivin (sc-177779, mouse, 1:500), p21(sc-6246, mouse, 1:500), β-actin (sc-47778, mouse, 1:1000), Puma (sc-374223, mouse, 1:500), Bax (sc-7480, mouse, 1:500), Bak (sc-832, mouse, 1:500). Primary antibody of Abcam (Cambridge, UK) was: DR5 (ab8416, rabbit, 1:1000). Secondary antibodies were: peroxidase-labeled goat anti-rabbit and goat anti-mouse (Dako, Hamburg, Germany; 1:5000).

2.7. Statistical Analyses

Each finding was proven by at least two independent experiments. For all assays, each independent experiment itself consisted of at least three independent values (three individual wells that were seeded, treated and analyzed individually). Thus, we had at least six values in one group, which were used for statistical analysis. Statistical significance was determined by Student's t-test and is indicated by asterisks in the figures (* $p < 0.05$; ** $p < 0.01$; *** $p < 0.001$).

For semi-quantitative protein analysis, Western blot signals were quantified by densitometry using Fusion-Capt Advance software (Vilber Lourmat, Collégien, France), values were normalized by the respective β-actin values and median values were formed from each two independent experiments (independent cell extracts).

3. Results

3.1. Decreased cSCC Cell Proliferation, Induction of Apoptosis and Loss of Cell Viability

As indirubin and its derivatives represent promising candidates for cSCC therapy, we investigated the effects of three indirubin derivatives (DKP-071, -073, -184; Figure 1a) in four representative cSCC cell lines (SCL-I, SCL-II, SCC-12 and SCC-13). As the death ligand TRAIL is expressed by immune cells in an antitumor immune response and as TRAIL agonists were already tested in clinical trials, combinations of the three indirubins with TRAIL were also investigated.

As cell proliferation represents an important issue in anticancer treatment, it was monitored by quantitative WST-1 assays, which determine live cells, in cSCC cell lines treated with 10 µM indirubin ± 50 ng/mL TRAIL. Cell proliferation rates at 24 h of treatment were generally reduced in cSCC cells by DKP-071, -073 and -184, reaching values of 30%, 29% and 48% (SCL-I), of 72%, 77% and 83% (SCL-II), of 50%, 48% and 79% (SCC-12)

as well as of 41%, 22% and 57% (SCC-13) (Figure 1b). These antiproliferative effects were further strongly enhanced by the combination of indirubins with TRAIL (Figure 1b).

Even more pronounced combination effects were seen at the level of cell viability, as determined by calcein staining and flow cytometry. At 24 h, cell viability was almost completely abolished by the combinations of DKP-071 or DKP-073 with TRAIL (<10%), whereas cell viability after single treatments with DKP-071 and DKP-073 ranged between 35% and 80%. The effects of DKP-184 were generally somewhat less pronounced (Figure 1c).

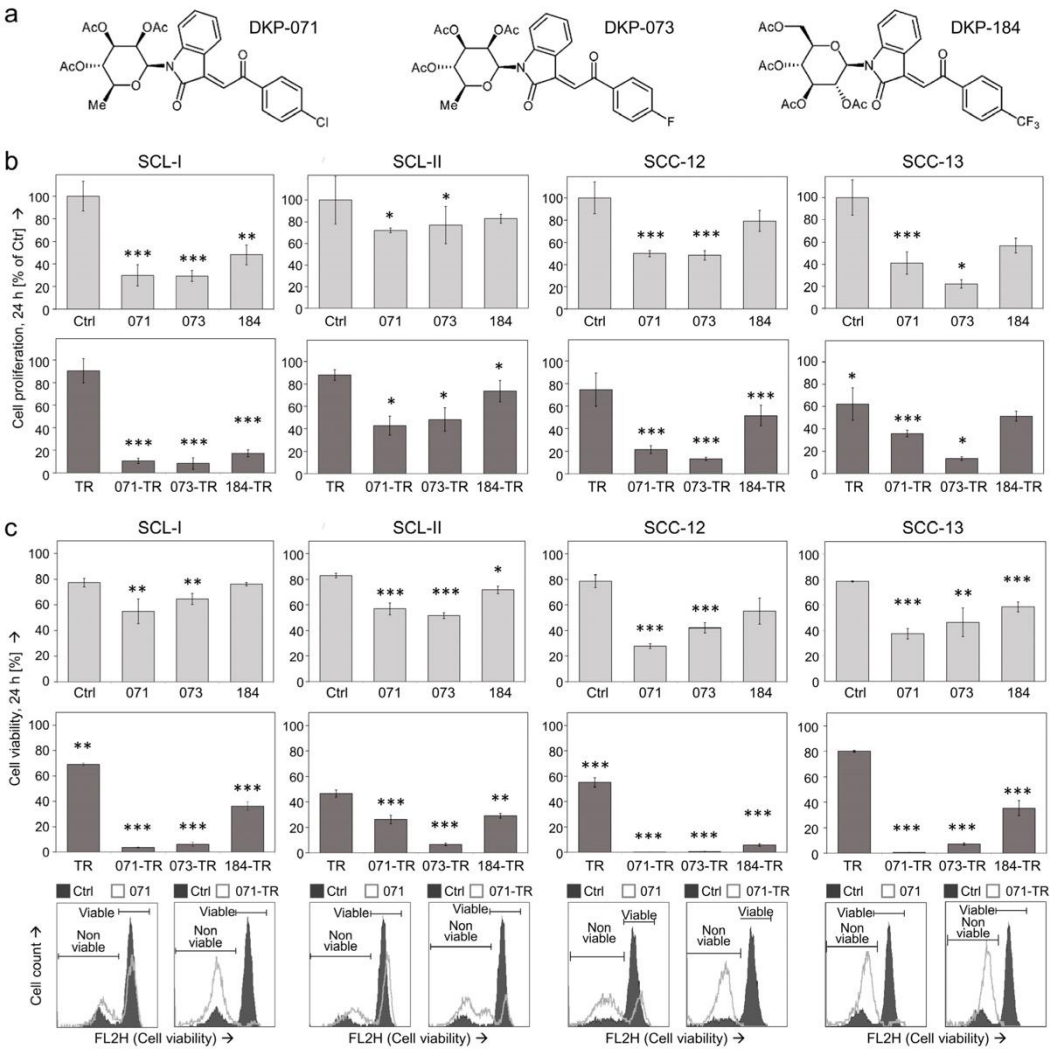

Figure 1. *Cont.*

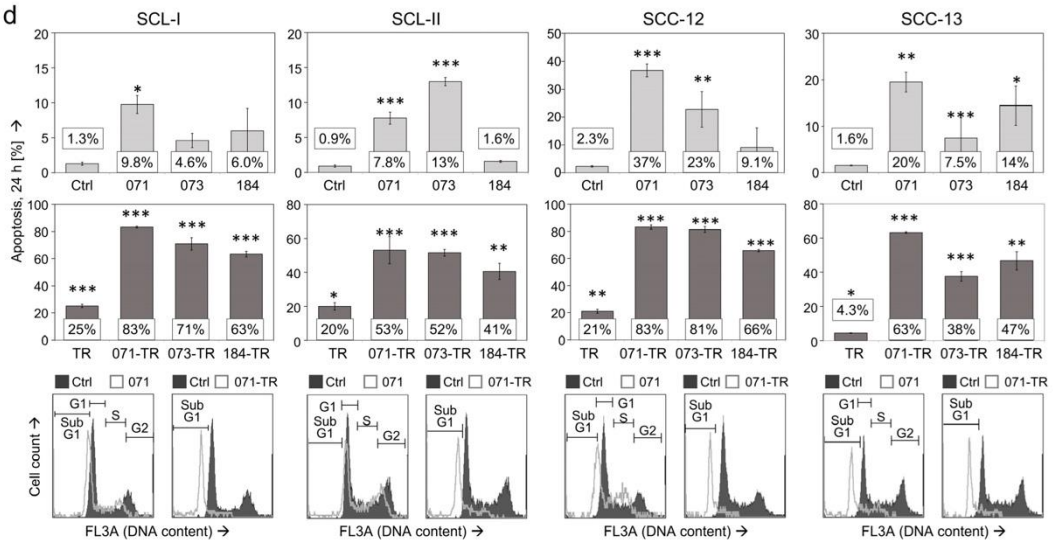

Figure 1. Decreased cell proliferation, cell viability and apoptosis induction. (**a**) Chemical structures of indirubin derivatives DKP-071, DKP-073 and DKP-184 are shown. (**b**) Cell proliferation was quantified by WST-1 assay in four cSCC cell lines at 24 h of treatment with indirubins (DKP-071, -073 and -184, 10 μM), TRAIL (TR; 50 ng/mL) or the combinations, as indicated. (**c**) Cell viability was determined by calcein-AM staining in cSCC cell lines at 24 h (treatment as above). (**c**) Apoptotic cells characterized by DNA fragmentation were identified by flow cytometry after propidium iodide staining as sub-G1 cells (cell cycle analyses, treatment as above). (**b**–**d**) Mean values are shown of triplicates of representative experiments (at least two independent experiments, each one with triplicates). (**c**,**d**) Examples of flow cytometry measurements are provided below (overlays of treated cells vs. controls). (**d**) The percentages of apoptotic cells are also indicated. Asterisks indicate statistical significance, as compared to controls (* $p < 0.05$; ** $p < 0.01$; *** $p < 0.001$).

Some induction of apoptosis was also seen at 24 h for DKP-071, -073 and -184 when applied alone, resulting in rates of 10%, 5% and 6% (SCL-I), 8%, 13% and 2% (SCL-II), 37%, 23% and 9% (SCC-12) as well as 19%, 8% and 14% (SCC-13) (Figure 1d). Most striking, however, was the enhancement of apoptosis by the combination of indirubins and TRAIL, resulting in apoptosis rates of 84%, 70% and 63% (SCL-I), 53%, 51% and 40% (SCL-II), 83%, 81% and 65% (SCC-12) and 63%, 38% and 47% (SCC-13) (Figure 1d). Of note, in response to indirubin treatments, the whole cell populations analyzed by flow cytometry were responsive and shifted in the direction of the sub-G1 area. Thus, the same marker for sub-G1 cell populations was used as in the controls (Figure 1d, insets). The high apoptosis values were approved by the particularly strong caspase activation, seen after combination treatments in Western blots (shown below).

The effects on apoptosis and cell viability were not associated with cytotoxicity, as determined by quantification of release of lactate dehydrogenase (LDH). There was no indication of increased cell necrosis in terms of LDH release, after treatment with the three indirubin derivatives as well as after combination treatments with TRAIL. This was found both at 4 h, excluding direct cytotoxic effects of the substances, as well as at 24 h, also largely excluding secondary necrotic effects (Supplementary Figure S1a,b).

The effects of indirubin derivatives were much stronger than those of non-substituted indirubin. This was shown in SCL-I and SCC-12 by applying equimolar concentrations (5, 10, 20 μM) of DKP-071 and non-substituted indirubin. While DKP-071 significantly triggered apoptosis and loss of cell viability when applied in concentrations of 10 and 20 μM, the effects of non-substituted indirubin were much less pronounced and resulted in only less than 5% apoptosis and at maximum in a reduction of cell viability to 67%,

when applied at 20 μM (Supplementary Figure S2a,b). However, the effects of indirubin derivatives appeared as not absolutely tumor-specific, as also some response was seen in HaCaT immortalized keratinocytes (up to 13% apoptosis, decrease of cell viability to 33%, Supplementary Figure S3). Thus, the combination of indirubin derivatives and TRAIL appeared as a promising strategy for targeting of cSCC cells.

3.2. Changes of Mitochondrial Membrane Potential

Addressing the mechanisms that mediate the antitumor effects of indirubins in cSCC cells, we determined changes in mitochondrial membrane potential (MMP) in response to indirubin treatments, applying $TMRM^+$ staining and flow cytometry. Loss of MMP was seen in SCL-I, SCC-12 and SCC-13 already at 4 h (44–78%, for DKP-071 and -073), indicative of an activation of mitochondrial apoptosis pathways (Figure 2a). Only SCL-II showed a delayed response, with no effects at 4 h but strong loss of MMP at 24 h (80%, 75% for DKP-071 and -073; Figure 2b). Thus, loss of MMP appeared as an early effect (4 h), at least in cell lines SCL-I, SCC-12 and SCC-13. At this time, apoptosis and loss of cell viability were not clearly evident. Thus, we can conclude that loss of MMP represents an initial effect, not secondary to cell death.

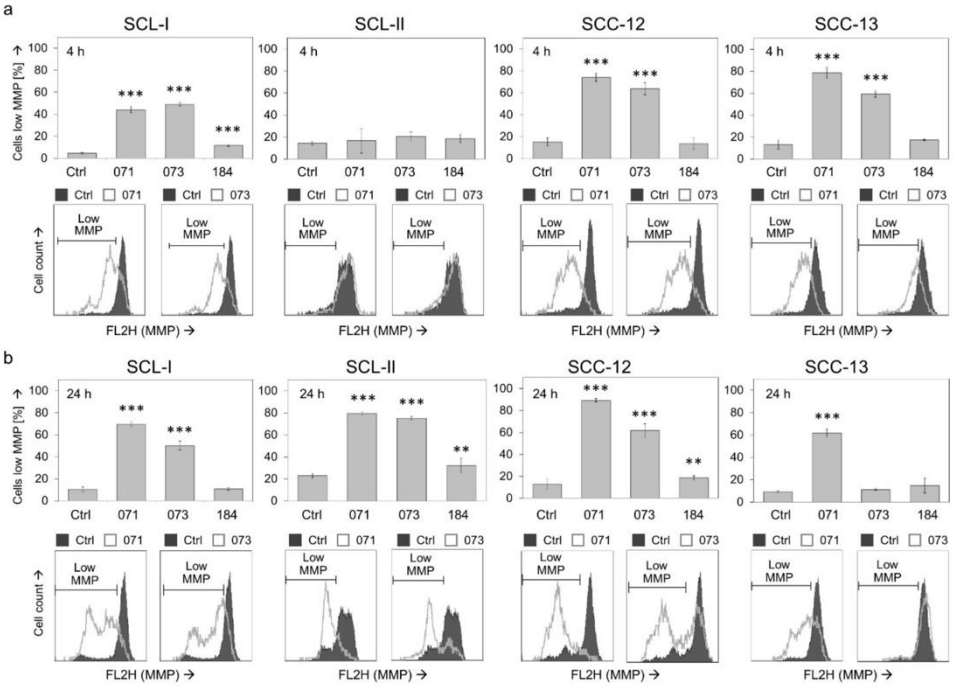

Figure 2. Loss of mitochondrial membrane potential (MMP). Percentages of cells with low MMP were determined by $TMRM^+$ staining at 4 h (**a**) and at 24 h (**b**) of treatment with indirubins (DKP-071, -073 and -184, 10 μM) in four cSCC cell lines. Cells with low MMP are defined by less staining than the main peak of control cells. Example flow cytometry measurements of controls and treatments are provided below (overlays of treated cells vs. controls), and cell fractions with low MMP are indicated. Mean values and SDs are shown of a representative experiment (two independent experiments, each one with triplicates). Asterisks indicate statistical significance, as compared to controls (** $p < 0.01$; *** $p < 0.001$).

3.3. High ROS Production in Response to Indirubin Derivatives in cSCC Cells

Increased evidence in recent years has shown that reactive oxygen species (ROS) may have vital roles in skin cancer therapy, related to induction of apoptosis. Production of ROS in response to indirubin treatment appeared as a very general and early effect in cSCC cells, as determined by H_2DCF-DA staining and flow cytometry. Of note, the effects of indirubins on ROS levels were complete, namely the whole cell population shifted to higher ROS levels, as seen in flow cytometry (Figure 3, insets). Thus, at 4 h of indirubin treatment, the cell proportions with high ROS levels were generally between 60% and 90% (Figure 3). Increased ROS levels appeared as a most pronounced response, affected in each cell line in response to the indirubin derivatives.

We aimed to see whether ROS production correlated with the effects on cell viability and apoptosis. Thus, ROS levels were quantified in response to increasing concentrations (2.5, 5, 10 and 20 μM) of a selected indirubin (DKP-071) in two cell lines (SCL-I and SCC-12). In parallel, assays for apoptosis and cell viability were performed. The experiments revealed that strong ROS production was seen only at concentrations of 10 and 20 μM, while 2.5 and 5 μM were much less effective (Supplementary Figure S4). Similarly, significant loss of cell viability and induction of apoptosis were also seen only for these higher concentrations (Supplementary Figure S2a,b). Thus, high ROS production correlated with loss of cell viability and apoptosis induction.

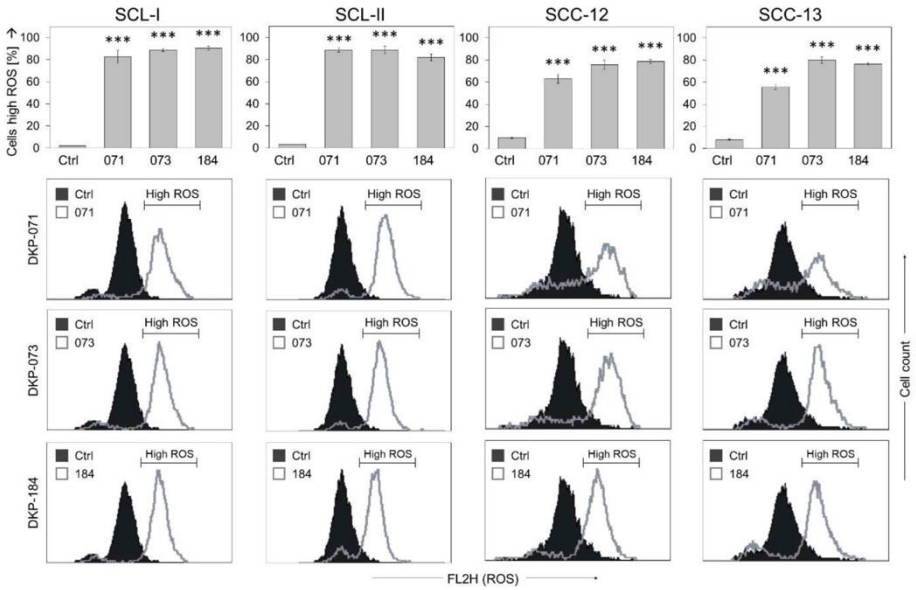

Figure 3. Changes in ROS production. ROS levels were determined by H_2DCF-DA staining in four cSCC cell lines at 4 h of treatment with indirubins (DKP-071, -073 and -184, 10 μM). Example cytometry measurements of controls and treatments are provided below (overlays of treated cells vs. controls), and cell fractions with high ROS are indicated. Mean values and SDs are shown of a representative experiment (two independent experiments, each one with triplicates). Asterisks (***) indicate high statistical significance, as compared to controls ($p < 0.001$).

ROS production was also determined at different times: 1, 2, 4 and 24 h. The main finding was that ROS comes particularly early, as shown in SCL-I and SCC-12 at 1 h (>90% cells with high ROS), and high ROS levels remained at least for 4 h (Supplementary Figure S5a), while at 24 h, percentages appeared as somewhat reduced (30–80%), possibly due to some ongoing cell proliferation (Supplementary Figure S5b).

3.4. Strong Caspase Activation in Course of Combined Treatment

Apoptosis can be regulated by caspase-dependent as well as by caspase-independent mechanisms. Thus, activation of the caspase cascade was investigated by Western blot analysis exemplarily in one of the 4 cell lines (SCL-I). Analyses included the effector caspases-3, -6 and -7, the initiator caspase-8 of the extrinsic pathway, the initiator caspase-9 of the intrinsic pathway as well as caspase-4, which may be involved in endoplasmic reticulum stress-induced apoptosis [14].

Treatment with indirubins alone showed some effects on caspase processing, indicative of their activation, however, the strongest caspase activation was obtained in the combinations of indirubins with TRAIL, in agreement with the apoptotic rates shown above. Thus, the proforms of caspase-4 (86 kDa), caspase-6 (35 kDa), caspase-7 (37 kDa), caspase-8 (55 kDa) and caspase-9 (47 kDa) were almost completely degraded at 24 h in response to DKP-071/TRAIL and DKP-073/TRAIL treatment (Figure 4). In parallel, characteristic processing products were obtained, such as of caspase-3 (20, 18, 16 kDa), caspase-7 (20 kDa), caspase-8 (43, 41, 18 kDa) and caspase-9 (37, 17 kDa), as well as some other intermediate or secondary processing products (Figure 4). Densitometric, semiquantitative analyses and normalization with the β-actin signals largely confirmed this strong regulation of caspases. The caspase processing in DKP-184-treated cells was generally somewhat weaker than DKP-071 and -073 (Figure 4), also in parallel with the apoptosis values provided above. Collectively, these data indicate complete activation of caspase cascades by indirubin/TRAIL combinations.

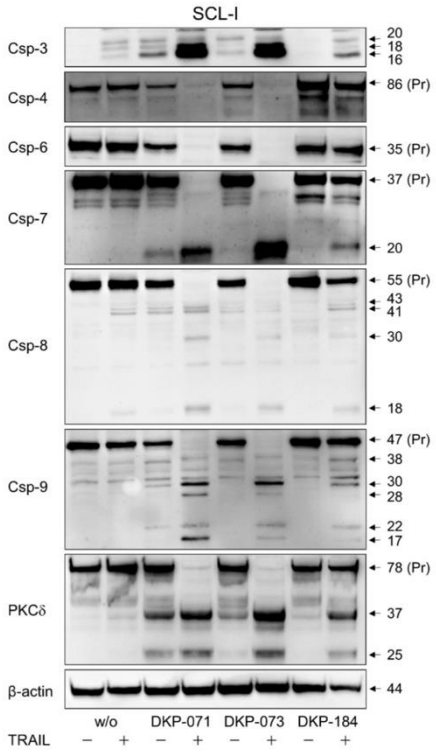

Figure 4. Enhanced caspase activation in course of combined treatment. Protein extracts of SCL-I cells treated for 24 h with indirubins (DKP-071, -073 and -184, 10 μM), TRAIL (50 ng/mL) or the combinations

were analyzed by Western blotting and compared to control cells. Equal protein amounts (30 µg per lane) were separated by SDS-PAGE, and consistent blotting was proven by Ponceau staining as well as by evaluation of β-actin expression. Proforms (Pr) and characteristic cleavage products are indicated, such as for caspase-3 (20, 18, 16 kDa), caspase-4 (86 kDa), caspase-6 (35 kDa), caspase-7 (37, 20 kDa), caspase-8 (55, 43, 41, 18 kDa), caspase-9 (47, 38, 17 kDa) and PKCδ (78, 37, 25 kDa). Besides these, some intermediate and secondary cleavage products were seen. Two independent series of protein extracts and independent Western blots revealed highly comparable results.

Proapoptotic pathways may also be initiated by protein kinase C delta (PKCδ), which is activated through processing of its 78 kDa proform [20,21]. Here, we show significant processing of PKCδ in SCL-I in response to treatment with DKP-071 and DKP-073, and even stronger in response to the combinations with TRAIL, indicated by loss of its pro-form and characteristic cleavage products of 37 and 25 kDa (Figure 4). Additionally, in SCL-II and SCC-12, indications of PKCδ activation by DKP-071 and -073 were visible by induction of the 37 kDa fragment (Figure 5a). However, PKCδ may play an only contributory role here, as indirubin-mediated proapoptotic effects could not be prevented by the PKC inhibitor bisindolylmaleimide I (data not shown).

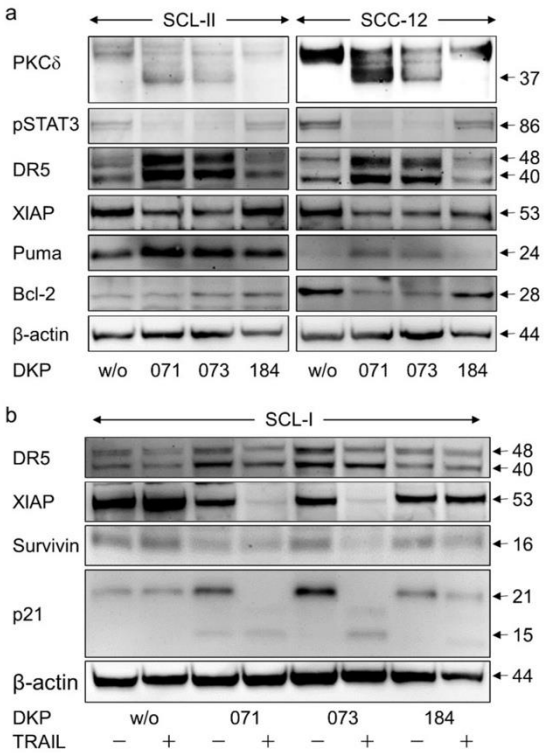

Figure 5. Expression of apoptosis agonists. (**a**) Cell lines SCL-II and SCC-12 were treated for 24 h with indirubins (DKP-071, -073 and -184; 10 µM). (**b**) Cell line SCL-I was treated for 24 h with indirubins (DKP-071, -073 and -184, 10 µM) ± TRAIL (50 ng/mL). (**a**,**b**) Expression of PKCδ(fragment 37 kDa),

pSTAT3 (86 kDa), TRAIL-R2/DR5 (48, 40 kDa), XIAP (53 kDa), Puma (24 kDa), Bcl-2 (28 kDa), survivin (16 kDa) and p21 (21, 15 kDa) was analyzed by Western blotting. Equal protein amounts (30 µg per lane) were separated by SDS-PAGE, and consistent blotting was proven by Ponceau staining as well as by evaluation of β-actin expression. Size of proteins (in kDa) is indicated on the right side. Largely similar results were obtained in three independent Western blot experiments using three independent series of cell extracts.

3.5. Regulation of Characteristic Mediators of Apoptosis and Cell Proliferation

To further address the mechanisms of antitumor effects mediated by indirubin derivatives in cSCC cells, the expression of several regulators of apoptosis and cell proliferation was investigated by Western blotting. Thus, pSTAT3 was downregulated in SCL-II and SCC-12 by DKP-071 and -073 (median factor of 2–3, according to densitometric analysis; Figure 5a), indicating an inhibition of the pSTAT3 survival pathway. The TRAIL receptor, DR5, was upregulated by DKP-071 and -073 in SCL-I, SCL-II and SCC-12 (median factors 2–3; Figure 5a,b). The caspase-3 antagonist XIAP (chromosome X-linked inhibitor of apoptosis protein) was downregulated by all three indirubins in SCC-12 and SCL-II as well as by DKP-071 and -073 in SCL-I (factors of 3–10; Figure 5a,b). Additionally, the cIAP survivin appeared as downregulated by the combinations (Figure 5b).

Intrinsic apoptosis pathways are critically controlled by the family of pro- and anti-apoptotic Bcl-2 proteins. Here, we found upregulation of the proapoptotic Bcl-2 protein Puma in SCL-II and SCC-12 (factors of 2–4), whereas antiapoptotic Bcl-2 was downregulated in SCC-12 (factor of 2; Figure 5a). In contrast, no significant changes were obtained for the anti-apoptotic Bcl-2 family members Mcl-1 and Bcl-w or the multidomain proapoptotic family members Bax and Bak (data not shown). Finally, upregulation of the CDK inhibitor p21 was seen in SCL-I in response to indirubin treatment (factor of 4). In course of strongly induced apoptosis after combination treatment, however, it was degraded, as seen by an increased 15 kDa fragment (Figure 5b). Thus, several different pathways appeared as affected by indirubin derivatives in cSCC cells.

3.6. Function of Caspases

To prove the significance of caspase activation for the antitumor effects of indirubin derivatives, the pan-caspase inhibitor QVD-Oph was applied. Both decrease of cell viability and induction of apoptosis mediated by indirubin/TRAIL combinations were strongly diminished by QVD-Oph. Thus, in SCL-II, cell viability rates decreased by combinations of TRAIL with DKP-071/073/184 (12%, 42% and 8%) were recovered to 45%, 38% and 66%, respectively. Similarly, in SCC-12, decreased cell viability rates by indirubin/TRAIL combinations (4%, 3% and 13%) were recovered to 65%, 52% and 69%, respectively (Figure 6a).

Comparably, apoptosis that was induced in SCL-II by indirubin/TRAIL combinations (40%, 36%, 57%) was reduced by QVD-Oph to 13%, 16% and 5%, respectively. Similarly, in SCC-12, induced apoptosis by combination treatments (56%, 57% and 54%) was reduced by QVD-Oph to 11%, 14% and 6%, respectively (Figure 6b).

Cell proliferation rates were investigated in SCL-I for indirubin treatment alone and for combinations with TRAIL. Thus, decreased cell proliferation in response to indirubins alone (29–48%) were restored to 35–69%, and decreased cell proliferation in response to indirubin/TRAIL combinations (8–17%) was restored to 36–69% (Figure 6c).

In clear contrast, QVD-Oph pretreatment remained without an effect on loss of MMP, as demonstrated in SCL-I and SCC-12 (Figure 6d), and it remained without an effect on the indirubin-mediated increase of ROS levels, as shown in all 4 cell lines (Figure 6e). Thus, caspases appeared as strongly contributing to induction of apoptosis and loss of cell viability, but they were not upstream of mitochondrial activation and ROS production.

3.7. Critical Roles of ROS

To prove the significance of ROS induction for the antitumor effects of indirubin derivatives in cSCC cells, the antioxidant N-acetylcysteine (NAC) was applied. Pretreat-

ment with NAC (1 mM) for 1 h almost completely abolished ROS production in all four cell lines (Figure 7a). This also resulted in almost completely restored cell viability. Thus, cell viability rates that were decreased by combinations of TRAIL with DKP-071 and -073 to values of 4–18% were improved by NAC pretreatment to values >63% (controls at 80–90%) (Figure 7b).

Largely comparable findings were obtained at the apoptosis level. Thus, apoptosis induced in SCL-I by combinations of TRAIL with DKP-071/073/184 (48%, 46%, 32%) was reduced by NAC to 24%, 7% and 6%. In SCL-II, apoptosis induced by indirubin/TRAIL combinations (25%, 21%, 16%) was reduced by NAC to 5%, 10% and 8%. Similarly, apoptosis was reduced by NAC in SCC-12 from 41%, 40% and 48% to 23%, 21% and 22%, as well as in SCC-13 from 48%, 41% and 21% to 2%, 2% and 3%, respectively (Figure 8a).

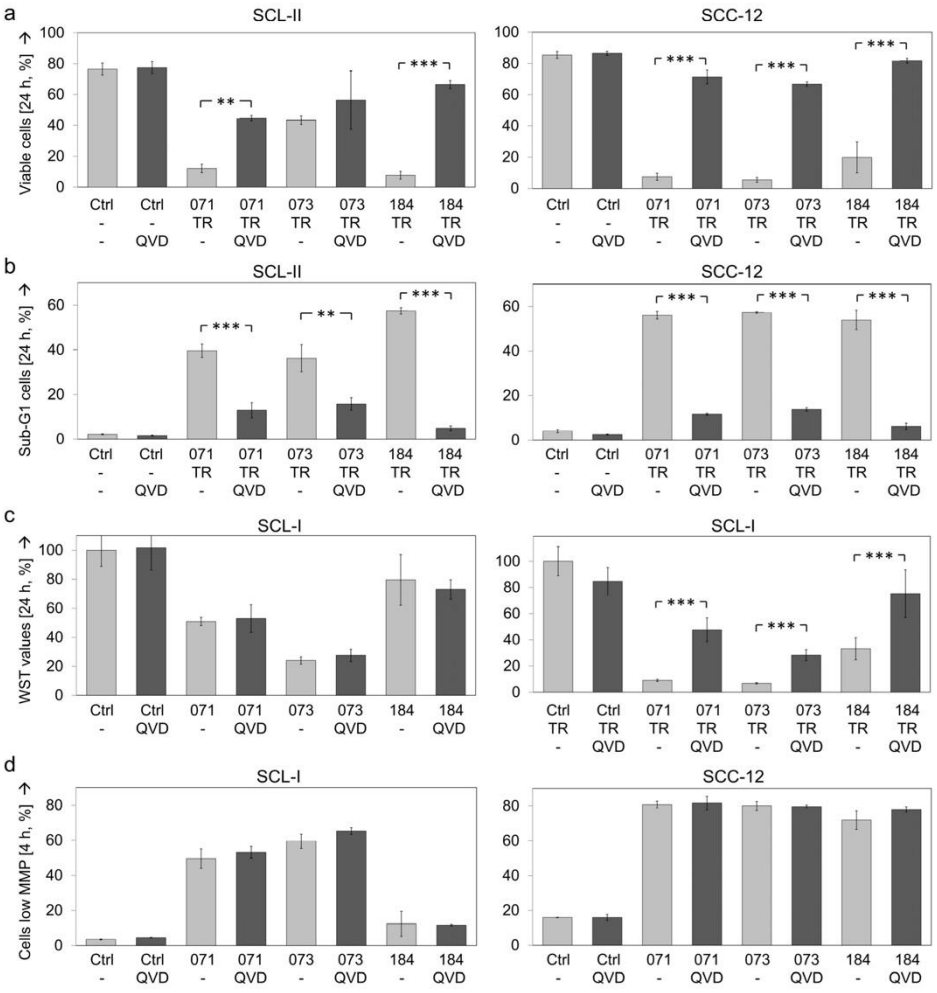

Figure 6. *Cont.*

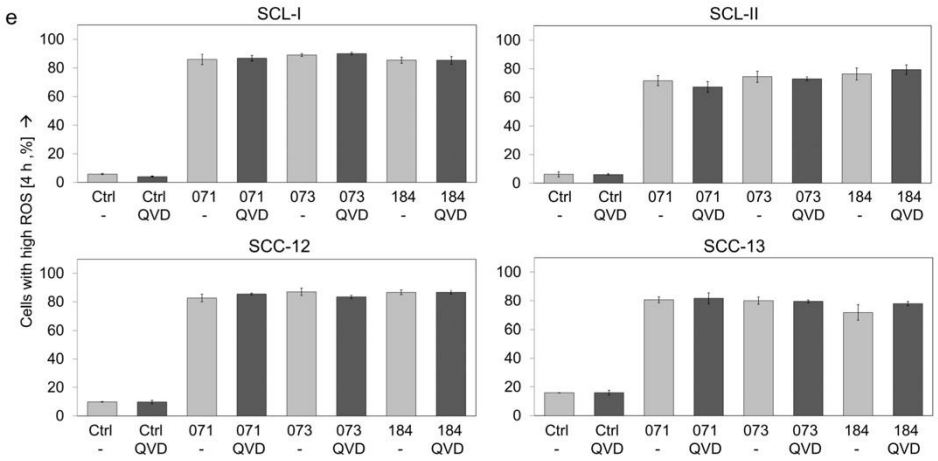

Figure 6. Inhibition of apoptosis by caspase antagonist. The antagonistic effects of the pan-caspase inhibitor QVD-Oph (QVD, 10 μM, 1 h pretreatment) on indirubins' antitumor activity are shown. (**a**) Cell viability was determined by calcein-AM staining in SCL-II and SCC-12 at 24 h in response to the combinations of indirubins (DKP-071, -073 and -184, 10 μM) and TRAIL (TR; 50 ng/mL). (**b**) Apoptotic cells were quantified by cell cycle analyses (propidium iodide staining, flow cytometry) as sub-G1 cells characterized by DNA fragmentation (treatment as above). (**c**) Cell proliferation was quantified by WST-1 assay in SCL-I at 24 h of treatment with indirubins, TRAIL or combinations. (**d**) Loss of MMP was investigated in SCL-I and SCC-12 at 4 h of treatment with indirubins (10 μM). (**e**) ROS production was investigated in the four cell lines at 4 h of treatment with indirubins (10 μM). (**a**–**e**) Mean values and SDs are shown of a representative experiment (two independent experiments, each one with triplicates). Asterisks indicate statistical significance, when cells ± QVD-Oph were compared (** $p < 0.01$; *** $p < 0.001$).

Cell proliferation rates (WST-1 assay) in response to indirubins ± TRAIL were determined in SCL-I. Also here, decreased cell proliferation rates by indirubins alone (29–48%) and in combinations with TRAIL (8–17%) were largely restored to control levels (>78%; Figure 8b). Inhibition of ROS production also strongly affected the loss of MMP. Thus, loss of MMP in SCL-I (50% and 59% by DKP-071/073) and in SCC-12 (63%, 78% of cells) was almost completely abolished by NAC (Figure 8c).

The antagonistic effects of ROS scavenging through NAC were further investigated in SCL-I and SCC-12 by Western blotting. Thus, processing/activation of effector caspases-3, -6 and -7 by DKP-071/TRAIL treatment was completely abolished by NAC, as it was also abolished by the pan-caspase inhibitor QVD-Oph. Interestingly, caspase-8 processing was also diminished by NAC but not by QVD-Oph (Figure 9), indicating that initiator caspase-8 activation was also downstream of ROS induction.

Additionally, most other activation steps identified in response to indirubin treatment, such as PKCδ and STAT3 activation as well as the downregulation of XIAP and survivin, appeared as downstream of ROS, as they were also reverted by NAC pretreatment (Figure 9). These data clearly favor ROS as the master regulator of indirubin-mediated effects in cSCC cells.

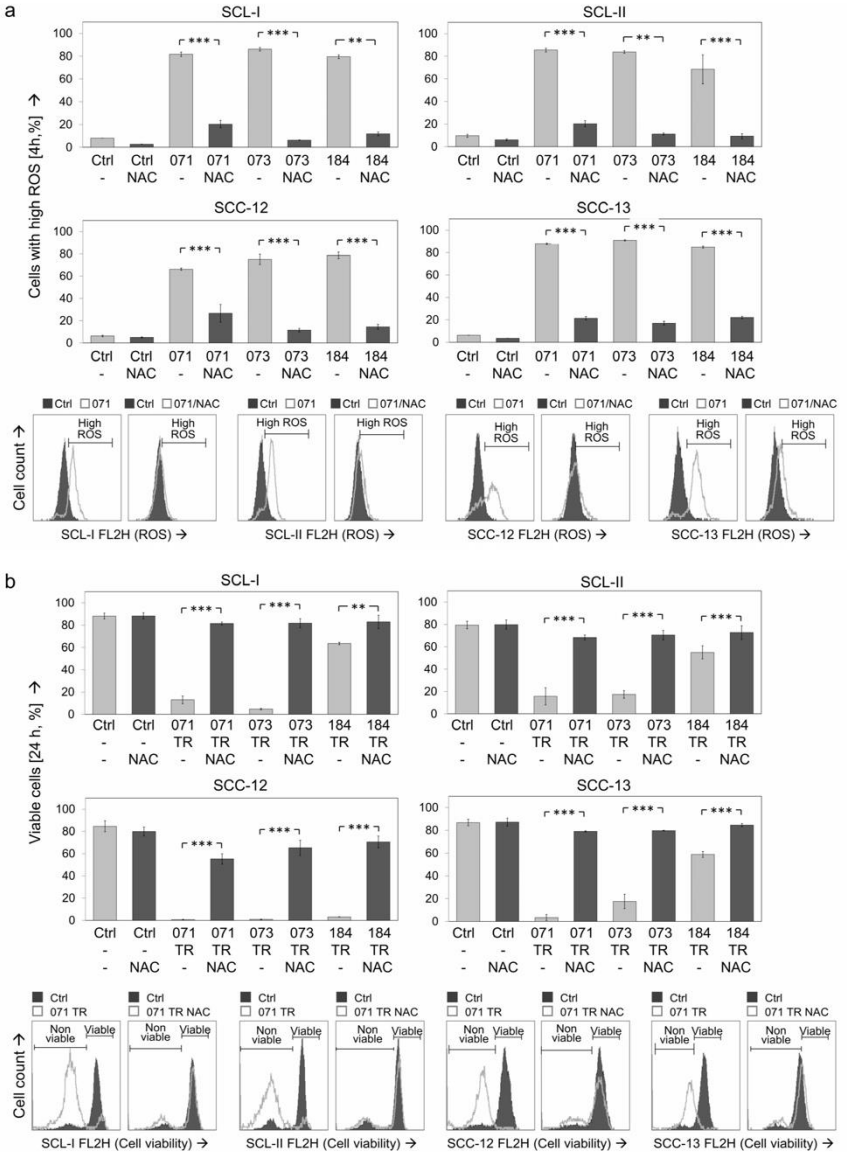

Figure 7. Antagonistic effects of NAC on ROS production and cell viability. The antagonistic effects of the antioxidant N-acetylcysteine (NAC, 1 mM, 1 h pretreatment) were investigated. (**a**) ROS production, as determined by H_2DCF-DA staining, is shown in the four cSCC cell lines at 4 h of treatment with indirubins (DKP-071, -073 and -184, 10 µM). (**b**) Cell viability was determined by calcein staining in cell lines at 24 h in response to the combinations of indirubins (DKP-071, -073 and -184, 10 µM) and TRAIL (TR; 50 ng/mL). (**a**,**b**) Examples of flow cytometry measurements are provided below (overlays of treated cells vs. controls). Bar charts, mean values and SDs are shown of a representative experiment (two independent experiments, each one with triplicates). Asterisks indicate statistical significance, when cells ± NAC were compared (** $p < 0.01$; *** $p < 0.001$).

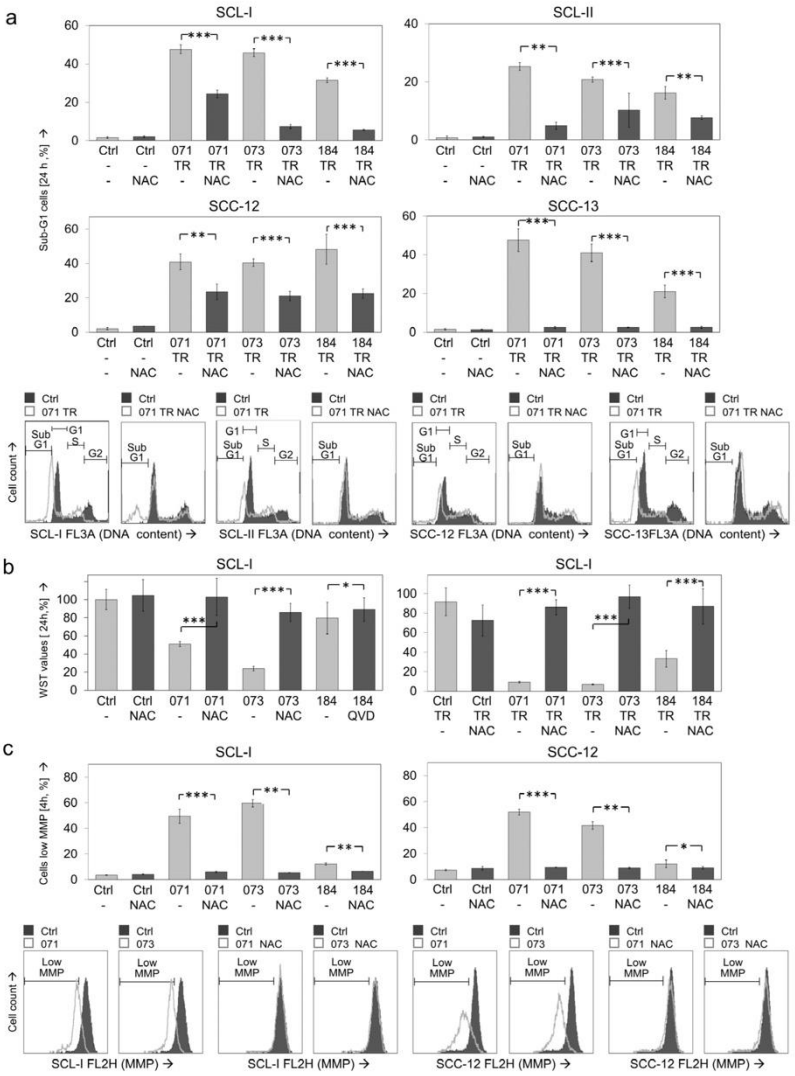

Figure 8. Effects of NAC on apoptosis, cell proliferation and MMP. The antagonistic effects of the antioxidant N-acetylcysteine (NAC, 1 mM, 1 h pretreatment) were investigated. Cells were treated with combinations of indirubins (DKP-071, -073 and -184, 10 μM) and TRAIL (TR; 50 ng/mL) or with indirubins alone, as indicated. (**a**) Apoptosis was determined at 24 h by cell cycle analysis and quantification of sub-G1 cells in four cSCC cell lines. (**b**) Cell proliferation was quantified by WST-1 assay in SCL-I at 24 h. (**c**) Loss of MMP was investigated in SCL-I and SCC-12 at 4 h of treatment. (**a**, **c**) Examples of flow cytometry measurements are provided below (overlays of treated cells vs. controls). (**a**–**c**) Bar charts, mean values and SDs are shown of a representative experiment. Two independent experiments were performed, each one with triplicates. Asterisks indicate statistical significance, when cells ± NAC were compared (* $p < 0.05$; ** $p < 0.01$; *** $p < 0.001$).

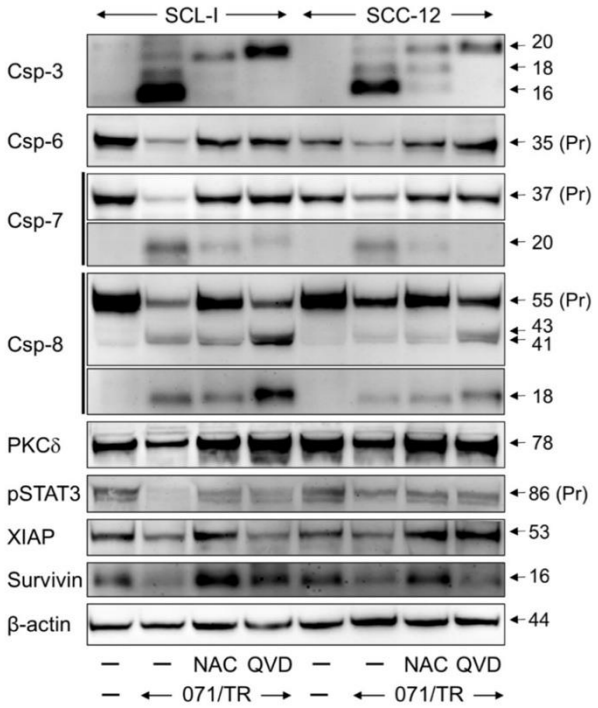

Figure 9. Effects on expression of apoptosis regulators. Expression analysis of characteristic apoptosis regulator proteins in SCL-I and SCC-12 is shown by Western blotting. Cells received pretreatment for 1 h with N-acetylcysteine (NAC, 1 mM) or QVD-Oph (QVD, 10 μM), followed by combination of DKP-071 (071; 10 μM) and TRAIL (TR; 50 ng/mL). Proteins had been extracted at 24 h of treatment. Size of proteins (in kDa) is indicated on the right side, as determined in comparison to a protein size marker run in parallel. Expression of β-actin is shown as loading control. Largely similar results were obtained in three independent Western blot experiments using three independent series of cell extracts.

4. Discussion

Epithelial skin cancer represents the most common malignancy worldwide. Thus, cutaneous squamous cell carcinoma (cSCC) ranks at second place (~20%) following basal cell carcinoma (~77%) [35]. The incidence of actinic keratosis is even higher, which is defined as carcinoma in situ of cSCC and thus needs treatment [36]. Present standard care of cSCC is mainly based on surgical excision and on chemotherapy. However, frequent side effects and insufficient efficacy of chemotherapy as well as infections by surgery represent major problems [37,38]. With the success of new, targeted therapies, these also gain particular attention for cSCC. Targeted therapy may in particular apply for actinic keratosis, which is often widely distributed but not severe enough for chemotherapeutic treatment.

The natural compound indirubin was identified as an active component of the traditional Chinese medicine Danggui Longhui Wan, used for treatment of chronic and inflammatory diseases [39]. The antitumor activity of indirubin was considered, and clinical trials proved its activity in chronic myeloid leukemia and chronic granulocytic leukemia as well as in head and neck cancer. Importantly, no severe toxicity and side effects have been reported [27,28,40].

Indirubin activity may be further enhanced by chemical modifications, and several new derivatives were described that showed antitumor activities in in vitro and in vivo tumor models, such as for non-small cell lung cancer, glioblastoma, breast, bladder, thyroid, hepatocellular and colorectal cancer [41–46]. We have previously reported a series of new indirubin derivatives based on N-glycosylated 3-alkylideneoxindoles containing halogen substituents [30,32]. Two derivatives (DKP-071 and DKP-073) have been previously tested in melanoma and cutaneous T-cell lymphoma cells, where they induced apoptosis in combination with the death ligand TRAIL and affected cell viability [25,47].

In epithelial skin cancer, such as cSCC and basal cell carcinoma, indirubins have not been reported thus far. Here, we show a particularly high efficacy of these derivatives in cSCC cells, which was much stronger as compared to equimolar concentrations of non-substituted indirubin. The active concentration of 10 μM appeared as moderate and may also be reached in tumor tissue.

Indirubin effects were strongly enhanced in combinations with the death ligand TRAIL. TRAIL is a promising candidate for tumor therapy itself, but TRAIL or TRAIL receptor agonistic antibodies have revealed only limited efficacy in clinical trials so far [6]. Thus, the identification of suitable combination partners appears of particular interest. Enhancement of TRAIL-induced apoptosis in cSCC has also previously been shown in combinations with diclofenac and celecoxib [24,33]. As death ligands represent basic elements of an antitumor immune response driven by cytotoxic T-lymphocytes and natural killer cells [6], it is also conceivable that indirubins might enhance an immune response against cSCC in patients. However, first, cytotoxicity studies and investigations of possible side effects on immune cells are needed. Although non-substituted indirubins were quite well-tolerated in clinical trials, no in vivo data are so far available on the compounds investigated here. As many different normal cell types cannot be tested in vitro and as normal cells may reveal largely different characteristics in culture, tolerability of the substances needs to be thoroughly tested in animal models.

The mode of action of indirubins in cancer cells still largely remains in the dark. Inhibition of protein kinases such as JAK, Src, GSK-3β (glycogen synthase kinase), aurora kinase A and cyclin-dependent kinases (CDKs) have been reported [39,48]. Three major types of cell death were distinguished, namely apoptosis, autophagy and necrosis. In principle, apoptosis can be mediated by caspase-dependent or caspase-independent pathways [23]. Intrinsic apoptosis is further characterized by mitochondrial outer membrane permeability as well as by activation of executioner caspases, mainly caspase-3. Here, we saw strong activation of proapoptotic caspase cascades by indirubins alone and even more by combinations with TRAIL. The essential role of caspases was proven by a pan-caspase inhibitor, which almost completely abolished apoptosis induced by indirubins alone as well as by indirubin/TRAIL combinations.

Proapoptotic caspase cascades may be blocked by cIAPs (cellular inhibitor of apoptosis proteins), as XIAP and survivin inhibit effector caspases and caspase-9 [49]. Thus, downregulation of XIAP and survivin seen here in cSCC cells may contribute to the strongly activated caspase cascade. Downregulation of survivin and XIAP by indirubin derivatives has also been seen in breast cancer, melanoma and CTCL cells [25,47,50,51].

There were strong indications that indirubins induce intrinsic apoptosis pathways, and a number of arguments could be collected. Thus, intrinsic apoptosis is characterized by MOMP (mitochondrial outer membrane permeability) and activation of executioner caspases, mainly caspase-3. MOMP leads to loss of the mitochondrial transmembrane potential, associated with cytochrome c release and caspase-9 activation [8]. In a caspase cascade, caspase-3 can activate other effector caspases (-6 and -7) as well as—in a positive feedback loop—caspase-8. Caspase-3 drives DNA fragmentation, e.g., via cleavage of the inhibitor of caspase-activated DNAse (ICAD). Of particular importance for our present findings, intrinsic apoptosis can be initiated by a variety of microenvironmental perturbations, which in particular also include overload of reactive oxygen species (ROS) [8,52]. Loss of MMP in response to indirubins was also seen in melanoma and CTCL cells [25,47]. Intrinsic

apoptosis pathways are critically controlled by the family of pro- and anti-apoptotic Bcl-2 proteins [9]. In relation to loss of MMP, we identified the downregulation of antiapoptotic Bcl-2, while proapoptotic Puma was upregulated by indirubins in cSCC cells.

In many cancer cells, persistent activation of STAT3 pathways can promote tumor cell proliferation, survival, angiogenesis and immune evasion. STAT3 activation may be induced via JAK, Src or other tyrosine kinases [51]. Related to its inhibitory activity against JAK, indirubin-induced apoptosis has been related to STAT3 inhibition, as seen in breast cancer, prostate cancer and melanoma cells [47,50]. Downregulation of phosphorylated STAT3 (active) in response to indirubin is also described here in cSCC cells. STAT3 acts as a transcription factor and its inhibition may result in the downregulation of several antiapoptotic factors, including Bcl-2 and survivin [53], which was also seen here in cSCC cells.

A proapoptotic function of PKCδ has been described in response to DNA-damaging agents, UV radiation, phorbol 12-myristate-12-acetate as well as in response to ROS. PKCδ is activated through processing of its 78 kDa proform, which releases a 41 and a 37 kDa fragment [20,21]. In CTCL cells, PKCδ appeared as a master regulator in PEP005-induced apoptosis [54]. Processing of PKCδ in response to indirubins was also shown here by downregulation of the 78 kDa proform and induction of characteristic fragments of 37 and 25 kDa, whereas the 41 kDa fragment was not efficiently detected by the used antibody. PKCδ activation appeared as downstream of caspase-3, as its processing could be inhibited by caspase inhibition. However, PKCδ may have an only contributory role in this setting, as a PKC inhibitor did not prevent the effects of DKPs.

We furthermore found upregulation of TRAIL receptor-1 (DR5) [55], which may contribute to the enhanced TRAIL sensitivity in cSCC cells. Finally, p21 represents a well-known CDK inhibitor [10]. Its upregulation in cSCC cells by indirubins may critically contribute to the inhibition of cell proliferation seen here. Upregulation of TRAIL receptors by indirubins has also been seen in hepatoma, cervical, colon cancer and melanoma cells [47,56,57], whereas upregulation of p21 by indirubin was reported in human laryngeal carcinoma cells [58].

A particular role is described here for reactive oxygen species (ROS). Besides their described functions in tissue damaging and aging [22], reactive oxygen species (ROS) can also mediate proapoptotic signaling in cancer cells and may explain the proapoptotic effects of several anticancer therapies, as demonstrated in skin cancer cells [23–25,47]. Concerning the activities of indirubin derivatives, we had previously shown ROS production by indirubins in melanoma and CTCL cells. As shown in the present study, cSCC cells also responded with massive ROS production already at 4 h of indirubin treatment. Thus, ROS production appears as a general mechanism of indirubins in cutaneous cancer cells. Interestingly, not only apoptotic cells but the whole cell population showed increased ROS levels, as demonstrated by flow cytometry. Thus, all tumor cells could be targeted.

Based on our previous data, ROS could act as a signaling molecule in melanoma and CTCL cells by affecting intrinsic, mitochondrial as well as extrinsic, death receptor-mediated apoptosis pathways [25,47]. Additionally, in cSCC cells, indirubin derivatives mediated highly pleiotropic effects, enclosing caspases, mitochondrial membrane potential, PKCδ, STAT3, p21 and Bcl-2 proteins. Our data strongly suggest ROS as the unique master regulator of these pathways in cSCC cells. Indeed, production of reactive oxygen species turned out as upstream of all other identified effects. Namely, the antioxidant NAC completely abolished the proapoptotic effects of indirubins, restored cell viability and cell proliferation as well as prevented all other effects induced by indirubins. ROS production was also reported for other cSCC therapies, such as for chemotherapy, photothermal therapy [59] and photodynamic therapy [60,61].

5. Conclusions

In conclusion, these data suggest indirubin derivatives as possibly promising candidates for therapy of epithelial skin cancer, provided that they may also be tolerated in vivo

and in the clinical setting. The identification of ROS as particularly responsive for indirubin-mediated antitumor effects opens new perceptions in cSCC therapy. ROS induction should be considered and may also be suitable for early monitoring of therapeutic effects.

Supplementary Materials: The following are available online at https://www.mdpi.com/article/10.3390/antiox10101514/s1. Figure S1: Cytotoxicity in 4 cell lines (a) Exp 1 (b) Exp 2, Figure S2: Dose dependency for DKP-071 / Comparison with non-substituted Indirubin (a) Cell viability (b) Apoptosis, Figure S3: Apoptosis and cell viability in HaCaT cells in response to DKPs, Figure S4: Dose dependency of ROS production for DKP-071 and Figure S5: Time dependency of ROS production for DKP-071 (a) 1–4 h (b) 24 h.

Author Contributions: J.Z., data curation, formal analysis, investigation, methodology; P.L., formal analysis, methodology; C.U., formal analysis, resources; J.E., formal analysis, funding acquisition, investigation, methodology, project administration, resources, supervision. All authors have read and agreed to the published version of the manuscript.

Funding: J.Z. received a stipendium from the China Scholarship Council (CSC), Beijing 100044, China.

Institutional Review Board Statement: Not applicable.

Informed Consent Statement: Not applicable.

Data Availability Statement: The data presented in this study are available in article and Supplementary Materials.

Acknowledgments: The study was supported by the research fund of the Charité-Universitätsmedizin Berlin.

Conflicts of Interest: The authors declare no conflict of interest.

References

1. Alam, M.; Ratner, D. Cutaneous squamous-cell carcinoma. *N. Engl. J. Med.* **2001**, *344*, 975–983. [CrossRef] [PubMed]
2. Szewczyk, M.; Pazdrowski, J.; Golusiński, P.; Dańczak-Pazdrowska, A.; Marszałek, S.; Golusiński, W. Analysis of selected risk factors for nodal metastases in head and neck cutaneous squamous cell carcinoma. *Eur. Arch. Otorhinolaryngol.* **2015**, *272*, 3007–3012. [CrossRef] [PubMed]
3. Amaral, T.; Osewold, M.; Presser, D.; Meiwes, A.; Garbe, C.; Leiter, U. Advanced cutaneous squamous cell carcinoma: Real world data of patient profiles and treatment patterns. *J. Eur. Acad. Derm. Venereol.* **2019**, *33* (Suppl. S8), 44–51. [CrossRef] [PubMed]
4. Agbai, O.N.; Buster, K.; Sanchez, M.; Hernandez, C.; Kundu, R.V.; Chiu, M.; Roberts, W.E.; Draelos, Z.D.; Bhushan, R.; Taylor, S.C.; et al. Skin cancer and photoprotection in people of color: A review and recommendations for physicians and the public. *J. Am. Acad. Derm.* **2014**, *70*, 748–762. [CrossRef]
5. Halder, R.M.; Bridgeman-Shah, S. Skin cancer in African Americans. *Cancer* **1995**, *75*, 667–673. [CrossRef]
6. Eberle, J. Countering TRAIL Resistance in Melanoma. *Cancers* **2019**, *11*, 656. [CrossRef]
7. Hanahan, D.; Weinberg, R.A. Hallmarks of Cancer: The Next Generation. *Cell* **2011**, *144*, 646–674. [CrossRef]
8. Galluzzi, L.; Vitale, I.; Aaronson, S.A.; Abrams, J.M.; Adam, D.; Agostinis, P.; Alnemri, E.S.; Altucci, L.; Amelio, I.; Andrews, D.W.; et al. Molecular mechanisms of cell death: Recommendations of the Nomenclature Committee on Cell Death 2018. *Cell Death Differ.* **2018**, *25*, 486–541. [CrossRef]
9. Chipuk, J.E.; Moldoveanu, T.; Llambi, F.; Parsons, M.J.; Green, D.R. The BCL-2 Family Reunion. *Mol. Cell* **2010**, *37*, 299–310. [CrossRef]
10. Karimian, A.; Ahmadi, Y.; Yousefi, B. Multiple functions of p21 in cell cycle, apoptosis and transcriptional regulation after DNA damage. *DNA Repair* **2016**, *42*, 63–71. [CrossRef]
11. Krammer, P.H.; Arnold, R.; Lavrik, I.N. Life and death in peripheral T cells. *Nat. Rev. Immunol.* **2007**, *7*, 532–542. [CrossRef]
12. Ashkenazi, A.; Holland, P.; Eckhardt, S.G. Ligand-based targeting of apoptosis in cancer: The potential of recombinant human apoptosis ligand 2/tumor necrosis factor-related apoptosis-inducing ligand (rhApo2L/TRAIL). *J. Clin. Oncol.* **2008**, *26*, 3621–3630. [CrossRef]
13. Walczak, H.; Miller, R.E.; Ariail, K.; Gliniak, B.; Griffith, T.S.; Kubin, M.; Chin, W.; Jones, J.; Woodward, A.; Le, T.; et al. Tumoricidal activity of tumor necrosis factor related apoptosis-inducing ligand in vivo. *Nat. Med.* **1999**, *5*, 157–163. [CrossRef]
14. Hitomi, J.; Katayama, T.; Eguchi, Y.; Kudo, T.; Taniguchi, M.; Koyama, Y.; Manabe, T.; Yamagishi, S.; Bando, Y.; Imaizumi, K.; et al. Involvement of caspase-4 in endoplasmic reticulum stress-induced apoptosis and A beta-induced cell death. *J. Cell Biol.* **2004**, *165*, 347–356. [CrossRef]
15. Martinon, F.; Tschopp, J. Inflammatory caspases and inflammasomes: Master switches of inflammation. *Cell Death Differ.* **2007**, *14*, 10–22. [CrossRef]
16. Fischer, U.; Janicke, R.U.; Schulze-Osthoff, K. Many cuts to ruin: A comprehensive update of caspase substrates. *Cell Death Differ.* **2003**, *10*, 76–100. [CrossRef]

17. Yuan, Z.L.; Guan, Y.J.; Wang, L.; Wei, W.; Kane, A.B.; Chin, Y.E. Central role of the threonine residue within the p+1 loop of receptor tyrosine kinase in STAT3 constitutive phosphorylation in metastatic cancer cells. *Mol. Cell Biol.* **2004**, *24*, 9390–9400. [CrossRef]
18. Benhadji, K.A.; Serova, M.; Ghoul, A.; Cvitkovic, E.; Le Tourneau, C.; Ogbourne, S.M.; Lokiec, F.; Calvo, F.; Hammel, P.; Faivre, S.; et al. Antiproliferative activity of PEP005, a novel ingenol angelate that modulates PKC functions, alone and in combination with cytotoxic agents in human colon cancer cells. *Brit. J. Cancer* **2008**, *99*, 1808–1815. [CrossRef]
19. Zhang, J.; Anastasiadis, P.Z.; Liu, Y.; Thompson, E.A.; Fields, A.P. Protein kinase C (PKC) beta II induces cell invasion through a Ras/Mek-, PKC iota/Rac1-dependent signaling pathway. *J. Biol. Chem.* **2004**, *279*, 22118–22123. [CrossRef]
20. Zhao, M.; Xia, L.; Chen, G.Q. Protein Kinase C delta in Apoptosis: A Brief Overview. *Arch. Immunol. Ex.* **2012**, *60*, 361–372. [CrossRef]
21. Kato, K.; Yamanouchi, D.; Esbona, K.; Kamiya, K.; Zhang, F.; Kent, K.C.; Liu, B. Caspase-mediated protein kinase C-delta cleavage is necessary for apoptosis of vascular smooth muscle cells. *Am. J. Physiol. Heart C* **2009**, *297*, H2253–H2261. [CrossRef]
22. Sies, H.; Jones, D.P. Reactive oxygen species (ROS) as pleiotropic physiological signalling agents. *Nat. Rev. Mol. Cell Biol.* **2020**, *21*, 363–383. [CrossRef]
23. Franke, J.C.; Plotz, M.; Prokop, A.; Geilen, C.C.; Schmalz, H.G.; Eberle, J. New caspase-independent but ROS-dependent apoptosis pathways are targeted in melanoma cells by an iron-containing cytosine analogue. *Biochem. Pharm.* **2010**, *79*, 575–586. [CrossRef]
24. Zhu, J.Q.; May, S.; Ulrich, C.; Stockfleth, E.; Eberle, J. High ROS Production by Celecoxib and Enhanced Sensitivity for Death Ligand-Induced Apoptosis in Cutaneous SCC Cell Lines. *Int. J. Mol. Sci.* **2021**, *22*, 3622. [CrossRef]
25. Soltan, M.Y.; Sumarni, U.; Assaf, C.; Langer, P.; Reidel, U.; Eberle, J. Key Role of Reactive Oxygen Species (ROS) in Indirubin Derivative-Induced Cell Death in Cutaneous T-Cell Lymphoma Cells. *Int. J. Mol. Sci.* **2019**, *20*, 1158. [CrossRef]
26. Quast, S.A.; Berger, A.; Eberle, J. ROS-dependent phosphorylation of Bax by wortmannin sensitizes melanoma cells for TRAIL-induced apoptosis. *Cell Death Dis.* **2013**, *4*, e839. [CrossRef]
27. Blazevic, T.; Heiss, E.H.; Atanasov, A.G.; Breuss, J.M.; Dirsch, V.M.; Uhrin, P. Indirubin and Indirubin Derivatives for Counteracting Proliferative Diseases. *Evidence-Based Compl. Alt.* **2015**, *2015*, 654098. [CrossRef] [PubMed]
28. Xiao, Z.; Hao, Y.; Liu, B.; Qian, L. Indirubin and meisoindigo in the treatment of chronic myelogenous leukemia in China. *Leuk. Lymphoma* **2002**, *43*, 1763–1768. [CrossRef] [PubMed]
29. Sun, B.; Wang, J.H.; Liu, L.H.; Mao, L.F.; Peng, L.Z.; Wang, Y.W. Synthesis and activity of novel indirubin derivatives. *Chem. Biol. Drug Des.* **2021**, *97*, 565–571. [CrossRef] [PubMed]
30. Libnow, S.; Methling, K.; Hein, M.; Michalik, D.; Harms, M.; Wende, K.; Flemming, A.; Kockerling, M.; Reinke, H.; Bednarski, P.J.; et al. Synthesis of indirubin-N ′-glycosides and their anti-proliferative activity against human cancer cell lines. *Bioorgan. Med. Chem.* **2008**, *16*, 5570–5583. [CrossRef] [PubMed]
31. Erben, F.; Kleeblatt, D.; Sonneck, M.; Hein, M.; Feist, H.; Fahrenwaldt, T.; Fischer, C.; Matin, A.; Iqbal, J.; Plotz, M.; et al. Synthesis and antiproliferative activity of selenoindirubins and selenoindirubin-N-glycosides. *Org. Biomol. Chem.* **2013**, *11*, 3963–3978. [CrossRef]
32. Kleeblatt, D.; Becker, M.; Plotz, M.; Schonherr, M.; Villinger, A.; Hein, M.; Eberle, J.; Kunz, M.; Rahman, Q.; Langer, P. Synthesis and bioactivity of N-glycosylated 3-(2-oxo-2-arylethylidene)-indolin-2-ones. *Rsc. Adv.* **2015**, *5*, 20769–20782. [CrossRef]
33. Fecker, L.F.; Stockfleth, E.; Braun, F.K.; Rodust, P.M.; Schwarz, C.; Kohler, A.; Leverkus, M.; Eberle, J. Enhanced Death Ligand-Induced Apoptosis in Cutaneous SCC Cells by Treatment with Diclofenac/Hyaluronic Acid Correlates with Downregulation of c-FLIP. *J. Invest. Derm.* **2010**, *130*, 2098–2109. [CrossRef]
34. Boukamp, P.; Petrussevska, R.T.; Breitkreutz, D.; Hornung, J.; Markham, A.; Fusenig, N.E. Normal keratinization in a spontaneously immortalized aneuploid human keratinocyte cell line. *J. Cell Biol.* **1988**, *106*, 761–771. [CrossRef]
35. Bray, F.; Ferlay, J.; Soerjomataram, I.; Siegel, R.L.; Torre, L.A.; Jemal, A. Global cancer statistics 2018: GLOBOCAN estimates of incidence and mortality worldwide for 36 cancers in 185 countries. *CA Cancer J. Clin.* **2018**, *68*, 394–424. [CrossRef]
36. Rosenberg, A.R.; Tabacchi, M.; Ngo, K.H.; Wallendorf, M.; Rosman, I.S.; Cornelius, L.A.; Demehri, S. Skin cancer precursor immunotherapy for squamous cell carcinoma prevention. *JCI Insight* **2019**, *4*, e125476. [CrossRef]
37. Marur, S.; Forastiere, A.A. Head and Neck Squamous Cell Carcinoma: Update on Epidemiology, Diagnosis, and Treatment. *Mayo Clin. Proc.* **2016**, *91*, 386–396. [CrossRef]
38. Dothager, R.S.; Putt, K.S.; Allen, B.J.; Leslie, B.J.; Nesterenko, V.; Hergenrother, P.J. Synthesis and identification of small molecules that potently induce apoptosis in melanoma cells through G1 cell cycle arrest. *J. Am. Chem. Soc.* **2005**, *127*, 8686–8696. [CrossRef]
39. Schafer, M.; Semmler, M.L.; Bernhardt, T.; Fischer, T.; Kakkassery, V.; Ramer, R.; Hein, M.; Bekeschus, S.; Langer, P.; Hinz, B.; et al. Small Molecules in the Treatment of Squamous Cell Carcinomas: Focus on Indirubins. *Cancers* **2021**, *13*, 1770. [CrossRef]
40. You, W.C.; Hsieh, C.C.; Huang, J.T. Effect of extracts from indigowood root (Isatis indigotica Fort.) on immune responses in radiation-induced mucositis. *J. Altern. Complement. Med.* **2009**, *15*, 771–778. [CrossRef]
41. Ahn, M.Y.; Kim, T.H.; Kwon, S.M.; Yoon, H.E.; Kim, H.S.; Kim, J.I.; Kim, Y.C.; Kang, K.W.; Ahn, S.G.; Yoon, J.H. 5-Nitro-5′-hydroxy-indirubin-3′-oxime (AGM130), an indirubin-3′-oxime derivative, inhibits tumor growth by inducing apoptosis against non-small cell lung cancer in vitro and in vivo. *Eur. J. Pharm. Sci.* **2015**, *79*, 122–131. [CrossRef]
42. Zhang, Y.M.; Du, Z.X.; Zhuang, Z.R.; Wang, Y.J.; Wang, F.; Liu, S.; Wang, H.; Feng, H.R.; Li, H.Y.; Wang, L.Y.; et al. E804 induces growth arrest, differentiation and apoptosis of glioblastoma cells by blocking Stat3 signaling. *J. Neuro Oncol.* **2015**, *125*, 265–275. [CrossRef]

43. Braig, S.; Bischoff, F.; Abhari, B.A.; Meijer, L.; Fulda, S.; Skaltsounis, L.; Vollmar, A.M. The pleiotropic profile of the indirubin derivative 6BIO overcomes TRAIL resistance in cancer. *Biochem. Pharm.* **2014**, *91*, 157–167. [CrossRef]
44. Ndolo, K.M.; Park, K.R.; Lee, H.J.; Bin Yoon, K.; Kim, Y.C.; Han, S.Y. Characterization of the Indirubin Derivative LDD970 as a Small Molecule Aurora Kinase A Inhibitor in Human Colorectal Cancer Cells. *Immune Netw.* **2017**, *17*, 110–115. [CrossRef]
45. Lee, H.J.; Jeong, P.; Moon, Y.; Choi, J.; Heo, J.D.; Kim, Y.C.; Han, S.Y. Characterization of LDD-2633 as a Novel RET Kinase Inhibitor with Anti-Tumor Effects in Thyroid Cancer. *Pharm. Base* **2021**, *14*, 38. [CrossRef]
46. Tanaka, T.; Saito, H.; Miyairi, S.; Kobayashi, S. 7-Hydorxyindirubin is capable of specifically inhibiting anticancer drug-induced YB-1 nuclear translocation without showing cytotoxicity in HepG2 hepatocellular carcinoma cells. *Biochem. Biophys. Res. Commun.* **2021**, *544*, 15–21. [CrossRef]
47. Zhivkova, V.; Kiecker, F.; Langer, P.; Eberle, J. Crucial role of reactive oxygen species (ROS) for the proapoptotic effects of indirubin derivative DKP-073 in melanoma cells. *Mol. Carcinog.* **2019**, *58*, 258–269. [CrossRef]
48. Kunz, M.; Driller, K.M.; Hein, M.; Libnow, S.; Hohensee, I.; Ramer, R.; Hinz, B.; Berger, A.; Eberle, J.; Langer, P. Synthesis of thia-analogous indirubin N-Glycosides and their influence on melanoma cell growth and apoptosis. *ChemMedChem* **2010**, *5*, 534–539. [CrossRef]
49. Deveraux, Q.L.; Takahashi, R.; Salvesen, G.S.; Reed, J.C. X-linked IAP is a direct inhibitor of cell-death proteases. *Nature* **1997**, *388*, 300–304. [CrossRef]
50. Nam, S.; Buettner, R.; Turkson, J.; Kim, D.; Cheng, J.Q.; Muehlbeyer, S.; Hippe, F.; Vatter, S.; Merz, K.H.; Eisenbrand, G.; et al. Indirubin derivatives inhibit Stat3 signaling and induce apoptosis in human cancer cells. *Proc. Natl. Acad. Sci. USA* **2005**, *102*, 5998–6003. [CrossRef]
51. Liu, L.; Gaboriaud, N.; Vougogianopoulou, K.; Tian, Y.; Wu, J.; Wen, W.; Skaltsounis, L.; Jove, R. MLS-2384, a new 6-bromoindirubin derivative with dual JAK/Src kinase inhibitory activity, suppresses growth of diverse cancer cells. *Cancer Biol.* **2014**, *15*, 178–184. [CrossRef] [PubMed]
52. Chipuk, J.E.; Green, D.R. How do BCL-2 proteins induce mitochondrial outer membrane permeabilization? *Trends Cell Biol.* **2008**, *18*, 157–164. [CrossRef] [PubMed]
53. Banerjee, K.; Resat, H. Constitutive activation of STAT3 in breast cancer cells: A review. *Int. J. Cancer* **2016**, *138*, 2570–2578. [CrossRef] [PubMed]
54. Sumarni, U.; Reidel, U.; Eberle, J. Targeting Cutaneous T-Cell Lymphoma Cells by Ingenol Mebutate (PEP005) Correlates with PKC delta Activation, ROS Induction as Well as Downregulation of XIAP and c-FLIP. *Cells* **2021**, *10*, 987. [CrossRef]
55. Kurbanov, B.M.; Geilen, C.C.; Fecker, L.F.; Orfanos, C.E.; Eberle, J. Efficient TRAIL-R1/DR4-mediated apoptosis in melanoma cells by tumor necrosis factor-related apoptosis-inducing ligand (TRAIL). *J. Invest. Derm.* **2005**, *125*, 1010–1019. [CrossRef]
56. Shi, J.; Shen, H.M. Critical role of Bid and Bax in indirubin-3′-monoxime-induced apoptosis in human cancer cells. *Biochem. Pharm.* **2008**, *75*, 1729–1742. [CrossRef]
57. Berger, A.; Quast, S.A.; Plotz, M.; Hein, M.; Kunz, M.; Langer, P.; Eberle, J. Sensitization of melanoma cells for death ligand-induced apoptosis by an indirubin derivative-Enhancement of both extrinsic and intrinsic apoptosis pathways. *Biochem. Pharm.* **2011**, *81*, 71–81. [CrossRef]
58. Kameswaran, T.R.; Ramanibai, R. Indirubin-3-monooxime induced cell cycle arrest and apoptosis in Hep-2 human laryngeal carcinoma cells. *Biomed. Pharm.* **2009**, *63*, 146–154. [CrossRef]
59. Liu, P.; Yang, W.T.; Shi, L.; Zhang, H.Y.; Xu, Y.; Wang, P.R.; Zhang, G.L.; Chen, W.R.; Zhang, B.B.; Wang, X.L. Concurrent photothermal therapy and photodynamic therapy for cutaneous squamous cell carcinoma by gold nanoclusters under a single NIR laser irradiation. *J. Mater. Chem. B* **2019**, *7*, 6924–6933. [CrossRef]
60. Austin, E.; Koo, E.; Jagdeo, J. Thermal photodynamic therapy increases apoptosis and reactive oxygen species generation in cutaneous and mucosal squamous cell carcinoma cells. *Sci. Rep.* **2018**, *8*, 12599.
61. Niu, T.H.; Tian, Y.; Wang, G.Y.; Guo, G.J.; Tong, Y.; Shi, Y. Inhibition of ROS-NF-kappa B-dependent autophagy enhances Hypocrellin A united LED red light-induced apoptosis in squamous carcinoma A431 cells. *Cell Signal.* **2020**, *69*. [CrossRef]

Auszug aus der Journal Summary List (3)

Journal Data Filtered By: **Selected JCR Year: 2020** Selected Editions: SCIE,SSCI Selected Categories: **"BIOCHEMISTRY and MOLECULAR BIOLOGY"** Selected Category Scheme: WoS

Gesamtanzahl: 297 Journale

Rank	Full Journal Title	Total Cites	Journal Impact Factor	Eigenfactor Score
1	NATURE MEDICINE	114,401	53.440	0.184050
2	CELL	320,407	41.582	0.526960
3	Molecular Cancer	24,931	27.401	0.030030
4	Annual Review of Biochemistry	24,394	23.643	0.021450
5	Signal Transduction and Targeted Therapy	3,848	18.187	0.005730
6	MOLECULAR CELL	86,299	17.970	0.161840
7	TRENDS IN MICROBIOLOGY	17,553	17.079	0.022820
8	NUCLEIC ACIDS RESEARCH	248,139	16.971	0.387070
9	MOLECULAR BIOLOGY AND EVOLUTION	61,557	16.240	0.082270
10	PROGRESS IN LIPID RESEARCH	7,328	16.195	0.004530
11	MOLECULAR PSYCHIATRY	28,622	15.992	0.046220
12	CELL DEATH AND DIFFERENTIATION	27,701	15.828	0.028730
13	NATURE STRUCTURAL & MOLECULAR BIOLOGY	32,038	15.369	0.051210
14	Nature Chemical Biology	27,428	15.040	0.047880
15	MOLECULAR ASPECTS OF MEDICINE	8,136	14.235	0.006640
16	TRENDS IN BIOCHEMICAL SCIENCES	22,003	13.807	0.025760
17	NATURAL PRODUCT REPORTS	13,293	13.423	0.011160
18	Molecular Plant	15,778	13.164	0.026860
19	Advances in Carbohydrate Chemistry and Biochemistry	752	12.200	0.000200
20	TRENDS IN MOLECULAR MEDICINE	13,213	11.951	0.014720

Rank	Full Journal Title	Total Cites	Journal Impact Factor	Eigenfactor Score
21	Redox Biology	15,982	11.799	0.024930
22	EMBO JOURNAL	76,189	11.598	0.055000
23	MATRIX BIOLOGY	8,972	11.583	0.011010
24	Molecular Systems Biology	10,149	11.429	0.016300
25	PLANT CELL	64,794	11.277	0.036260
26	CURRENT BIOLOGY	78,289	10.834	0.116100
27	BIOCHIMICA ET BIOPHYSICA ACTA-REVIEWS ON CANCER	7,025	10.680	0.007000
28	Cell Systems	5,813	10.304	0.035330
29	ONCOGENE	77,576	9.867	0.059180
30	CELLULAR AND MOLECULAR LIFE SCIENCES	34,003	9.261	0.033790
31	GENOME RESEARCH	47,141	9.043	0.064690
32	CURRENT OPINION IN CHEMICAL BIOLOGY	12,240	8.822	0.014190
33	EMBO REPORTS	19,502	8.807	0.027490
34	EXPERIMENTAL AND MOLECULAR MEDICINE	8,780	8.718	0.013260
35	ANTIOXIDANTS & REDOX SIGNALING	26,971	8.401	0.016700
36	CRITICAL REVIEWS IN BIOCHEMISTRY AND MOLECULAR BIOLOGY	4,576	8.250	0.005370
37	Science Signaling	15,954	8.192	0.023910
38	Cell Chemical Biology	5,236	8.116	0.018050
39	PLOS BIOLOGY	39,598	8.029	0.059920
40	Essays in Biochemistry	3,629	8.000	0.006450
41	BIOINORGANIC CHEMISTRY AND APPLICATIONS	1,406	7.778	0.000890

Selected JCR Year: 2020; Selected Categories: "BIOCHEMISTRY and MOLECULAR BIOLOGY"

Rank	Full Journal Title	Total Cites	Journal Impact Factor	Eigenfactor Score
42	Acta Crystallographica Section D-Structural Biology	23,670	7.652	0.020190
43	CYTOKINE & GROWTH FACTOR REVIEWS	7,650	7.638	0.005850
44	FREE RADICAL BIOLOGY AND MEDICINE	52,714	7.376	0.034180
45	Computational and Structural Biotechnology Journal	3,620	7.271	0.006770
46	AMYLOID-JOURNAL OF PROTEIN FOLDING DISORDERS	2,202	7.141	0.003280
47	Cell and Bioscience	3,184	7.133	0.004320
48	Genes & Diseases	1,850	7.103	0.003170
49	Molecular Ecology Resources	13,390	7.090	0.016690
50	Journal of Integrative Plant Biology	6,749	7.061	0.006430
51	BIOMACROMOLECULES	45,724	6.988	0.026020
52	INTERNATIONAL JOURNAL OF BIOLOGICAL MACROMOLECULES	79,246	6.953	0.073720
53	AMERICAN JOURNAL OF RESPIRATORY CELL AND MOLECULAR BIOLOGY	15,280	6.914	0.015050
54	International Review of Cell and Molecular Biology	3,057	6.813	0.004320
55	CURRENT OPINION IN STRUCTURAL BIOLOGY	12,448	6.809	0.018970
56	PROTEIN SCIENCE	16,581	6.725	0.021220
57	International Journal of Biological Sciences	10,778	6.580	0.010540
58	Open Biology	4,059	6.411	0.010280
59	MOLECULAR MEDICINE	6,230	6.354	0.004160
60	Antioxidants	9,076	6.312	0.009480
61	JOURNAL OF PHOTOCHEMISTRY AND PHOTOBIOLOGY B-BIOLOGY	17,015	6.252	0.012740

Selected JCR Year: 2020; Selected Categories: "BIOCHEMISTRY and MOLECULAR BIOLOGY"

Publication 3

antioxidants

MDPI

Article

Inhibition of Cell Proliferation and Cell Viability by Sinecatechins in Cutaneous SCC Cells Is Related to an Imbalance of ROS and Loss of Mitochondrial Membrane Potential

Jiaqi Zhu [1,2], Bernd Gillissen [3], Dieu Linh Dang Tran [1,4], Stefanie May [1], Claas Ulrich [1], Eggert Stockfleth [5] and Jürgen Eberle [1,*]

[1] Skin Cancer Centre Charité, Department of Dermatology and Allergy, Charité–Universitätsmedizin Berlin, Charitéplatz 1, 10117 Berlin, Germany; jiaqi.zhu@charite.de (J.Z.); tran-dieu-linh.dang@charite.de (D.L.D.T.); stefanie.may@charite.de (S.M.); claas.ulrich@charite.de (C.U.)
[2] Department of Gynecology and Obstetrics, Jilin University, 130001 Changchun, China
[3] Department of Hematology, Oncology and Tumor Immunology, Charité–Universitätsmedizin Berlin, 13125 Berlin, Germany; bernhard.gillissen@charite.de
[4] Beuth-Hochschule für Technik Berlin–University of Applied Sciences, Luxemburger Str. 10, 13353 Berlin, Germany
[5] Dermatologie, Venerologie und Allergologie, Klinikum Bochum, Ruhr-Universität Bochum, Gudrunstr. 56, 44791 Bochum, Germany; e.stockfleth@klinikum-bochum.de
* Correspondence: juergen.eberle@charite.de; Tel.: +49-30-450-518-383

Citation: Zhu, J.; Gillissen, B.; Dang Tran, D.L.; May, S.; Ulrich, C.; Stockfleth, E.; Eberle, J. Inhibition of Cell Proliferation and Cell Viability by Sinecatechins in Cutaneous SCC Cells Is Related to an Imbalance of ROS and Loss of Mitochondrial Membrane Potential. *Antioxidants* **2022**, *11*, 1416. https://doi.org/10.3390/antiox11071416

Academic Editor: Salvador Máñez Aliño

Received: 20 June 2022
Accepted: 18 July 2022
Published: 21 July 2022

Abstract: The term sinecatechins designates an extract containing a high percentage of catechins obtained from green tea, which is commercially registered as Veregen or Polyphenon E (PE) and may be considered for treatment of cutaneous squamous cell carcinoma (cSCC) and actinic keratosis (AK). As shown here, treatment of four cSCC cell lines with 200 µg/mL of PE resulted in strong, dose-dependent decrease in cell proliferation (20–30%) as well as strongly decreased cell viability (4–21% of controls, 48 h). Effects correlated with loss of mitochondrial membrane potential, whereas early apoptosis was less pronounced. At the protein level, some activation of caspase-3 and enhanced expression of the CDK inhibitor p21 were found. Loss of MMP and induced cell death were, however, largely independent of caspases and of the proapoptotic Bcl-2 proteins Bax and Bak, suggesting that sinecatechins induce also non-apoptotic, alternative cell death pathways, in addition to apoptosis. Reactive oxygen species (ROS) were downregulated in response to PE at 4 h, followed by an increase at 24 h. The contributory role of initially reduced ROS was supported by the antioxidant N-acetyl cysteine, which in combination with PE further enhanced the negative effects on cell viability. Thus, sinecatechins inhibited cell proliferation and viability of cSCC cells, which could suggest the use of PE for AK treatment. The mechanisms appear as linked to an imbalance of ROS levels.

Keywords: cancer; therapy; cell viability; reactive oxygen species; apoptosis

1. Introduction

About 20% of skin malignancies and skin cancer deaths worldwide result from cutaneous squamous cell carcinoma (cSCC) [1,2]. Thus, following basal cell carcinoma, cSCC is the second most common skin cancer in Caucasians and East Asians [3,4]. Actinic keratosis (AK) is characterized by a particularly high prevalence and is mainly located on sun-exposed areas of the skin. Clinical and subclinical lesions often coexist across a large area described as field cancerization [5]. As AK derives from neoplastic epidermal

keratinocytes, and as lesions have the potential to transform into invasive cSCC, AK was defined as cSCC in situ, and its treatment is crucial [6].

Several therapies have been established for AK/cSCC in recent years, and the green tea extract sinecatechins (PE) represent a promising candidate [7,8]. PE contains a particularly high proportion of epigallocatechin-3-gallate (EGCG; 55%) as well as other polyphenolic compounds as epigallocatechin, epicatechin-3-gallate, epicatechin, gallocatechins, and gallocatechin gallate [9]. For EGCG, inhibition of cell proliferation and induction of apoptosis have already been reported in mammary carcinoma, lung cancer and gastric cancer cells [10–12].

Cell proliferation is critically regulated by cyclin-dependent kinases (CDK 1/2/4/6), which mediate retinoblastoma (Rb) protein phosphorylation, thus resulting in E2F transcription factor-induced gene expression and activation of the cell cycle [13]. On the other hand, a panel of CDK inhibitors as of the INK4 family (p15, p16, p18, and p19) as well as of the Cip/Kip family (p21, p27 and p57) can prevent cell cycle progression [14]. While CDK inhibitors critically control cell proliferation in normal cells, they may be downregulated or abolished in cancer [15].

Induction of apoptosis represents an important goal in cancer therapy [16], and intrinsic proapoptotic pathways are activated by different anticancer drugs. This relies on mitochondrial membrane permeability and loss of mitochondrial membrane potential, which may further result in caspase activation [17]. The major effector caspase (caspase-3) cleaves multiple death substrates, which finally results in DNA fragmentation and apoptosis induction. Caspase-3 itself can be activated by the initiator caspase of the extrinsic apoptosis pathway (caspase-8) or by the initiator caspase of the intrinsic apoptosis pathway (caspase-9) [18]. The intrinsic, mitochondrial apoptotic pathways are mainly controlled by pro- and antiapoptotic Bcl-2 proteins. Here, the functionally related, proapoptotic, multidomain proteins Bax and Bak play essential roles, because, once activated, they cause mitochondrial outer membrane permeability and release of proapoptotic components from the intermembrane space into the cytosol [17]. In particular, mitochondria-mediated apoptosis is prevented in Bax/Bak knockout cells [19–21].

Reactive oxygen species are involved in different signaling pathways and play important roles in disease of the neuronal, cardiovascular, and nervous systems as well as in aging [22]. ROS have been further related to apoptosis induction in cancer cells, as recently shown in cSCC cells for celecoxib [23] and for indirubin derivatives [24].

Besides the often discussed possible roles of sinecatechins in cancer prevention, they were also suggested as therapeutic strategy for skin cancer as for AK [7]. Nevertheless, there is still only limited information on its direct effects and mechanisms in skin cancer cells. We therefore investigated its effects in four cSCC cell lines, which also represent cell culture models of AK. In particular, inhibition of cell proliferation, loss of cell viability, induction of apoptosis and molecular mechanisms were addressed.

2. Materials and Methods

2.1. Cells and Treatment

The effects of sinecatechins were studied in four established cSCC cell lines: SCL-I, SCL-II, SCC-12, and SCC-13. As AK is defined as cSCC in situ, these cell lines also serve as models for AK. SCC-12 and SCC-13 were kindly provided by Prof. J.G. Rheinwald (Department of Dermatology, Brigham and Women's Hospital, Harvard Medical School, Boston, MA, USA); SCL-I and SCL-II were kindly provided by Prof. N.E. Fusenig (DKFZ, Heidelberg, Germany). SCC-12 and SCC-13 derive from rapidly growing, well-differentiated SCCs of the epidermis; SCL-I and SCL-II derive from squamous cell carcinomas of human skin. All four cell lines form monolayers in cell culture; atypical and poor stratification of colonies had been reported as well as tumorgenicity in nude mice [25,26]. SCL-I has shown resistance to diclofenac in a previous project, while the other cell lines were sensitive [27]. SCC cells were cultured at 5% CO_2 in growth medium RPMI 1640 (Life

Technologies, Darmstadt, Germany), which was supplemented with FCS (10%), glutamine (2 mM), non-essential amino acids and antibiotics.

For determination of Bax/Bak dependency, HCT-116 colon carcinoma wild-type cells (HCT-116 WT) and the isogenic double knockout subline HCT-116-Bax$^{-/-}$/Bak$^{-/-}$ (HCT-116 KO) were used, which had been kindly provided by Dr. R.J. Youle, National Institutes of Health, Bethesda, MD, USA [19]. HCT-116 cells were grown at 37 °C and 5% CO_2 in DMEM growth medium (Invitrogen (Karlsruhe, Germany) supplemented with 10% FCS, penicillin and streptomycin. For control, normal human fibroblast cells (MRC-5) were used, which were derived from embryonic lung tissue (CCL-171, ATCC, Manassas, VA, USA).

Most assays were performed in 24-well plates, and 5×10^4 cells were seeded per well. Sinecatechins (PE) was supplied by CPM Aenova (Feldkirchen, Germany); stock solutions were prepared in aqua iniectabilia at concentrations of 5 mg/mL, sterilized by filtration (0.2 µm filters) and stored at −80 °C. Light protection was applied at all steps. PE was applied in concentrations of 10, 25, 50, 100, and 200 µg/mL. For positive control, cells were treated with EGCG (Epigallocatechin gallate; Sigma-Aldrich E4143; 25 and 100 µg/mL). For further apoptosis control, cells were treated with an indirubin derivative (DKP-071, 10 µM) and/or TRAIL (TNF-related apoptosis inducing ligand; KillerTRAIL, Adipogen, San Diego, CA, AG-40T-0001; 50 ng/mL). The pan-caspase inhibitor Q-VD-OPH (Merck, Darmstadt, Germany, 5 µM) was applied 1 h before the other treatments.

2.2. Cell Proliferation

Relative cell proliferation rates were determined by WST-1 assay (Roche Diagnostics, Penzberg, Germany), which is based on staining cells with the water-soluble tetrazolium salt WST-1. In metabolically active cells, WST-1 is converted to formazan dye by mitochondrial dehydrogenases. The assay was quantified in an ELISA reader at 450 nm. As the enzyme activity is restricted to viable cells, the read-out reflects both cell numbers and cell viability. Thus, reduced WST-1 values may reflect either less cells (reduced cell proliferation) or less mitochondrial enzyme in single cells (less viable).

2.3. Apoptosis Induction and Cell Viability

For quantification of apoptosis by cell cycle analysis, cells were harvested by trypsinization and were dissolved in a hypotonic buffer containing sodium citrate (0.1%), triton-x 100 (0.1%) and propidium iodide (PI, Sigma-Aldrich, St. Louis, MO, USA, 40 µg/mL), in PBS. In this way, cells were lysed, and isolated cell nuclei were stained for at least 1 h with propidium iodide at 4 °C. Nuclei in cell cycle phases G1, G2 and S-phase as well as apoptotic sub-G1 nuclei were identified by flow cytometry at FL3A using a FACS Calibur (BD Bioscience, Bedford, MA, USA). As small DNA fragments are washed out of the nuclei by this procedure, apoptotic cells with DNA fragmentation are characterized by nuclei with less DNA (sub-G1 populations).

As an independent cell death assay, cells were stained with Annexin V-fluorescein isothiocyanate (AnnV) and propidium iodide (PI). In brief, cells harvested by trypsin/EDTA were washed twice with cold PBS and resuspended at 1×10^6 cells/mL in 10 mM Hepes (pH 7.4), 140 mM NaCl, 2.5 mM $CaCl_2$. For 100 µL of cell suspension (1×10^5 cells), 5 µL of AnnV-FITC (BD Biosciences, Heidelberg, Germany) and 10 µL PI (20 mg/mL, Sigma-Aldrich) were added, and cells were incubated for 10 min on ice. Subsequently, samples were analyzed using a FACScan and CELLQuest software (Becton Dickinson, Heidelberg, Germany).

For determination of cell viability, cells were stained with calcein-AM (PromoCell, Heidelberg, Germany), which is transported through the cellular membrane into live cells. Upon transport, cellular esterases cut off the AM groups, the molecules bind to calcium within cells resulting in acquiring strong green fluorescence. As dead cells largely lack esterases, only live cells are efficiently marked. Cells were grown and treated in 24-well plates; they were harvested by trypsinization and stained with calcein-AM (0.5 µM) at 37

°C for 1 h. Before measurement by flow cytometry (FL2H), cells were washed two-times with PBS. Due to the evaluation by flow cytometry, the percentage of viable and non-viable cells can be determined, independently of the total cell number. As controls in calcein assays, cells without calcein labelling were also compared, and the effect of PE treatment on cell size was determined by monitoring FSC (forward scatter) in flow cytometry.

2.4. Mitochondrial Membrane Potential

For determination of the loss of mitochondrial membrane potential, cells were stained with the fluorescent dye tetramethylrhodamine-6-maleimide ($TMRM^+$; Sigma-Aldrich). $TMRM^+$ is transported into mitochondria with sufficient high mitochondrial membrane potential. Cells were grown and treated in 24-well plates; they were harvested by trypsinization and stained by $TMRM^+$ (1 μM, 20 min, 37 °C). After 2× washing with PBS, cells were measured by flow cytometry (FL2H).

For microscopic visualization of MMP as well as of morphological changes in course of apoptosis, SCC cells were seeded into 6-well plates (2×10^5 cells/2 mL) and treated for 24 h. Thereafter, cells were incubated for 30 min with 2 μg/mL JC-1 (5,5′,6,6′-tetrachloro-1,1′,3,3′-tetraethyl-benzimidazolylcarbocyanin iodide; Life Technologies) and with 0.2 μg/mL Hoechst-33342 (Sigma-Aldrich Chemie, Taufkirchen, Germany). After staining, microscopy images were taken with an Axiovert 200 inverse fluorescence microscope (Carl Zeiss, Jena, Germany) equipped with appropriate fluorescence filter sets and a Hamamatsu ORCA-ER digital camera.

2.5. Analysis of Reactive Oxygen Species

To determine intracellular ROS levels, cells were stained with the cell-permeable and non-fluorescent chemical 2′,7′-dichlorodihydrofluorescein diacetate (H_2DCF-DA; D-399, Thermo Fisher Scientific, Hennigsdorf, Germany), which is oxidized in cells with high ROS levels to the fluorescent 2′,7′-dichlorodihydrofluorescein (DCF). Cells were grown in 24-well plates and were pre-incubated for 1 h with H_2DCF-DA (10 μM), before starting treatment with other effectors. After 4–24 h of treatment, cells were harvested by trypsinization, washed two-times with PBS and were then analyzed by flow cytometry (FL1H). As positive controls, cells were treated with 1 mM H_2O_2 for 1 h. The antioxidant N-acetylcysteine (NAC, Sigma-Aldrich, Taufkirchen, Germany; 1 mM) was applied simultaneously with PE, aiming at a further decrease in PE-reduced ROS levels.

2.6. Western Blotting

For Western blotting, total proteins were extracted by lysing the cells in cell lysis buffer, containing 150 mM NaCl, 1 mM EDTA, 1% NP-40, 50 mM Tris-HCl, pH 8.0, and inhibitors for proteases and phosphatases. After SDS polyacrylamide gel electrophoresis, proteins were transferred by electro blotting to nitrocellulose membranes.

The following primary antibodies were used: Cleaved caspase-3 (9664, rabbit, 1:1000; Cell Signaling, Danvers, MA, USA); Caspase-8 (9746, mouse, 1:1000; Cell Signaling), Caspase-9 (9502, rabbit, 1:1000; Cell Signaling); p21 (sc-6246, mouse, 1:200; Santa Cruz Biotech, Dallas, TX, USA); p19 (sc-1063, rabbit, 1:200; Santa Cruz Biotech); β-actin (sc-47778, mouse, 1:200; Santa Cruz Biotech). The following secondary antibodies were used: peroxidase-labeled goat anti-rabbit and goat anti-mouse (Dako, Hamburg, Germany; 1:5000).

2.7. Statistical Analyses

Results of assays were generally proven by two to three independent experiments. Each individual experiment was consisted of triplicate values (three wells that were seeded, treated and analyzed individually). Thus for statistical analysis, there were at least six values in each group. For calculation of statistical significance, Student's t-test was used, and significance is indicated by asterisks in all figures (* $p < 0.05$). Western blot experiments were repeated at least once by using two independent series of protein extracts.

For semi-quantitative analysis, selected protein bands were quantified by densitometry, normalized by the respective β-actin signals, and median values were formed from two independent experiments.

3. Results

3.1. Dose-Dependent Inhibition of Cell Proliferation by Sinecatechins (PE)

The targeting of cancer cell proliferation and reduction of cell numbers represent important goals in anticancer therapy. Effects on cell proliferation were investigated in cSCC cell lines SCL-I, SCL-II, SCC-12, and SCC-13 in response to increasing concentrations of PE (10, 25, 50, 100 and 200 µg/mL). As determined by quantitative WST-1 assays, PE resulted in strong and dose-dependent decrease in cell counts in all four cell lines. Effects were somewhat stronger at 48 h as compared to 24 h. Thus at 48 h, cell proliferation was decreased by 100/200 µg/mL PE to 43%/22% (SCL-I), 29%/19% (SCL-II), 39%/29% (SCC-12) and to 37%/24% (SCC-13), respectively (Figure 1). For comparison, cells were treated with 25 and 100 µg/mL EGCG. Largely comparable effects were obtained as for 50 and for 200 µg/mL of PE, respectively, reflecting the roughly 55% of EGCG in PE (Figure 1). The IC50 values for PE treatment at 48 h were determined with 89 (SCL-I), 61 (SCL-II), 25 (SCC-12) and 82 µg/mL (SCC-13). For control, we investigated MRC-5 normal human fibroblasts, which were seeded and treated in an identical way as cSCC cells. In contrast to cSCC cells, no significant antiproliferative effects were found in MRC-5 at 24 h or 48 h (10–200 µg/mL PE), as determined by WST-1 assay (Supplementary Figure S1A).

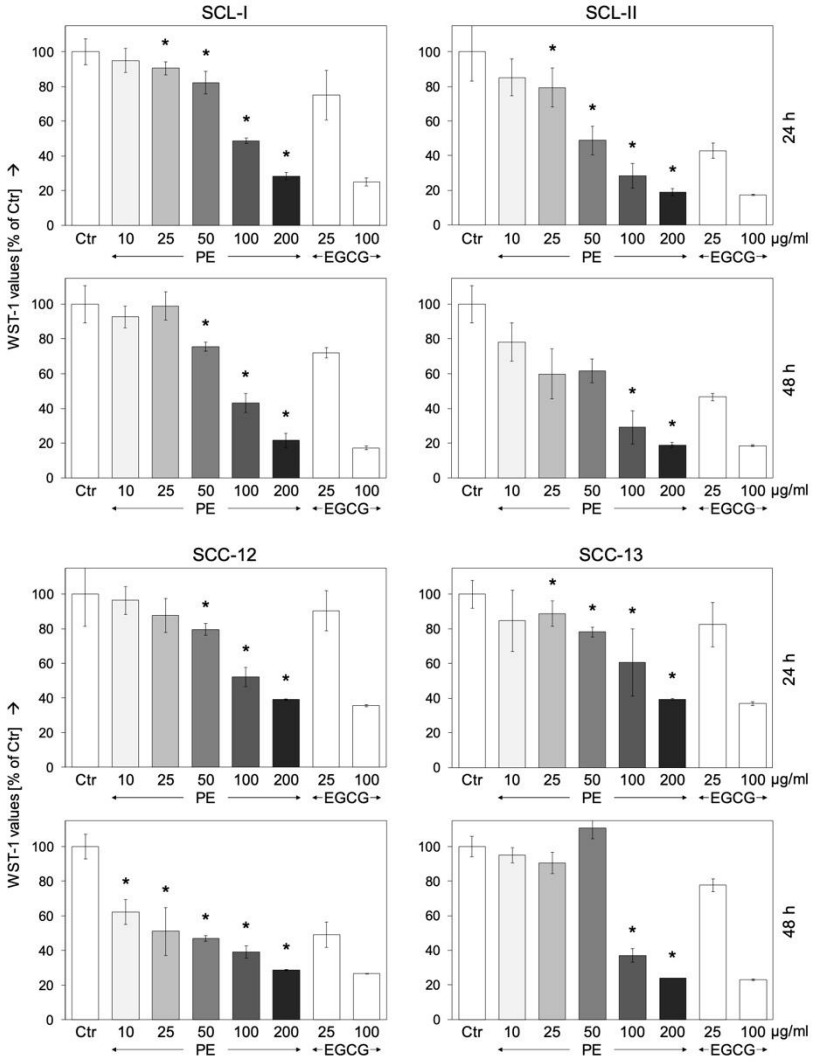

Figure 1. Reduced cell proliferation by PE. SCL-I, SCL-II, SCC-12, and SCC-13 were seeded in 96-well pates and were treated with increasing concentrations of PE (10–200 µg/mL). As controls, EGCG was used at 25 and 100 µg/mL. Cell proliferation was quantified by WST-1 assay at 24 h and at 48 h of treatment. One of two independent experiments is shown here, each one consisting of triplicate values. Effects on cell proliferation are shown as percentages of non-treated controls (Ctr = 100%). Statistical significance of PE treatments was calculated from all individual values (#6) and is indicated by asterisks ($p < 0.05$, as compared to Ctr).

3.2. Strongly Reduced Cell Viability and Moderate Induction of Early Apoptosis

The effects of PE in cSCC cells were further investigated at the levels of cell viability (calcein-AM staining) and apoptosis (propidium iodide staining). Reduced cell proliferation rates, as shown above, coincided with strongly reduced cell viability at 24 h and 48 h. Thus, numbers of viable cell were reduced by PE (200 μg/mL) at 48 h to 4% (SCL-I), 16% (SCL-II), 4% (SCC-12) and 3% (SCC-13), respectively (non-treated controls: 53–90%; Figure 2A,B). In parallel with loss of cell viability, cell size somewhat decreased, as determined by reduced FSC (forward scatter) in flow cytometry. Thus, PE-200 resulted in decreased FSC of 68%, 67%, 90%, and 49%, in SCL-I, SCL-II, SCC-12, and SCC-13, respectively, as compared to controls (data not shown). The reduced size alone, however, cannot explain the strongly reduced calcein staining. Comparable loss of cell viability was obtained at 48 h with 100 μg/mL of EGCG, reflecting the 55% of EGCG in PE. MRC-5 normal human fibroblasts were again seeded and treated in an identical way as cSCC cells and were used as control. In contrast to cSCC cells, no significant loss of cell viability was found in MRC-5 at 24 h or 48 h (50–200 μg/mL PE), as determined by calcein staining (Supplementary Figure S1B).

In contrast to strongly reduced cell viability, effects on apoptosis induction, as determined by cell cycle analysis (sub-G1 cell populations), remained on a lower level reaching at maximum 13% +/− 7% in SCL-II and 14% +/− 4% in SCC-13 (48 h, PE-200; Figure 2C). In SCL-I and SCL-II, cell death was also investigated at 24 h by Annexin V-FITC / PI staining (AnnV/PI). As positive controls for apoptosis induction, cells were treated with a combination of an indirubin derivative (DKP-071) and TRAIL, as reported previously [24]. Early apoptotic cells were identified as AnnV(+)/PI(−) (Figure 2D). While early apoptosis was strongly enhanced by DKP/TRAIL in both cell lines (28%, 40%), PE-induced early apoptosis remained on a lower level (7–11%, Figure 2E), comparable to the values obtained by cell cycle analysis, shown above. On the other hand, numbers of AnnV(+)/PI(+) cells (late apoptosis or necrosis) were strongly enhanced at 24 h in SCL-I (29%) and SCL-II (39%; Figure 2D,E).

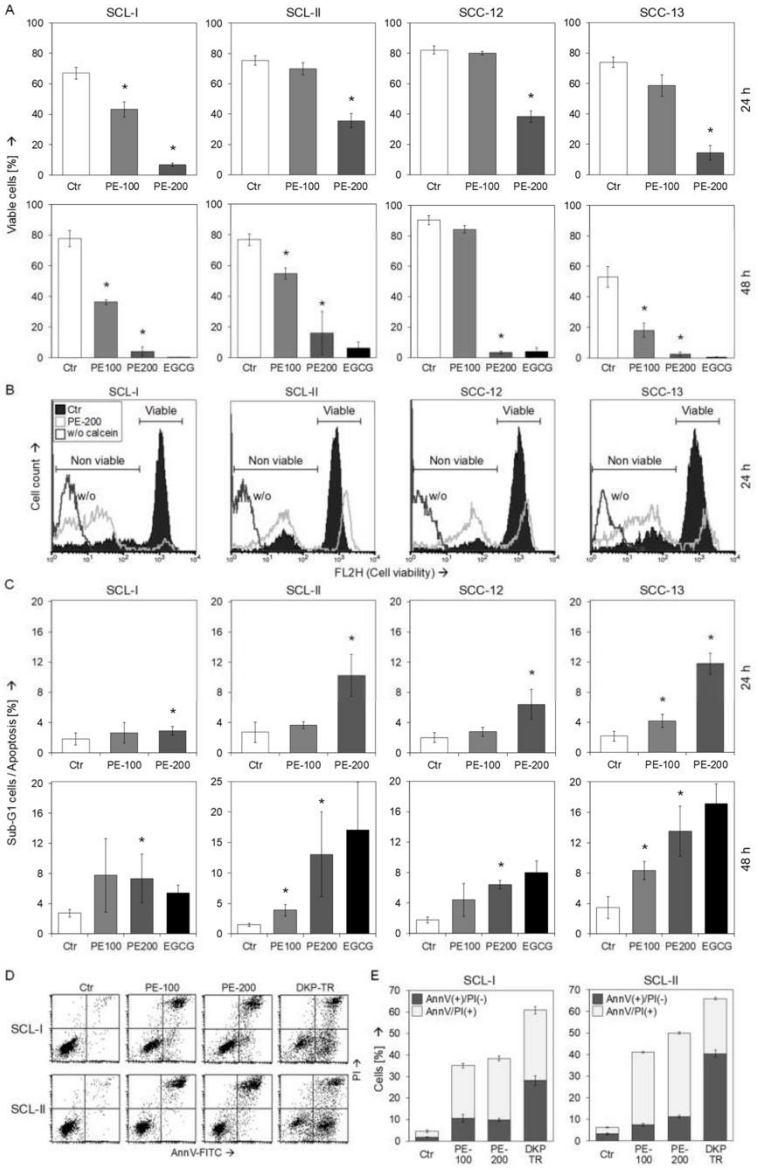

Figure 2. Reduced cell viability by PE. (**A**–**C**) SCL-I, SCL-II, SCC-12, and SCC-13 were seeded in 24-well plates and were treated with PE (100, 200 µg/mL) for 24 h and 48 h, respectively. For control, cells were also treated with 100 µg EGCG for 48 h. (**A**) Cell viability was determined by calcein-AM staining and flow cytometry. Values represent the percentage of cells with high calcein staining (=

viable cells). (**B**) Examples of flow cytometry reading are shown for the cell lines at 24 h and 200 μg/mL PE treatment (overlays of treated cells vs. Ctr, logarithmic scale). Non-viable and viable cell populations are indicated. For control, cells are also shown without calcein staining (PE-200-treated, w/o). (**C**) Apoptosis was quantified by propidium iodide staining and flow cytometry (cell cycle analyses). Values represent the percentage of sub-G1 cells (=apoptotic cells). (**A**,**C**) Each one of at least two independent experiments is shown; each independent experiment consisted of triplicate values. Statistical significance for PE treatments was calculated from all individual values (#6) and is indicated by asterisks ($p < 0.05$, as compared to Ctr). (**D**) For SCL-I and SCL-II, induced cell death by PE-100 and PE-200 was determined by AnnV/PI staining. Treatment with the indirubin derivative DKP-071 in combination with TRAIL was used as control (DKP/TR). Representative flow cytometry histograms are shown of treated and control cells. (E) Mean values and SDs of AnnV(+)/PI(+) cells and of AnnV(+)/PI(−) cells are shown (in %). Mean values and SDs correspond to each six individual values obtained in two independent experiments with triplicates.

3.3. Loss of Mitochondrial Membrane Potential

Maintenance of mitochondrial membrane potential (MMP) represents a critical issue in viable cells, and its early loss may be a characteristic feature of activation of intrinsic, proapoptotic pathways. We thus monitored MMP in response to PE at 24 h by applying $TMRM^+$ staining and flow cytometry. In contrast to only moderately induced early apoptosis (Figure 2C,E), loss of MMP at 24 h appeared as a strong effect. As seen in flow cytometry charts, almost the whole cell populations of SCL-I, SCL-II, SCC-12, and SCC-13 were shifted, resulting in values of 75%, 97%, 61%, and 84% of cells with low MMP (200 μg/mL PE; Figure 3A).

Loss of MMP in PE-treated cells was further visualized by JC-1/ Hoechst-33342 double staining. While cell nuclei are stained blue with Hoechst-33342, the cationic dye JC-1 accumulates in mitochondria of viable cells, where it forms red fluorescent aggregates. Upon loss of MMP, however, JC-1 locates to the cytosol and fluorescence shifts from red to green. Treatment with an indirubin derivative (DKP-071, 10 μM) in combination with TRAIL was applied as positive control, as reported previously [24]. Whereas vital control cells were characterized by red-stained mitochondria, PE-100 and PE-200 treatment resulted in complete loss of red mitochondrial staining, reflecting loss of MMP. Only blue nuclear staining and green cytosolic staining remained, due to fact that cytosolic JC-1 is green (Figure 3B). However, upon PE treatment, there was only little incidence of a typical apoptotic cell morphology characterized by rounding and detachment of cells as well as by membrane blebbing, which was typically seen in positive control cells (DKP-071/TRAIL, Figure 3B). Thus, loss of MMP by PE appeared as a strong effect but was decoupled from apoptosis induction.

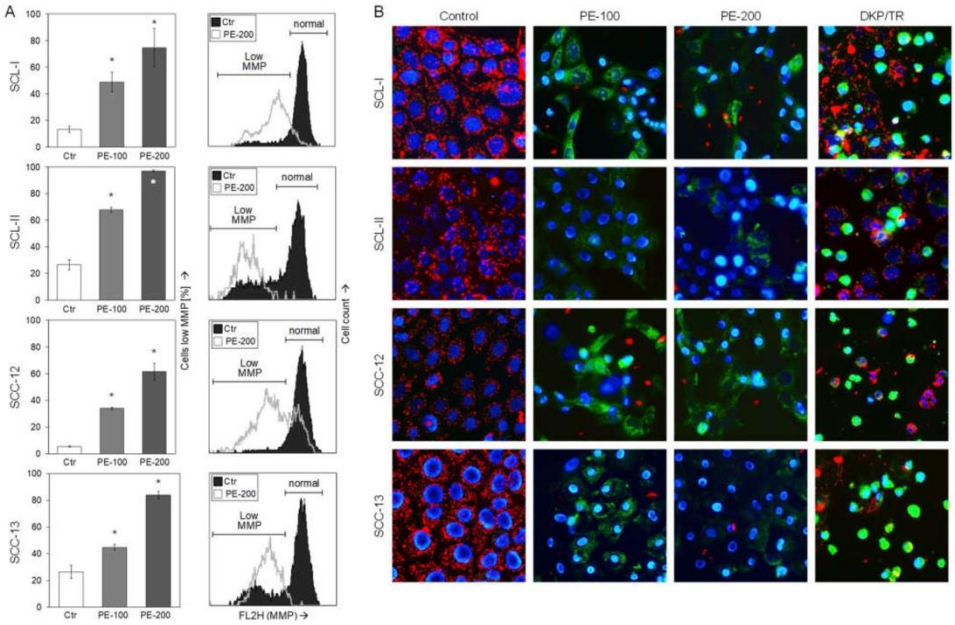

Figure 3. Loss of mitochondrial membrane potential. (**A**) SCL-I, SCL-II, SCC-12, and SCC-13 were seeded in 24-well pates and were treated with PE (100, 200 µg/mL) for 24 h. Mitochondrial membrane potential (MMP) was determined at 24 h by TMRM⁺ staining and flow cytometry. Values represent the percentage of cells with low MMP. Right, examples of flow cytometry reading are shown for 200 µg/mL treatment (overlays of treated cells vs. Ctr). Cell populations with low and normal MMP are indicated. One of two independent experiments is shown; each individual experiment consisted of triplicate values. Statistical significance was calculated from all individual values (#6) and is indicated by asterisks ($p < 0.05$, as compared to Ctr). (**B**) Cells were treated with PE-100 and PE-200 as well as with DKP-071 (10 µM)in combination with TRAIL (DKP/TR, positive control). For microscopic visualization of low MMP, cells were stained with JC-1 and counterstained with Hoechst-33342 at 24 h of treatment. Blue, nuclear staining; red, mitochondria with high (normal) MMP; faint green, JC-1-stained cytosol; bright green or turquoise, rounded and detached cells.

3.4. Caspase Activation and Upregulation of p21

To identify protein factors that may mediate apoptosis induction as well as inhibition of cell proliferation and cell viability by PE, the cell cycle inhibitors p19 and p21, the main effector caspase-3 as well as proapoptotic initiator caspases (−8 and −9) were investigated by Western blotting (Figure 4). Some induction of caspase-3 processing was seen in response to PE treatment (characteristic cleavage products of 18 and 16 kDa), indicative of caspase-3 activation. However, this remained on a relatively low level, as seen in comparison with a positive control consisting of SCC-12 cells treated with the indirubin derivative DKP-071 in combination with TRAIL [24]. Semi-quantitative analyses revealed induction factors of 3x − 4x for the active p16 caspase-3 cleavage product after PE treatment, while p16 was induced > 60-fold in the positive control. Similarly, only weak activation was seen for initiator caspases of the proapoptotic extrinsic and intrinsic pathways. Thus, caspase-8 proform was downregulated to 64% in SCL-II by 200 mg/mL PE, and caspase-9 cleavage products (35/37 kDa) were slightly upregulated by 200 µg/mL PE in SCL-I (1.7x) and in

SCC-12 (3.7x). The weak caspase processing was in agreement with only moderately induced apoptosis described above.

As concerning inhibition of cell proliferation, we found dose-dependent upregulation of the CDK inhibitor p21 (21 kDa) by PE-200 in two cell lines (SCL-I, 2.9-fold; SCC-12, 3.1-fold), whereas there was no upregulation in SCL-II. Also, a representative of the INK4A family, p19, was not upregulated (Figure 4).

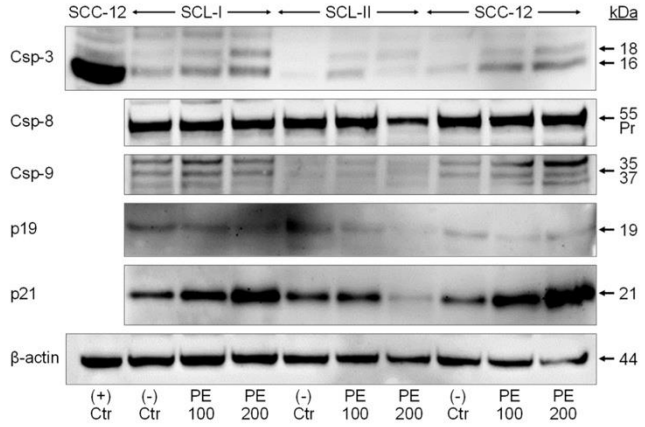

Figure 4. Weak caspase activation. Expression of caspase-3, caspase-8, caspase-9, p19, and p21 is shown by Western blotting in cell lines SCL-I, SCL-II, and SCC-12. Cells were treated for 24 h with PE (100, 200 μg/mL). Protein size (in kDa) is indicated on the right side, as determined in comparison to a protein size marker separated in parallel. Caspase activation is seen either by characteristic cleavage products, as 18/16 kDa for caspase-3 and 35/37 kDa for caspase-9 or by loss of the caspase-8 proform (55 kDa). For demonstrating full caspase-3 activation, a positive control is shown, (+)Ctr, consisting of SCC-12 cells treated with an indirubin derivative in combination with the death ligand TRAIL (TNF-related apoptosis-inducing ligand [24]. Expression of β-actin is shown as loading control. Largely similar results were obtained in two independent Western blot experiments using independent series of cell extracts.

3.5. No Dependence on Caspases or the Proapoptotic Bcl-2 Proteins Bax and Bak

As seen in Figure 2D,E, PE treatment resulted in less increase in early apoptotic cells characterized by AnnV(+)/PI(−), whereas numbers of late apoptotic/necrotic cells characterized by AnnV(+)/PI(+) were strongly increased. To further prove, whether cells may die by apoptosis, i.e., via a caspase-dependent pathway, and to evaluate the possible significance of caspases in PE-induced cell death, the pan-caspase inhibitor Q-VD-Oph was applied in SCL-I and SCL-II, and cell death was evaluated by AnnV/PI staining. When considering AnnV(+)/PI(−) cells (early apoptosis), the applied positive control (DKP-071/TRAIL) induced apoptosis in 30% and 43% of SCL-I and SCL-II cells, respectively. This proapoptotic effect was completely prevented by 10 μM Q-VD-Oph (Figure 5A). Similarly, induction of AnnV(+)/PI(+) cells by DKP-071/TRAIL was strongly reduced in SCL-I and was prevented in SCL-II by Q-VD-Oph, indicating late apoptotic (secondary necrotic) cells. In contrast, cell death induced by PE-200 was not significantly decreased by Q-VD-Oph, indicating also caspase-independent and non-apoptotic pathways induced by PE.

Mitochondrial apoptosis is typically mediated by either one of the multi-domain Bcl-2 proteins Bax or Bak [17]. Their possible role in PE-induced cell death was evaluated in a

cell culture model based on HCT-116 colon carcinoma cells. While HCT-116 WT cells express functional Bax and Bak, the double knockout strain is deficient for both proteins (HCT-116 KO), as described by Wang and Joule [19]. In our experiments, HCT-116 WT cells were sensitive for TRAIL (46% apoptosis) as well as showed a comparable response to PE treatment at 24 h as cSCC cells. Indicating the important roles of Bax/Bak in these cells, TRAIL-induced apoptosis was completely abolished in HCT-116 KO cells, whereas PE-mediated effects were much less decreased in KO cells (Figure 5B). When considering both AnnV(+)/PI(−) and AnnV(+)/PI(+) cells, the effects of PE-100 decreased from 26% to 19%, and the effects of PE-200 decreased from 35% to 28%.

To further analyze the possible role of Bax/Bak in PE-induced loss of MMP, HCT-116 WT and KO cells were stained with JC-1/Hoechst-33342. Again, the effects of TRAIL, here loss of MMP, were completely blocked in Bax/Bak-deficient cells, whereas loss of MMP by PE was less affected (Figure 5C). Together, these data indicate that also Bax and Bak were not essentially required for PE-induced cell death and loss of MMP, again suggesting the additional role of non-apoptotic, alternative pathways involved in PE-induced cell death.

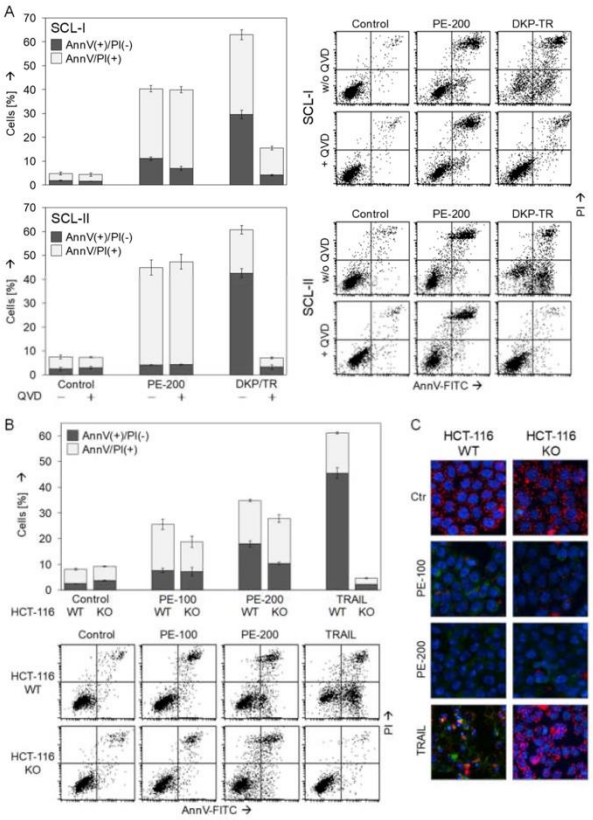

Figure 5. Less effects of caspase inhibition and Bax/Bak knockdown. (**A**) SCL-I and SCL-II cells were treated with 200 μg/mL PE (PE-200) or with an indirubin derivative DKP-071 in combination

with TRAIL (DKP/TR, positive control). In addition, cells received the pancaspase inhibitor Q-VD-Oph (10 μM), when indicated. (**B**,**C**) HCT-116 WT cells and HCT-116 double knockout cells for Bax and Bak (KO) were treated with PE (100 or 200 μg/mL) or with TRAIL (positive control). A, B) Cell death analysis by AnnV/PI staining and flow cytometry was performed after 24 h. Representative flow cytometry histograms of treated and control cells are shown on the right side or below. Mean values and SDs of two cell death fractions, namely AnnV(+)/PI(−) and AnnV(+)/PI(+) cells are shown (in %). (**C**) For microscopic visualization of low MMP and of morphological changes, cells were double stained with JC-1/Hoechst-33342 at 24 h. Blue, nuclear staining; red, mitochondria with high (normal) MMP; faint green, JC-1-stained cytosol; bright green or turquoise, rounded and detached cells.

3.6. Role of Reactive Oxygen Species

Increasing evidence in recent years has shown that the control of reactive oxygen species may play vital roles in cellular homeostasis, and induced ROS production can trigger apoptosis programs in cancer cells. On the other hand, antioxidative activities have been described for EGCG, a major constituent of PE [9]. Thus, the control of ROS in response to PE appeared of particular interest.

Indeed, reduced ROS levels were obtained in all four cell lines as an early response to PE treatment (100/200 μg/mL), as determined by the ROS-sensitive dye H_2DCF-DA and flow cytometry. Thus, ROS were reduced in response to 200 μg/mL at 4 h to 26% (SCL-I), 69% (SCL-II), 40% (SCC-12) and 26% (SCC-13), respectively. As seen from the cytometry charts, the whole cell populations appeared as responsive (Figure 6A).

The situation, however, reversed at 24 h. Then, ROS levels were enhanced in response to PE. Values of 420% (SCL-II), 160% (SCC-12) and 180% (SCC-13) were determined for 200 μg/mL PE, and again almost all cells appeared as responsive, as seen in the cytometry charts (Figure 6B). In SCL-I, the early reduction of ROS was also abolished, but its induction at 24 h was not significant (114%).

In order to assess the relations between ROS and the observed loss of cell viability in response to PE, we used the antioxidant N-acetyl cysteine (NAC, 1 mM). While NAC itself remained almost without effect on cell viability, it significantly further enhanced the reduction of cell viability by PE. Thus, viability values at 24 h decreased from 16% to 1% (SCL-I), from 51% to 5% (SCL-II), from 41% to 9% (SCC-12) and from 8% to 6% (SCC-13), respectively (Figure 6C). A similar tendency was seen for the WST-1 values at 24 h, when cells were treated with a combination of PE-100 and NAC (1 mM), as compared to PE treatment alone. Thus, WST-1 values decreased from 34% to 27% (SCL-I), 20% to 13% (SCL-II), 28% to 23% (SCC-12) and from 33% to 21% (SCC-13) (Figure 6D). These data suggest that the PE-mediated ROS imbalance may be the signal for its inhibitory effects.

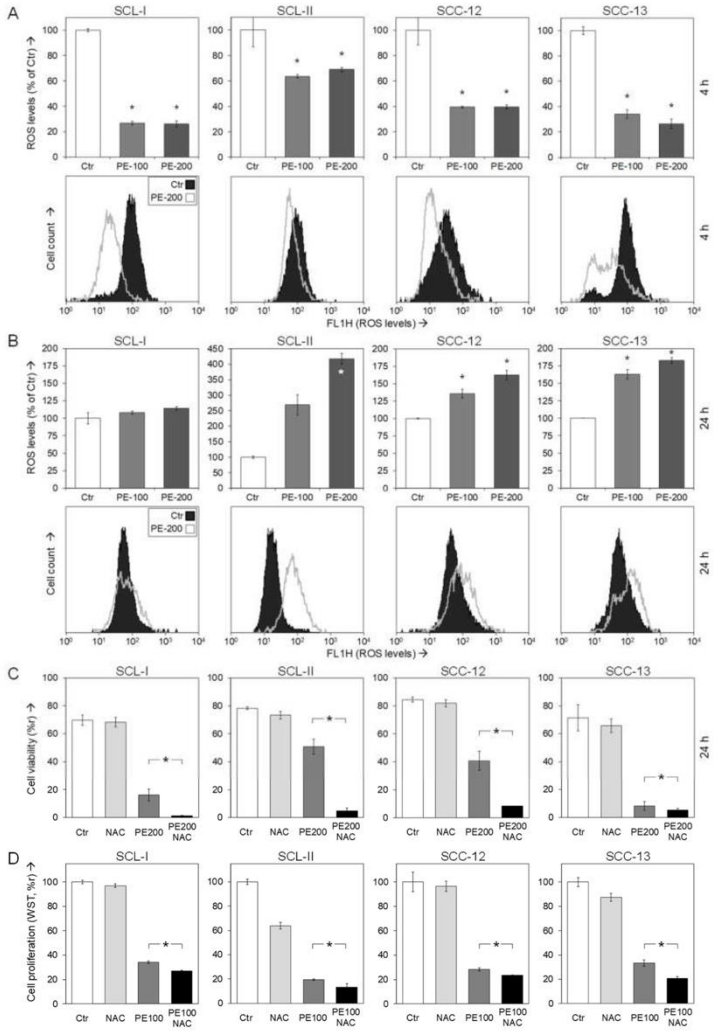

Figure 6. Dysregulation of ROS by PE. (**A**,**B**) SCC cells were seeded in 24-well plates and treated with PE (100, 200 μg/mL) for 4 h (**A**) and for 24 h (**B**), respectively. Cellular levels of ROS were determined by H2DCF-DA staining and flow cytometry. Values represent means of ROS levels in cells in percent, as compared to non-treated controls (Ctr, 100%). Examples of flow cytometry readings are shown below (overlays of cells treated with 200 μg/mL PE vs. Ctr). Each one of two independent experiments is shown; each individual experiment consisted of triplicate values. Statistical significance was calculated from all individual values (#6) and is indicated by asterisks ($p < 0.05$, as compared to Ctr). (**C**) SCC cell lines seeded in 24-well plates were treated with PE (200 μg/mL) +/− N-acetylcysteine (NAC, 1 mM), as indicated. Cell viability was determined at 24 h of treatment by calcein-AM staining and flow cytometry. Values represent the percentage of cells with high calcein staining (viable cells). (**D**) SCC cell lines seeded in 96-well plates (10,000 cells/well) were treated

with PE (100 µg/mL) +/− 1 mM NAC, as indicated. Cell proliferation rates were determined at 24 h of treatment by WST-1 assay. (**C**,**D**) At least two independent experiments revealed highly comparable results; each individual experiment consisted of triplicate values. Statistical significance of differences between PE/NAC-treated cells and PE-treated cells was calculated from all individual values in a group (at least 6) and is indicated by asterisks ($p < 0.05$).

4. Discussion

Due to high incidence and malignant progression, cSCC represents a severe health problem worldwide [3,4]. Additionally, treatment of field cancerization in AK is crucial, concerning the high risk to proceed to invasive cSCC [6]. Polyphenols as green tea extracts are under basic research for their potential use as antitumor agents [28,29]. Thus, sinecatechins (PE) includes a mixture of different catechin derivatives and other green tea components as epigallocatechin-3-gallate (EGCG), epigallocatechin, epicatechin-3-gallate, epicatechin, gallocatechins, gallocatechin gallate, gallic acid, caffeine, and theobromine [9].

PE ointment has been approved in 2006 for treatment of genital warts, after extensive testing in clinical trials, which showed complete clearance in more than 50% of patients and few side effects [30,31]. Based on this experience, it was also suggested for treatment of AK [7]. Although there is a large body of literature on green tea and skin cancer, a large part of the literature deals with the protective effects of green tea extracts, e.g., against irradiation-induced carcinogenesis [32], while other papers focus on the clinical use of PE for treatment of AK [7,8]. On the other hand, there is much less information on its direct mechanisms and mode of action in skin cancer cells. We thus investigated the effects of PE in cutaneous SCC cell lines, which represent suitable models for cSCC as well as for AK, due to the definition of AK as cSCC in situ. The effects of PE may be furthermore compared to those of epigallocatechin gallate (EGCG), which represents the most abundant catechin in green tea [9], and was here applied as a positive control.

Significant antitumor effects were obtained at the levels of cSCC cell proliferation and viability. Effects were comparable to the effects of EGCG, when used at half the concentration. Considering the 55% of EGCG in sinecatechins, these findings strongly suggestthat EGCG was the active compound here. PE treatment resulted in less induction of early apoptotic cells, whereas numbers of late apoptotic/necrotic cells were strongly increased, as shown by Annexin V/PI double staining. Also in mammary carcinoma cells (MCF-7), strong antiproliferative effects (up to 90%) had been reported in response to EGCG, while apoptosis was only at 6% [10]. In contrast, more pronounced apoptosis induction by EGCG was reported in other cancer cells. Thus, in lung cancer cells (H1299, A549), apoptosis induction by EGCG was up to 40% [11]. In gastric cancer cells (SGC7901), inhibition of cell proliferation was up to 70-fold, and apoptosis was up to 25% [12]. In ER-negative breast cancer cells (MDA-MB-468), EGCG resulted in strongly inhibited cell proliferation, loss of cell viability (up to 80%) as well as induced apoptosis (up to 70%) [33]. Furthermore, in colorectal cancer cells (SW480, SW620, LS411N), EGCG resulted in significant inhibition of cell proliferation and induction of apoptosis (up to 60%) [34]. Thus, while green tea components strongly induced apoptosis in other cell types, this effect could be masked in cSCC cells.

When raising the question of possible effects in normal cells, which may result in side effects in the clinical setting, it may be considered that green tea extracts have been used in traditional Chinese medicine for many years and PE topical treatment has been tested in several clinical trials. Major side effects are not known and have not been reported from the clinical trials. Thus, polyphenon E was approved for treatment of genital warts [30,31]. Here, the effects of PE were investigated in normal human fibroblasts, which did not show significant inhibition at the levels of cell viability and cell proliferation. Comparably, almost no inhibitory effects were reported for PE in combination with lactoferrin in normal human gingival fibroblast cells [35]. Additionally, EGCG and PE preferentially inhibited growth of colon cancer cells when compared with a normal human fetal colon cell line [36].

Inhibition of cell proliferation by PE correlated with dose-dependent upregulation of the cyclin-dependent kinase (CDK) inhibitor $p21^{Cip1}$ in two of three investigated cSCC cell lines. This inhibitor mainly targets CDK2, although capable of inhibiting also other cyclin/CDK complexes [37,38]. Besides p21, the family of Cip/Kip inhibitors includes also p27 and p57 [14]. Upregulation of p21 and p27 in response to EGCG has also been reported in MCF-7 breast carcinoma cells, in prostate carcinoma cells as well as in SCC-13 [39–41]. These CDK inhibitors may thus contribute to the antiproliferative effects of EGCG/PE, but the lack of p21 upregulation in SCL-II and its only limited upregulation in SCL-I and SCC-12 may suggest that this factor cannot be solely responsible for the antiproliferative effects induced by PE. Inhibition of cell proliferation may also be related to targeting EGFR and Notch pathways, as shown in SCC cells [42]. It is well known that the regulation of cell proliferation and viability is due to multiple factors and multiple pathways.

Concerning the mechanisms of PE-induced cell death in cSCC cells, loss of mitochondrial membrane potential (MMP), caspase activation and the roles of Bax and Bak were investigated. Significant caspase-3 activation in response to EGCG had been reported in bladder and colon cancer cells [43,44]. In cSCC cells, however, activation/processing of initiator caspases (-8 and -9) and the major effector caspase-3 remained on a lower level. Consistent with this, PE-mediated cell death was less affected by a pancaspase inhibitor (Q-VD-Oph), which, on the other hand, completely abolished apoptosis induced by an indirubin derivative in combination with TRAIL [24], used a positive control. This clearly indicated that also caspase-independent, non-apoptotic pathways were induced by PE in cSCC cells, besides some early induction of apoptosis.

Early loss of MMP often correlates with release of proapoptotic mitochondrial factors, e.g., cytochrome c, which then trigger intrinsic proapoptotic pathways via caspase-9/caspase-3 [17,18]. Thus, in HeLa cervical cancer cells, loss of MMP by EGCG was reported at 24 h [45,46]. Interestingly, PE resulted in a complete loss of MMP at 24 h in cSCC cells. However, there was only little incidence of typical apoptotic cell morphology upon PE treatment. Thus, loss of MMP by PE appeared as a strong effect but was decoupled from apoptosis induction.

Activation of intrinsic proapoptotic pathways typically depends on the multidomain proapoptotic proteins Bax and/or Bak [17]. Their possible role in PE-mediated cell death was evaluated in a cell culture model based on HCT-116 colon carcinoma cells [19–21], which showed a comparable response to PE as cSCC cells in Annexin V/PI staining as well as in JC-1 staining. While TRAIL-induced apoptosis was completely abolished in HCT-116 Bax/Bak double knockout cells, PE-mediated effects were less decreased. Together, these data indicate that neither caspases nor Bax or Bak were essentially required for the main effects of PE on cell death and loss of MMP. This was clearly suggestive for additional, non-apoptotic, alternative pathways involved in PE-induced cell death.

The intracellular formation of different kinds of reactive oxygen species can result in molecular damage and increased oxidative activity, and ROS are involved in multiple signaling pathways, including cell death signaling pathways. For different kinds of disease as of the neuronal, cardiovascular and nervous systems as well as in aging, ROS play important roles [22]. For polyphenols as for EGCG, antioxidative and thus protective effects have been reported, e.g., in cardiovascular disease, Alzheimer's disease and in skin damage [47–49].

On the other hand, reactive oxygen species may critically contribute to the induction of apoptosis and other cell death pathways in skin cancer cells, as shown for an iron-substituted nucleoside analogue in melanoma cells [50], for celecoxib in cSCC cells [23] and for indirubin derivatives in cutaneous T-cell lymphoma, melanoma and cSCC cells [24,51,52]. ROS may derive from mitochondrial leakage or other sources [53], but their relations to apoptosis pathways are still largely elusive to date. ROS production was also reported in different kinds of cSCC therapy, such as chemotherapy, photothermal, and photodynamic therapy [54–56].

While for other treatments the effects on ROS were rapid and strong upregulation, the effects of PE in cSCC cells were biphasic. Thus, PE resulted in an initial decrease in ROS (4 h) followed by a moderate ROS upregulation at 24 h. Increased ROS levels in response to EGCG had also been reported in HepG2 hepatocellular carcinoma cells [57], in primary effusion lymphoma cells [58] and in malignant mesothelioma cells [59]. In all three reports, ROS induction was also obtained at later times, namely 24 h.

Thus, polyphenols may exert both antioxidative and pro-oxidative activities. Ambivalent effects on ROS levels have also been reported for other agents. Thus, the antioxidant vitamin C may also reveal pro-oxidative activities in cancer cells [60]. Pro- and antioxidant effects have also been reported for flavonoids in plant extracts [61] and for different phenolic compounds in food [62]. The modulation of ROS appears as a suitable strategy for selective targeting cancer cells. Thus, cancer cells are often characterized by elevated ROS levels and may on one hand be more sensitive for ROS-inducing agents. On the other hand, cancer cells are adjusted to the elevated ROS levels and may thus be also more sensitive to a suppression of ROS, as shown here for PE. A switch from antioxidative to pro-oxidative activity may depend on the cellular redox systems, ROS balance by pro- and antioxidative enzymes, pH, iron and oxygen [63].

We suggest, that PE mediates an imbalance of ROS in cSCC cells, characterized by an initial decrease and subsequent increase. This may be responsible for the decreased cell viability observed in course of PE treatment in cSCC cells. The hypothesis was supported by the use of the additional antioxidant N-acetylcysteine (NAC). While NAC alone remained without significant effects on cSCC viability, the combination of PE with NAC resulted in a further strong decrease in cell viability. Of course, early antioxidative effects cannot be a sufficient step for decreasing cell viability. The green tea extract PE may have even more activities beyond its antioxidative effects that finally lead to the inhibition of cSCC cells.

5. Conclusions

Sinecatechins has been approved in 2006 as ointment for treatment of genital warts (Polyphenon E, Veregen). Based on these experiences, it was also suggested for treatment of actinic keratosis, however, mechanistic studies in skin cancer cells were rare. In this investigation, we demonstrate the particular high activity of sinecatechins in cSCC cells, which also serve as models for actinic keratosis. Induced cell death was, however, less related to classical apoptosis pathways, e.g., activation of caspases or of Bax and Bak. Rather, alternative cell death pathways were also involved, which enclose loss of MMP and a dysbalance of ROS, finally leading to loss of cell viability and cell proliferation. These data may support ideas for further development of PE in the treatment of AK. In general, the considering of targeted strategies for ROS may extend the therapeutic options in cancer therapy.

Supplementary Materials: The following supporting information can be downloaded at: www.mdpi.com/article/10.3390/antiox11071416/s1, Figure S1: MRC-5 cells (human fetal lung fibroblast cells) were seeded and treated in an identical way as cSCC cells. Cell proliferation (A), WST-1 assay) and cell viability (B), calcein staining) were performed at 24 h and at 48 h, respectively. Mean values and SDs were calculated for 6 (A) and 4 (B) individual wells.

Author Contributions: Conceptualization, J.E. and E.S.; methodology, J.Z., B.G. and J.E.; investigation, J.Z., B.G., D.L.D.T., and S.M.; resources, J.E. and C.U.; data curation, J.Z., D.L.D.T., S.M., and J.E.; writing—original draft preparation, J.E., J.Z. and B.G.; writing—review and editing, J.E., J.Z., B.G., C.U., and E.S.; supervision, J.E.; funding acquisition, J.E. and C.U. All authors have read and agreed to the published version of the manuscript.

Funding: This research was funded by the European skin cancer foundation (ESCF), Deutsches Stiftungszentrum, 45239 Essen, Germany; project S0251/10015/2020.

Institutional Review Board Statement: Not applicable.

Informed Consent Statement: Not applicable.

Data Availability Statement: Data is contained within the manuscript and supplementary materials.

Acknowledgments: We acknowledge support from the German Research Foundation (DFG) and the Open Access Publication Fund of Charité–Universitätsmedizin Berlin.

Conflicts of Interest: E.S. is working as a consultant for Aresus Pharma GmbH, Strausberg, Germany, and he holds patents for polyphenon E. Other authors declare no conflicts of interest. The funders had no role in the design of the study; in the collection, analyses, or interpretation of data; in the writing of the manuscript; or in the decision to publish the results.

References

1. Alam, M.; Ratner, D. Cutaneous squamous-cell carcinoma. *N. Engl. J. Med.* **2001**, *344*, 975–983. https://doi.org/10.1056/NEJM200103293441306.
2. Szewczyk, M.; Pazdrowski, J.; Golusiński, P.; Dańczak-Pazdrowska, A.; Marszałek, S.; Golusiński, W. Analysis of selected risk factors for nodal metastases in head and neck cutaneous squamous cell carcinoma. *Eur. Arch. Otorhinolaryngol.* **2015**, *272*, 3007–3012. https://doi.org/10.1007/s00405-014-3261-6.
3. Agbai, O.N.; Buster, K.; Sanchez, M.; Hernandez, C.; Kundu, R.V.; Chiu, M.; Roberts, W.E.; Draelos, Z.D.; Bhushan, R.; Taylor, S.C.; et al. Skin cancer and photoprotection in people of color: A review and recommendations for physicians and the public. *J. Am. Acad. Dermatol.* **2014**, *70*, 748–762. https://doi.org/10.1016/j.jaad.2013.11.038.
4. Amaral, T.; Osewold, M.; Presser, D.; Meiwes, A.; Garbe, C.; Leiter, U. Advanced cutaneous squamous cell carcinoma: Real world data of patient profiles and treatment patterns. *J. Eur. Acad. Dermatol. Venereol.* **2019**, *33* (Suppl. 8), 44–51. https://doi.org/10.1111/jdv.15845.
5. Stockfleth, E. The importance of treating the field in actinic keratosis. *J. Eur. Acad. Dermatol. Venereol.* **2017**, *31* (Suppl. 2), 8–11. https://doi.org/10.1111/jdv.14092.
6. Cramer, P.; Stockfleth, E. Actinic keratosis: Where do we stand and where is the future going to take us? *Expert Opin. Emerg. Drugs* **2020**, *25*, 49–58. https://doi.org/10.1080/14728214.2020.1730810.
7. Stockfleth, E.; Meyer, T. Sinecatechins (Polyphenon E) ointment for treatment of external genital warts and possible future indications. *Expert. Opin. Biol. Ther.* **2014**, *14*, 1033–1043. https://doi.org/10.1517/14712598.2014.913564.
8. Bobyr, I.; Campanati, A.; Offidani, A. "SENECA" Sinecatechins 10% ointment: A green tea extract for the treatment of actinic keratosis. Case series. *Dermatol. Ther.* **2018**, *31*, e12634. https://doi.org/10.1111/dth.12634.
9. Khan, N.; Mukhtar, H. Tea Polyphenols in Promotion of Human Health. *Nutrients* **2018**, *11*, 39. https://doi.org/10.3390/nu11010039.
10. Huang, C.Y.; Han, Z.; Li, X.; Xie, H.H.; Zhu, S.S. Mechanism of EGCG promoting apoptosis of MCF-7 cell line in human breast cancer. *Oncol. Lett.* **2017**, *14*, 3623–3627. https://doi.org/10.3892/ol.2017.6641.
11. Gu, J.J.; Qiao, K.S.; Sun, P.; Chen, P.; Li, Q. Study of EGCG induced apoptosis in lung cancer cells by inhibiting PI3K/Akt signaling pathway. *Eur. Rev. Med. Pharmacol. Sci.* **2018**, *22*, 4557–4563. https://doi.org/10.26355/eurrev_201807_15511.
12. Fu, J.D.; Yao, J.J.; Wang, H.; Cui, W.G.; Leng, J.; Ding, L.Y.; Fan, K.Y. Effects of EGCG on proliferation and apoptosis of gastric cancer SGC7901 cells via down-regulation of HIF-1α and VEGF under a hypoxic state. *Eur. Rev. Med. Pharmacol. Sci.* **2019**, *23*, 155–161. https://doi.org/10.26355/eurrev_201901_16759.
13. Roufayel, R.; Mezher, R.; Storey, K.B. The Role of Retinoblastoma Protein in Cell Cycle Regulation: An Updated Review. *Curr. Mol. Med.* **2021**, *21*, 620–629. https://doi.org/10.2174/1566524020666210104113003.
14. Roy, A.; Banerjee, S. p27 and leukemia: Cell cycle and beyond. *J. Cell. Physiol.* **2015**, *230*, 504–509. https://doi.org/10.1002/jcp.24819.
15. Li, J.; Poi, M.J.; Tsai, M.D. Regulatory mechanisms of tumor suppressor P16(INK4A) and their relevance to cancer. *Biochemistry* **2011**, *50*, 5566–5582. https://doi.org/10.1021/bi200642e.
16. Eberle, J. Countering TRAIL Resistance in Melanoma. *Cancers* **2019**, *11*, 656. https://doi.org/10.3390/cancers11050656.
17. Chipuk, J.E.; Moldoveanu, T.; Llambi, F.; Parsons, M.J.; Green, D.R. The BCL-2 family reunion. *Mol. Cell* **2010**, *37*, 299–310. https://doi.org/10.1016/j.molcel.2010.01.025.
18. Fischer, U.; Janicke, R.U.; Schulze-Osthoff, K. Many cuts to ruin: A comprehensive update of caspase substrates. *Cell Death Differ.* **2003**, *10*, 76–100. https://doi.org/10.1038/sj.cdd.4401160.
19. Wang, C.; Youle, R.J. Predominant requirement of Bax for apoptosis in HCT116 cells is determined by Mcl-1's inhibitory effect on Bak. *Oncogene* **2012**, *31*, 3177–3189. https://doi.org/10.1038/onc.2011.497.
20. Gillissen, B.; Richter, A.; Richter, A.; Overkamp, T.; Essmann, F.; Hemmati, P.G.; Preissner, R.; Belka, C.; Daniel, P.T. Targeted therapy of the XIAP/proteasome pathway overcomes TRAIL-resistance in carcinoma by switching apoptosis signaling to a Bax/Bak-independent 'type I' mode. *Cell Death Dis.* **2013**, *4*, e643. https://doi.org/10.1038/cddis.2013.67.
21. Gillissen, B.; Richter, A.; Richter, A.; Preissner, R.; Schulze-Osthoff, K.; Essmann, F.; Daniel, P.T. Bax/Bak-independent mitochondrial depolarization and reactive oxygen species induction by sorafenib overcome resistance to apoptosis in renal cell carcinoma. *J. Biol. Chem.* **2017**, *292*, 6478–6492. https://doi.org/10.1074/jbc.M116.754184.

22. Sies, H.; Jones, D.P. Reactive oxygen species (ROS) as pleiotropic physiological signalling agents. *Nat. Rev. Mol. Cell Biol.* **2020**, *21*, 363–383. https://doi.org/10.1038/s41580-020-0230-3.
23. Zhu, J.; May, S.; Ulrich, C.; Stockfleth, E.; Eberle, J. High ROS Production by Celecoxib and Enhanced Sensitivity for Death Ligand-Induced Apoptosis in Cutaneous SCC Cell Lines. *Int. J. Mol. Sci.* **2021**, *22*, 3622. https://doi.org/10.3390/ijms22073622.
24. Zhu, J.; Langer, P.; Ulrich, C.; Eberle, J. Crucial Role of Reactive Oxygen Species (ROS) for the Proapoptotic Effects of Indirubin Derivatives in Cutaneous SCC Cells. *Antioxidants* **2021**, *10*, 1514. https://doi.org/10.3390/antiox10101514.
25. Rheinwald, J.G.; Beckett, M.A. Tumorigenic keratinocyte lines requiring anchorage and fibroblast support cultured from human squamous cell carcinomas. *Cancer Res.* **1981**, *41*, 1657–1663.
26. Tilgen, W.; Boukamp, P.; Breitkreutz, D.; Dzarlieva, R.T.; Engstner, M.; Haag, D.; Fusenig, N.E. Preservation of morphological, functional, and karyotypic traits during long-term culture and in vivo passage of two human skin squamous cell carcinomas. *Cancer Res.* **1983**, *43*, 5995–6011.
27. Fecker, L.F.; Stockfleth, E.; Braun, F.K.; Rodust, P.M.; Schwarz, C.; Köhler, A.; Leverkus, M.; Eberle, J. Enhanced death ligand-induced apoptosis in cutaneous SCC cells by treatment with diclofenac/hyaluronic acid correlates with downregulation of c-FLIP. *J. Invest. Dermatol.* **2010**, *130*, 2098–2109. https://doi.org/10.1038/jid.2010.40.
28. Manach, C.; Scalbert, A.; Morand, C.; Rémésy, C.; Jiménez, L. Polyphenols: Food sources and bioavailability. *Am. J. Clin. Nutr.* **2004**, *79*, 727–747. https://doi.org/10.1093/ajcn/79.5.727.
29. Chen, D.; Wan, S.B.; Yang, H.; Yuan, J.; Chan, T.H.; Dou, Q.P. EGCG, green tea polyphenols and their synthetic analogs and prodrugs for human cancer prevention and treatment. *Adv. Clin. Chem.* **2011**, *53*, 155–177. https://doi.org/10.1016/b978-0-12-385855-9.00007-2.
30. Stockfleth, E.; Meyer, T. The use of sinecatechins (polyphenon E) ointment for treatment of external genital warts. *Expert Opin. Biol. Ther.* **2012**, *12*, 783–793. https://doi.org/10.1517/14712598.2012.676036.
31. Gross, G.; Meyer, K.G.; Pres, H.; Thielert, C.; Tawfik, H.; Mescheder, A. A randomized, double-blind, four-arm parallel-group, placebo-controlled Phase II/III study to investigate the clinical efficacy of two galenic formulations of Polyphenon E in the treatment of external genital warts. *J. Eur. Acad. Dermatol. Venereol.* **2007**, *21*, 1404–1412. https://doi.org/10.1111/j.1468-3083.2007.02441.x.
32. Prasanth, M.I.; Sivamaruthi, B.S.; Chaiyasut, C.; Tencomnao, T. A Review of the Role of Green Tea (Camellia sinensis) in Antiphotoaging, Stress Resistance, Neuroprotection, and Autophagy. *Nutrients* **2019**, *11*, 474. https://doi.org/10.3390/nu11020474.
33. Roy, A.M.; Baliga, M.S.; Katiyar, S.K. Epigallocatechin-3-gallate induces apoptosis in estrogen receptor-negative human breast carcinoma cells via modulation in protein expression of p53 and Bax and caspase-3 activation. *Mol. Cancer Ther.* **2005**, *4*, 81–90.
34. Luo, K.W.; Xia, J.; Cheng, B.H.; Gao, H.C.; Fu, L.W.; Luo, X.L. Tea polyphenol EGCG inhibited colorectal-cancer-cell proliferation and migration via downregulation of STAT3. *Gastroenterol. Rep.* **2021**, *9*, 59–70. https://doi.org/10.1093/gastro/goaa072.
35. Mohan, K.V.; Gunasekaran, P.; Varalakshmi, E.; Hara, Y.; Nagini, S. In vitro evaluation of the anticancer effect of lactoferrin and tea polyphenol combination on oral carcinoma cells. *Cell Biol. Int.* **2007**, *31*, 599–608. https://doi.org/10.1016/j.cellbi.2006.11.034.
36. Shimizu, M.; Deguchi, A.; Lim, J.T.; Moriwaki, H.; Kopelovich, L.; Weinstein, I.B. (-)-Epigallocatechin gallate and polyphenon E inhibit growth and activation of the epidermal growth factor receptor and human epidermal growth factor receptor-2 signaling pathways in human colon cancer cells. *Clin. Cancer Res.* **2005**, *11*, 2735–2746. https://doi.org/10.1158/1078-0432.Ccr-04-2014.
37. Xiong, Y.; Hannon, G.J.; Zhang, H.; Casso, D.; Kobayashi, R.; Beach, D. p21 is a universal inhibitor of cyclin kinases. *Nature* **1993**, *366*, 701–704. https://doi.org/10.1038/366701a0.
38. Abbas, T.; Dutta, A. p21 in cancer: Intricate networks and multiple activities. *Nat. Rev. Cancer* **2009**, *9*, 400–414. https://doi.org/10.1038/nrc2657.
39. Liang, Y.C.; Lin-Shiau, S.Y.; Chen, C.F.; Lin, J.K. Inhibition of cyclin-dependent kinases 2 and 4 activities as well as induction of Cdk inhibitors p21 and p27 during growth arrest of human breast carcinoma cells by (-)-epigallocatechin-3-gallate. *J. Cell. Biochem.* **1999**, *75*, 1–12.
40. Gupta, S.; Hussain, T.; Mukhtar, H. Molecular pathway for (-)-epigallocatechin-3-gallate-induced cell cycle arrest and apoptosis of human prostate carcinoma cells. *Arch. Biochem. Biophys.* **2003**, *410*, 177–185. https://doi.org/10.1016/s0003-9861(02)00668-9.
41. Balasubramanian, S.; Adhikary, G.; Eckert, R.L. The Bmi-1 polycomb protein antagonizes the (-)-epigallocatechin-3-gallate-dependent suppression of skin cancer cell survival. *Carcinogenesis* **2010**, *31*, 496–503. https://doi.org/10.1093/carcin/bgp314.
42. Liu, X.; Zhang, D.Y.; Zhang, W.; Zhao, X.; Yuan, C.; Ye, F. The effect of green tea extract and EGCG on the signaling network in squamous cell carcinoma. *Nutr. Cancer* **2011**, *63*, 466–475. https://doi.org/10.1080/01635581.2011.532901.
43. Luo, K.W.; Lung, W.Y.; Chun, X.; Luo, X.L.; Huang, W.R. EGCG inhibited bladder cancer T24 and 5637 cell proliferation and migration via PI3K/AKT pathway. *Oncotarget* **2018**, *9*, 12261–12272. https://doi.org/10.18632/oncotarget.24301.
44. Zhu, W.; Li, M.C.; Wang, F.R.; Mackenzie, G.G.; Oteiza, P.I. The inhibitory effect of ECG and EGCG dimeric procyanidins on colorectal cancer cells growth is associated with their actions at lipid rafts and the inhibition of the epidermal growth factor receptor signaling. *Biochem. Pharmacol.* **2020**, *175*, 113923. https://doi.org/10.1016/j.bcp.2020.113923.
45. Singh, M.; Singh, R.; Bhui, K.; Tyagi, S.; Mahmood, Z.; Shukla, Y. Tea polyphenols induce apoptosis through mitochondrial pathway and by inhibiting nuclear factor-kappaB and Akt activation in human cervical cancer cells. *Oncol. Res.* **2011**, *19*, 245–257. https://doi.org/10.3727/096504011x13021877989711.

46. Chakrabarty, S.; Nag, D.; Ganguli, A.; Das, A.; Ghosh Dastidar, D.; Chakrabarti, G. Theaflavin and epigallocatechin-3-gallate synergistically induce apoptosis through inhibition of PI3K/Akt signaling upon depolymerizing microtubules in HeLa cells. *J. Cell. Biochem.* **2019**, *120*, 5987–6003. https://doi.org/10.1002/jcb.27886.
47. Tipoe, G.L.; Leung, T.M.; Hung, M.W.; Fung, M.L. Green tea polyphenols as an anti-oxidant and anti-inflammatory agent for cardiovascular protection. *Cardiovasc. Hematol. Disord. Drug Targets* **2007**, *7*, 135–144. https://doi.org/10.2174/187152907780830905.
48. Singh, N.A.; Mandal, A.K.; Khan, Z.A. Potential neuroprotective properties of epigallocatechin-3-gallate (EGCG). *Nutr. J.* **2016**, *15*, 60. https://doi.org/10.1186/s12937-016-0179-4.
49. Avadhani, K.S.; Manikkath, J.; Tiwari, M.; Chandrasekhar, M.; Godavarthi, A.; Vidya, S.M.; Hariharapura, R.C.; Kalthur, G.; Udupa, N.; Mutalik, S. Skin delivery of epigallocatechin-3-gallate (EGCG) and hyaluronic acid loaded nano-transfersomes for antioxidant and anti-aging effects in UV radiation induced skin damage. *Drug Deliv.* **2017**, *24*, 61–74. https://doi.org/10.1080/10717544.2016.1228718.
50. Franke, J.C.; Plotz, M.; Prokop, A.; Geilen, C.C.; Schmalz, H.G.; Eberle, J. New caspase-independent but ROS-dependent apoptosis pathways are targeted in melanoma cells by an iron-containing cytosine analogue. *Biochem. Pharmacol.* **2010**, *79*, 575–586. https://doi.org/10.1016/j.bcp.2009.09.022.
51. Soltan, M.Y.; Sumarni, U.; Assaf, C.; Langer, P.; Reidel, U.; Eberle, J. Key Role of Reactive Oxygen Species (ROS) in Indirubin Derivative-Induced Cell Death in Cutaneous T-Cell Lymphoma Cells. *Int. J. Mol. Sci.* **2019**, *20*, 1158. https://doi.org/10.3390/ijms20051158.
52. Zhivkova, V.; Kiecker, F.; Langer, P.; Eberle, J. Crucial role of reactive oxygen species (ROS) for the proapoptotic effects of indirubin derivative DKP-073 in melanoma cells. *Mol. Carcinog.* **2019**, *58*, 258–269. https://doi.org/10.1002/mc.22924.
53. Quast, S.A.; Berger, A.; Eberle, J. ROS-dependent phosphorylation of Bax by wortmannin sensitizes melanoma cells for TRAIL-induced apoptosis. *Cell Death Dis.* **2013**, *4*, e839. https://doi.org/10.1038/cddis.2013.344.
54. Liu, P.; Yang, W.T.; Shi, L.; Zhang, H.Y.; Xu, Y.; Wang, P.R.; Zhang, G.L.; Chen, W.R.; Zhang, B.B.; Wang, X.L. Concurrent photothermal therapy and photodynamic therapy for cutaneous squamous cell carcinoma by gold nanoclusters under a single NIR laser irradiation. *J. Mater. Chem. B* **2019**, *7*, 6924–6933. https://doi.org/10.1039/c9tb01573f.
55. Austin, E.; Koo, E.; Jagdeo, J. Thermal photodynamic therapy increases apoptosis and reactive oxygen species generation in cutaneous and mucosal squamous cell carcinoma cells. *Sci. Rep.* **2018**, *8*, 12599. https://doi.org/10.1038/s41598-018-30908-6.
56. Niu, T.H.; Tian, Y.; Wang, G.Y.; Guo, G.J.; Tong, Y.; Shi, Y. Inhibition of ROS-NF-kappa B-dependent autophagy enhances Hypocrellin A united LED red light-induced apoptosis in squamous carcinoma A431 cells. *Cell. Signal.* **2020**, *69*, 109550. https://doi.org/10.1016/j.cellsig.2020.109550.
57. Khiewkamrop, P.; Phunsomboon, P.; Richert, L.; Pekthong, D.; Srisawang, P. Epistructured catechins, EGCG and EC facilitate apoptosis induction through targeting de novo lipogenesis pathway in HepG2 cells. *Cancer Cell Int.* **2018**, *18*, 46. https://doi.org/10.1186/s12935-018-0539-6.
58. Tsai, C.Y.; Chen, C.Y.; Chiou, Y.H.; Shyu, H.W.; Lin, K.H.; Chou, M.C.; Huang, M.H.; Wang, Y.F. Epigallocatechin-3-Gallate Suppresses Human Herpesvirus 8 Replication and Induces ROS Leading to Apoptosis and Autophagy in Primary Effusion Lymphoma Cells. *Int. J. Mol. Sci.* **2017**, *19*, 16. https://doi.org/10.3390/ijms19010016.
59. Ranzato, E.; Martinotti, S.; Magnelli, V.; Murer, B.; Biffo, S.; Mutti, L.; Burlando, B. Epigallocatechin-3-gallate induces mesothelioma cell death via H_2O_2-dependent T-type Ca^{2+} channel opening. *J. Cell. Mol. Med.* **2012**, *16*, 2667–2678. https://doi.org/10.1111/j.1582-4934.2012.01584.x.
60. Kaźmierczak-Barańska, J.; Boguszewska, K.; Adamus-Grabicka, A.; Karwowski, B.T. Two Faces of Vitamin C-Antioxidative and Pro-Oxidative Agent. *Nutrients* **2020**, *12*, 1501. https://doi.org/10.3390/nu12051501.
61. Chobot, V.; Hadacek, F.; Bachmann, G.; Weckwerth, W.; Kubicova, L. In Vitro Evaluation of Pro- and Antioxidant Effects of Flavonoid Tricetin in Comparison to Myricetin. *Molecules* **2020**, *25*, 5850. https://doi.org/10.3390/molecules25245850.
62. do Carmo, M.A.V.; Granato, D.; Azevedo, L. Antioxidant/pro-oxidant and antiproliferative activities of phenolic-rich foods and extracts: A cell-based point of view. *Adv. Food Nutr. Res.* **2021**, *98*, 253–280. https://doi.org/10.1016/bs.afnr.2021.02.010.
63. Moloney, J.N.; Cotter, T.G. ROS signalling in the biology of cancer. *Semin. Cell Dev. Biol.* **2018**, *80*, 50–64.

Curriculum Vitae

Mein Lebenslauf wird aus datenschutzrechtlichen Gründen in der elektronischen Version meiner Arbeit nicht veröffentlicht.

Publication list

1. **Zhu, J**., May, S., Ulrich, C., Stockfleth, E., & Eberle, J. (2021). High ROS Production by Celecoxib and Enhanced Sensitivity for Death Ligand-Induced Apoptosis in Cutaneous SCC Cell Lines. Int J Mol Sci, 22(7). doi:10.3390/ijms22073622. (IF= 4,556)
2. **Zhu, J**., Langer, P., Ulrich, C., & Eberle, J. (2021). Crucial Role of Reactive Oxygen Species (ROS) for the Proapoptotic Effects of Indirubin Derivatives in Cutaneous SCC Cells. Antioxidants (Basel), 10(10). doi:10.3390/antiox10101514. (IF= 5,014)
3. **Zhu, J**.; Gillissen, B.; Dang Tran, D.L.; May, S.; Ulrich, C.; Stockfleth, E.; Eberle, J. Inhibition of Cell Proliferation and Cell Viability by Sinecatechins in Cutaneous SCC Cells Is Related to an Imbalance of ROS and Loss of Mitochondrial Membrane Potential. Antioxidants 2022, 11, 1416. https://doi.org/ 10.3390/antiox11071416. (IF= 6,312)

Acknowledgments

Learning and living in Berlin has impressed a profound meaning into my life. After two and half special years, we witnessed the courage and wisdom of human beings bursting out in facing diseases and challenges and allowed me to explore more profound in scientific research. Everyone I have met here has accompanied me through such a marvelous and unforgettable time.

First of all, I thank my supervisors, PD. Dr. Jürgen Eberle gave me the valuable opportunity to work in our lab and complete my project.

Dr. Eberle was often enthusiastic in helping me to solve my difficulties. Without his enthusiastic support and sincere encouragement, I would never have been able to achieve this promotion and enjoy this special moment. Dr. Eberle has helped me on many occasions to discuss research ideas and revise my project manuscript. He always had great research ideas and under his guidance I learned the meaning of research, which will undoubtedly be very important for my future work. I am sure that this will continue to guide me on my future research journey and it will never end.

I am grateful to my friends Uly and Zina who not only helped me with my project, but we often discussed research and other life topics together. They have taught me a lot about international etiquette and culture. Their open-mindedness is an example to me. They always helps me whenever I have difficulties in life or in my studies. I believe that friendship knows no distance, even when I return to China.

I am also grateful to my friends Zhe Peng who helped me with my project and contribution to my dissertation submission. We often discussed research and other life topics together. We had a great time together.

I thank my friends Mengdi Xia and Dashan Wu for their help in my life and encouragement when I was at a low point in my experiments and life. They made me realize what a true friend is, especially Mengdi Xia, whose advice always made me better at cooking.

I thank my friend Yu Zhang for her help in my study and life, we often share the good moments in our lives.

Finally, I would like to thank my family, my father even though he has passed away and did not have the opportunity to see me graduate from my MD, but the thought of him has been my motivation to keep going. My mother, as well as my sister, for their support in my studies, even though they has missed me.

Thank you for all the support they have given me in the last two and a half years. Thank you!